

The Biosorption of Platinum and Palladium in Chloride Real Leach Solution by Modified Biomass

A Thesis Submitted to the College of Graduate and Postdoctoral Studies in Partial
Fulfillment of the Requirements for the Degree of Master of Science in the
Department of Chemical and Biological Engineering,
University of Saskatchewan, Saskatoon, SK
Canada

By

Yen Ning Lee

PERMISSION TO USE

In presenting this thesis in partial fulfillment of the requirements for a Postgraduate degree from the University of Saskatchewan, I agree that the Libraries of this University may make it freely available for inspection. I further agree that permission for copying of this thesis in any manner, in whole or in part, for scholarly purposes may be granted by the professor or professors who supervised my thesis work or, in their absence, by the Head of the Department or the Dean of the College in which my thesis work was done. It is understood that any copying or publication or use of this thesis or parts thereof for financial gain shall not be allowed without my written permission. It is also understood that due recognition shall be given to me and to the University of Saskatchewan in any scholarly use which may be made of any material in my thesis.

Requests for permission to copy or to make other use of materials in this thesis in whole or in part should be addressed to the Department of Chemical and Biological Engineering or the College of Graduate and Postdoctoral Studies listed below:

Head of the Department
Chemical and Biological Engineering
University of Saskatchewan
57 Campus Drive
Saskatoon, Saskatchewan S7N 5A9
Canada

College of Graduate and Postdoctoral Studies
Room 116 Thorvaldson Building
110 Science Place
Saskatoon, Saskatchewan S7N 5C9
Canada

ABSTRACT

Modern demands for technological goods have created a global problem of excess electronic wastes (e-wastes). Increasing demands of precious metals to supply factories around the world for these electronic goods may also pose a strain towards current global gold, platinum and palladium reserves. As e-wastes often contain prominent levels of toxic materials along with valuable metals, its recycling must be conducted on an industrial scale to ensure a steady supply of precious metals (PM) for future needs. Current conventional methods of recycling PM including pyrometallurgical and hydrometallurgical processes are often costly, environmentally unfriendly and potentially hazardous. Therefore, researchers have turned towards the study of biomass-based adsorbents, also known as biosorbents, for applications in PM recovery and recycling.

In the research presented in the thesis herein, wheat straw, canola meal and wood bark nuggets were used and immobilized with dithiooxamide (DTO), ethylenediamine (EN) and primary amine (PA) to create 12 novel biosorbents. These biosorbents were examined for their effectiveness in recovering platinum (Pt) and palladium (Pd) from real leach solution provided by a PM refining plant in Ontario. From these 12 biosorbents, it was determined that dithiooxamide-immobilized wood bark (DTO-WB) was the most effective. Being able to recover up to 97.4% Pt and 99.8% Pd from diluted leach solution, DTO-WB was selected as the biosorbent of focus for the rest of the research. Characterization analysis including Fourier-Transform Infrared Spectroscopy (FT-IR) and Carbon, Hydrogen, Nitrogen and Sulfur (CHNS) content analysis confirmed that DTO immobilization was successful on the structure of WB.

Further experimentation and data analysis revealed that the rate of adsorption of Pt and Pd on DTO-WB progressed via the pseudo-second order rate model. Adsorption isotherm model studies indicate that the adsorption of Pt and Pd by DTO-WB followed the Freundlich and Langmuir adsorption isotherm respectively. Calculated energy levels of activation by Pt and Pd suggests that adsorption progresses due to chemisorption. Thermodynamic studies reveal that DTO-WB adsorption of Pt and Pd is endothermic in nature and that adsorption efficiencies may be improved by increasing operating temperatures. Acknowledging that a variety of dissolved metals exists in real leach solution, performed co-adsorption experiments indicated that DTO-WB was efficient in recovering other PM, namely silver and rhodium. Selenium, a potentially

toxic element commonly present in drinking water was also adsorbed in significant numbers by DTO-WB, suggesting that the adsorbent may potentially be used in water-treatment research.

ACKNOWLEDGEMENTS

I would like to thank my supervisor Dr. Shafiq Alam for his technical advice and support as well as providing me an opportunity to work under him and helping me achieve my first step in entering the world of scientific research and academia. The fast progress of my research work and completion of this thesis would not have been possible if it were not for his expert guidance.

I am grateful for my advisory committee members, Dr. Venkatesh Meda and Dr. Lope Tabil for taking the time to provide me with suggestions that helped me to improve my research scope and analysis of data.

I would also like to thank Mr. Afolabi Ayeni, Mr. Mohammad H. Mahaninia, Mr. Richard Blondin and Ms. Heli Eunike for their help in technical laboratory work and assistance with analytical instruments.

It would have been impossible to conduct the analytical portion of this research without the expert service on ICP-OES measurements provided by the Geoanalytical Laboratories at the Saskatchewan Research Council with special thanks to Mr. Robert Millar and Ms. Cherryl Comahig for their professionalism.

My sincere gratitude goes to the financial support from the Department of Chemical and Biological Engineering and Dr. Alam for awarding me with the Chemical Engineering Devolved Scholarship and numerous teaching assistant positions.

I would also like to thank my bosses and colleagues at the University Club of the University of Saskatchewan for their camaraderie – you all bring a spark into my otherwise mundane life.

And above all, I would like to wholeheartedly thank my parents, Mr. Raymond Lee and Ms. Shu-Fong Chen for always believing that I can achieve my dreams, no matter what that may be. I would also like to thank my brother Mr. Yen-Ju Lee who always provides me with plenty of love and support in my academic endeavors. Lastly, I want to thank my dear friend Ms. Sutasana Chinotaikul who constantly encourages me in all aspects of my life.

DEDICATION

This thesis is dedicated to my parents

Mr. Raymond Lee and Ms. Shu-Fong Chen

Thank you for always being proud of me
even in times when I am not proud of myself.

TABLE OF CONTENTS

PERMISSION TO USE	i
ABSTRACT.....	ii
ACKNOWLEDGEMENTS.....	iv
DEDICATION.....	v
TABLE OF CONTENTS.....	vi
LIST OF TABLES.....	viii
LIST OF FIGURES	ix
LIST OF ABBREVIATIONS.....	xiii
CHAPTER 1: Introduction	1
1.1 Introduction	1
1.2 Knowledge gaps	7
1.3 Research objectives	8
1.4 Overall outline of the thesis	8
CHAPTER 2: Literature Review	9
2.1 Mechanisms of metal biosorption	9
2.2 Lignin content in wheat straw, canola meal and wood bark	12
2.3 Conventional methods of recovery and advantages of biosorption	14
2.4 Significance of immobilization	19
2.5 Effect of experimental conditions	21
2.6 Adsorption isotherm and thermodynamics	24
2.7 Summary of literature review.....	28
CHAPTER 3: Experimental Procedures	30
3.1 Materials and instrumentation.....	30
3.2 Pre-treatment of biomass.....	31
3.3 Dithiooxamide immobilization	33
3.4 Synthesis of crosslinked-lignophenol	35
3.5 Ethylenediamine immobilization	36

3.6	Primary amine immobilization.....	37
3.7	Determination of the biosorbent of focus.....	39
3.8	Adsorption experiments	43
3.9	Characterization of biosorbent	44
3.9.1	FT-IR analysis of DTO-WB	44
3.9.2	Characterization of DTO-WB.....	45
3.10	Data analysis	46
CHAPTER 4: Results and Discussions.....		47
4.1	Effect of adsorbent dose.....	47
4.2	Effect of initial solution metal concentration.....	48
4.3	Biosorption kinetics.....	50
4.4	Activation Energies of Pt and Pd adsorption	56
4.5	Biosorption isotherm models	57
4.6	Thermodynamic analysis of adsorption	63
4.7	Trace metal co-adsorption.....	65
CHAPTER 5: Conclusions and Recommendations.....		67
5.1	Summary of research and obtained results.....	67
5.2	Challenges encountered in present research.....	69
5.3	The biosorption potential of canola meal.....	70
5.4	Recommendations for future work.....	73
REFERENCES		75
APPENDIX A: Filtrate solutions from one-point adsorption.....		81
APPENDIX B: FT-IR spectra of all biosorbents.....		85
APPENDIX C: Permission to reuse figures and tables from existing literature.....		91

LIST OF TABLES

Table 1.1. List of some common Waste Electrical and Electronic Equipment (WEEE) and electronic waste (E-waste) items with typical life span and item weight.	2
Table 2.1. Typical component values of canola meal in animal feed with North American and Export standards.....	13
Table 2.2. Various possible alternatives to cyanide as a leaching agent, their operating properties and extent of research and level of commercialization.....	16
Table 3.1. All created adsorbents according to precursor biomasses and immobilization routes.	38
Table 3.2. Elemental assay of received pregnant leach solution without dilution.....	39
Table 3.3. Carbon, Hydrogen, Sulfur and Nitrogen percentages of dithiooxamide-immobilized wood bark and raw wood bark.....	45
Table 4.1. Summary of all obtained parameters from pseudo-first and pseudo-second order kinetic model fitting of the adsorption of platinum and palladium on dithiooxamide-immobilized wood bark.....	52
Table 4.2. Summary of various parameters obtained from the application of the linear Langmuir equation from experimental data for the adsorption of platinum and palladium by dithiooxamide-immobilized wood bark	58
Table 4.3. Summary of all obtained R^2 correlation coefficients for the Langmuir and Freundlich isotherm plots obtained from the adsorption of platinum and palladium by dithiooxamide-immobilized wood bark.	62
Table 4.4. Summary of all calculated thermodynamic parameters for the adsorption of platinum and palladium by dithiooxamide-immobilized wood bark.	65

LIST OF FIGURES

Fig 1.1. Global generation of Electrical and Electronic Equipment on the market in millions of tons in 2012.....	4
Fig 1.2. Global generation of electronic waste per capita in millions of tons in 2014.	4
Fig 1.3. The concentration in parts per million of 44 elements typically found on printed circuit boards ranging from 10^0 to 10^6 parts per million.....	5
Fig 1.4. Proposed model for the complexation between polyphenolic species and Fe(III) ions. ...	6
Fig 1.5. Flow chart for a typical method of recovering gold and silver via adsorption by crosslinked persimmon tannin gel.	7
Fig 2.1. A proposed structure of lignin.	10
Fig 2.2. Structure of tannic acid, a form of tannin	11
Fig 2.3. Cross-sectional diagram of a tree	14
Fig 2.4. The adsorption ratios of gold, platinum and palladium at equilibrium using grape-seed based biosorbent Gravinol-GA ₅₆₀ versus conventional ion-exchange resin S1A0A	17
Fig 2.5. Adsorption percentage of various metals in pregnant leach solution on unmodified microalgal residue and dithiooxamide-immobilized microalgae in varying hydrochloric acid concentrations.	18
Fig 2.6. Adsorption percentage of various metals in pregnant leach solution on ion-exchange resin DIAION WA20 and activated carbon in varying hydrochloric acid concentrations	18
Fig 2.7. Structure of dithiooxamide (DTO).	20
Fig 2.8. Trends of hard, soft and intermediate acids and bases.	21
Fig 2.9. Effect of pH on recovery of Au at varying times for modified bagasse biosorbent.....	22
Fig 2.10. The effect of adsorbent dose on the amount of gold (III) remaining in solution using kraft mill lignin biosorbent	23
Fig 2.11. Langmuir isotherm plot of palladium (II) adsorption by moss biomass at equilibrium	25
Fig 2.12. Freundlich isotherm plot for biosorption of palladium (II) on moss biomass at equilibrium.....	26
Fig 3.1. The Malvern Mastersizer 3000 used for determination of biosorbent particle size.	30
Fig 3.2. Raw wheat straw (WS) after grinding.	31
Fig 3.3. Wood bark (WB) as received and after grinding.....	32
Fig 3.4. Raw canola meal (CM) as received and after protein removal.	32

Fig 3.5. Schematic for the synthesis of dithiooxamide-immobilized microalgae.....	34
Fig 3.6. Laboratory set-up illustrating the chlorination of biomass.....	34
Fig 3.7. Creation of crosslinked-lignophenol biomass.	35
Fig 3.8. Schematic illustrating the addition of H ₂ SO ₄ into phenolic mixture in the creation of lignophenol.	36
Fig 3.9. Reaction of crosslinked-lignophenol with ethylenediamine.	37
Fig 3.10. Reaction of crosslinked-lignophenol with primary amine	38
Fig 3.11. Summary of all immobilization routes for biosorbent production.	38
Fig 3.12. All biosorbent and pregnant leach solution mixtures with diluted and undiluted leach solutions.	40
Fig 3.13. Comparison of all 12 biosorbents in their efficiency of adsorbing platinum and palladium from solution.....	42
Fig 3.14. Average adsorption percentages achieved by dithiooxamide-immobilized wood bark on platinum and palladium recovery from three trials.....	43
Fig 3.15. FT-IR spectra of dithiooxamide-immobilized wood bark.....	45
Fig 3.16. Particle size distribution of dithiooxamide-immobilized wood bark.....	46
Fig 4.1. Effect of solid-liquid ratio on platinum and palladium recovery using dithiooxamide-immobilized wood bark	47
Fig 4.2. Effect of initial concentration on the adsorptions of platinum and palladium ions on dithiooxamide-immobilized wood bark.....	49
Fig 4.3. Effect of stirring time on the amount of platinum and palladium adsorbed by dithiooxamide-immobilized wood bark at 25°C, 30°C and 40°C	50
Fig 4.4. Pseudo-first order plot for the adsorption data of platinum and palladium on dithiooxamide-immobilized wood bark biosorbent at various temperatures.....	54
Fig 4.5 Pseudo-second order plot for the adsorption data of platinum and palladium on dithiooxamide-immobilized wood bark biosorbent at various temperatures.....	55
Fig 4.6. Arrhenius plot obtained from the pseudo-first order kinetic data of platinum and palladium adsorption by dithiooxamide-immobilized wood bark.....	56
Fig 4.7. Experimental data plots for platinum and palladium adsorption by dithiooxamide-immobilized wood bark	59

Fig 4.8. Langmuir isotherm plots of platinum and palladium adsorption by dithiooxamide-immobilized wood bark.	60
Fig 4.9. Freundlich isotherm plots of platinum and palladium adsorption by dithiooxamide-immobilized wood bark.	61
Fig 4.10. Van't Hoff plot of the adsorption of platinum and palladium by dithiooxamide-immobilized wood bark.	64
Fig 4.11. Comparison of effectiveness in co-adsorption of all detectable metal species in received pregnant leach solution by dithiooxamide-immobilized wood bark at various temperatures..	66
Fig 5.1. Protein-free canola meal (CM), protein-intact benzene-ethanol washed canola meal (CM-P) and protein-intact unwashed canola meal (CM-NW) before adsorption.....	71
Fig 5.2. Protein-free canola meal (CM), protein-intact benzene-ethanol washed canola meal (CM-P) and protein-intact unwashed canola meal (CM-NW) in diluted pregnant leach solution after 24 hours of shaking.....	71
Fig 5.3. Adsorption efficiencies of protein-free canola meal (CM), protein-intact benzene-ethanol washed canola meal (CM-P) and protein-intact unwashed canola meal (CM-NW) in recovering platinum and palladium.....	72
Fig B.1. FT-IR spectra of raw wheat straw.....	85
Fig B.2. FT-IR spectra of raw wood bark.....	85
Fig B.3. FT-IR spectra of raw canola meal.....	86
Fig B.4. FT-IR spectra of dithiooxamide-immobilized wheat straw.....	86
Fig B.5. FT-IR spectra of dithiooxamide-immobilized wood bark.....	87
Fig B.6. FT-IR spectra of dithiooxamide-immobilized canola meal.....	87
Fig B.7. FT-IR spectra of ethylenediamine-immobilized wheat straw.....	88
Fig B.8. FT-IR spectra of ethylenediamine-immobilized wood bark.....	88
Fig B.9. FT-IR spectra of ethylenediamine-immobilized canola meal.....	89
Fig B.10. FT-IR spectra of primary amine-immobilized wheat straw.....	89
Fig B.11. FT-IR spectra of primary amine-immobilized wood bark.....	90
Fig B.12. FT-IR spectra of primary amine-immobilized canola meal.....	90
Fig C.1.....	91
Fig C.2.....	92
Fig C.3.....	92
Fig C.4.....	93

Fig C.5.....	94
Fig C.6.....	94
Fig C.7.....	95
Fig C.8.....	95
Fig C.9.....	95
Fig C.10.....	96
Fig C.11.....	97
Fig C.12.....	98
Fig C.13.....	98
Fig C.14.....	98
Fig C.15.....	98
Fig C.16.....	99
Fig C.17.....	100
Fig C.18.....	101

LIST OF ABBREVIATIONS

Terminology

BET = Brunauer-Emmett-Teller

CHNS = Carbon, hydrogen, nitrogen and sulfur

CM = Protein-removed canola meal

CM-NW = Unwashed canola meal

CM-P = Protein-retained benzene-ethanol washed canola meal

CPT = Crosslinked persimmon tannin

Da = Dalton

DTO = Dithiooxamide

EEE = Electrical and Electronic Equipment

EN = Ethylenediamine

FT-IR = Fourier-transform infrared spectroscopy

HSAB = Hard-Soft Acid-Base

ICP-OES = Inductively coupled plasma optical emission spectrometry

PA = Primary amine

PCB = Printed Circuit Boards

PEI = Polyethyleneimine

PGM = Platinum group metals

PLS = Pregnant leach solution

PM = Precious metals

PPM = Parts per million

RPM = Revolutions per minute

WB = Wood bark

WEEE = Waste Electrical and Electronic Equipment

WS = Wheat straw

Elements

Ag = Silver

Au = Gold

Cd = Cadmium

Co = Cobalt

Cu = Copper

Fe = Iron

Hg = Mercury

Ni = Nickel

Pb = Lead

Pd = Palladium

Pt = Platinum

Rh = Rhodium

Se = Selenium

Sn = Tin

Te = Tellurium

Zn = Zinc

CHAPTER 1: Introduction

1.1 Introduction

Precious metals (PM) are rare and naturally occurring metallic elements which include gold, silver and platinum group metals (PGM) comprising of platinum, palladium and rhodium [1]. Traditionally, the rarity and beauty of PM have made them a common material for currency and jewelry [2]. The ductility, non-corrosive nature and general stability of gold makes it a valuable components in the technology industry [1]. In industry, palladium is often used in cell phones as capacitors and catalytic converters found in fuel consuming vehicles typically contain platinum additives to help treat exhaust fumes [3,4]. Additionally, PM are also used extensively in printed circuit boards and other electronic components [5].

The rate of technology turnover in the current economic market means that newer, cheaper and more sophisticated electronic devices are being manufactured in larger volumes and are being developed in shorter amounts of time. Obsolete and otherwise unusable electronics are often referred to as e-waste and waste electrical and electronic equipment (WEEE). WEEE refers to the blanket term for all electricity consuming household products while e-wastes typically refer to high-tech consumer gadgets including mobile phones, televisions, radios and computers. To illustrate the concept of technology obsolescence, Table 1.1 illustrates common WEEE separated into categories that are and are not typically considered to be e-wastes as well as their typical lifespans. Due to the hazardous and valuable components that make up e-wastes, they must be handled and recycled in specialized manners different from municipal and industrial waste. Aside from previously mentioned PM, e-waste can also contain significant concentrations of mercury, cadmium and lead – all of which can contaminate the environment and cause detrimental effects to the human body [6]. While it is true that valuable PM and other metals can be recovered from the recycling of waste electronics, the strict environmental codes and high labor costs of developed countries makes disposing of e-wastes in landfills or its exportation to developing countries with lax environmental regulations for recycling a more financially sound decision [7].

Table 1.1. List of some common Waste Electrical and Electronic Equipment (WEEE) and electronic waste (e-waste) items with typical life span and item weight (Adapted from Robinson (2009) with permission from Elsevier. Please refer to Fig C.1 for permission details).

Item	Weight of Item (kg)	Typical life (year)
<i>WEEE not normally considered e-waste</i>		
Computer	25	3
Facsimile machine	3	5
High-fidelity system	10	10
Mobile telephone	0.1	2
Electronic games	3	5
Photocopier	60	8
Radio	2	10
Television	30	5
Video recorder and DVD player	5	5
<i>WEEE not normally considered e-waste</i>		
Air conditioning unit	55	12
Dish washer	50	10
Electric cooker	60	10
Electric heaters	5	20
Food mixer	1	5
Freezer	35	10
Hair dryer	1	10
Iron	1	10
Kettle	1	3
Microwave	15	7
Refrigerator	35	10
Telephone	1	5
Toaster	1	5
Tumble dryer	35	10
Vacuum cleaner	10	10
Washing machine	65	8

The outsourcing of e-waste recycling can greatly harm the environment as developing and transitioning nations do not have the elaborate processing methods devised with safety in mind as does regions across Europe and North America. Often times electronic products contain myriad hazardous substances, most notably, lead, mercury, arsenic, cadmium, chromium and non-decomposable plastics that may release toxic dioxins [8]. Typical practices of processing e-

waste in China, India and Nigeria involves fuming plastics off cables to recover copper components, as well as leaching circuit boards by using acid baths to recover PM [8]. With the lack of disciplinary actions from environmental agencies for irresponsible waste disposal, often times waste leach solutions contaminated with toxic heavy metals will be dumped either directly into the ground or in nearby streams which then contaminate the surroundings of populated communities [8].

As the world's largest manufacturers and consumers of electrical and electronic equipment (EEE), Fig 1.1 illustrates that Asia consumed approximately 26.69 million tons of electronics in 2012 – about half of the global amount [9]. Fig 1.2 indicates that in 2014, Asia generated about 16 million tons of e-waste in the year alone and as Asian nations continue to industrialize and develop, standards of living will increase, causing the consumption of EEE and the eventual generation of e-wastes to proliferate [9]. To illustrate the effect technological advancements have on the production of e-wastes, it was estimated that in the 10 years between 1997 and 2007 approximately 500 million tons of computers were discarded in the United States and by the end of 2010, 610 million tons of computers became obsolete in Japan [10]. As the prices of electronics continue to decrease and are made more available with the advancement of technology, surely newer electronic gadgets are now being designed with planned obsolescence in mind to push consumers towards purchasing newer products [9]. With this increase of potentially hazardous wastes becoming a growing concern globally, the safe handling of obsolete EEE must not be overlooked to protect the health of the public and the environment.

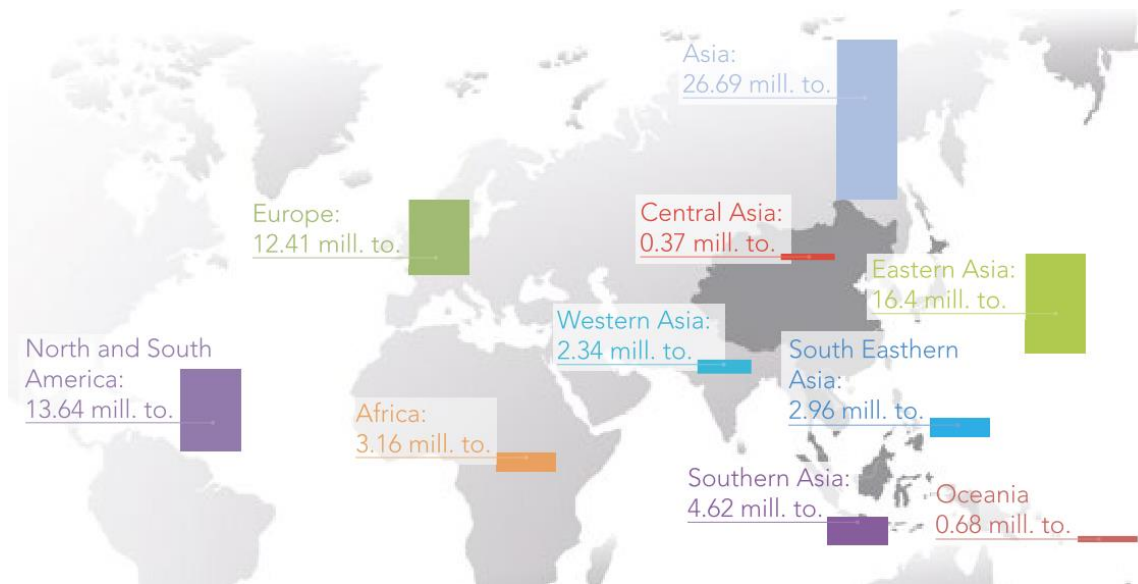


Fig 1.1. Global generation of Electrical and Electronic Equipment on the market in millions of tons in 2012 (Adapted from Honda et al. (2016) under creative commons. Please refer to Fig C.2 for permission details).

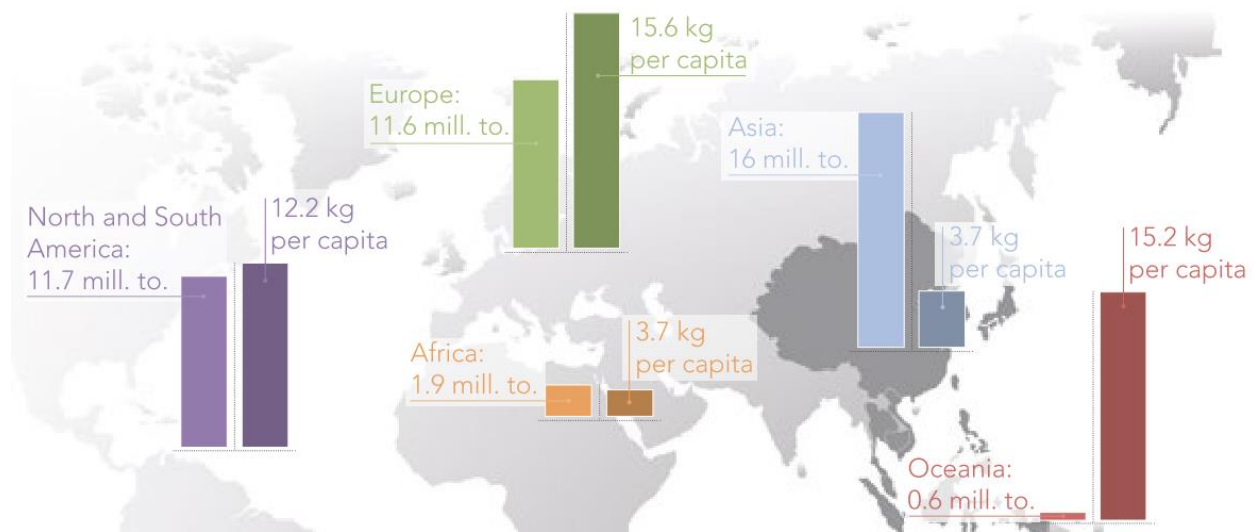


Fig 1.2. Global generation of electronic waste per capita in millions of tons in 2014 (Adapted from Honda et al. (2016) under creative commons. Please refer to Fig C.2 for permission details).

In addition to the problem of increased waste generation, the production boom of EEE also has potential to deplete the world’s natural resources. E-wastes by weight mainly comprises of approximately 60% metals and 15.21% plastics with various screen components making up another 11.87% [10]. Mobile phones contain anywhere from 60 to 64 elemental ingredients in minute amounts which are essential to the operation of the device [4]. In relation to this, the parts per million concentrations of typical elements found printed circuit boards (PCB) are exhibited

in Fig 1.3. Although gold and platinum have traditionally been regarded to have low supply risks due to its historically large geological reserves, its near universal use in the electronics and jewelry industry have potential to cause vulnerability to supply availability [11]. In the years between 2006 to 2015 there has been a steady decline in amount of gold found by miners, plunging as much as 85% over the decade [12]. To complicate matters, often times PM reserves are located within geopolitically unstable environments which adds a layer of difficulty in acquiring it [13]. Due to the issue of natural precious metal ores becoming progressively more difficult to obtain with the ever-increasing demand for electronic goods, great attention has been turned towards the recycling of precious metals.

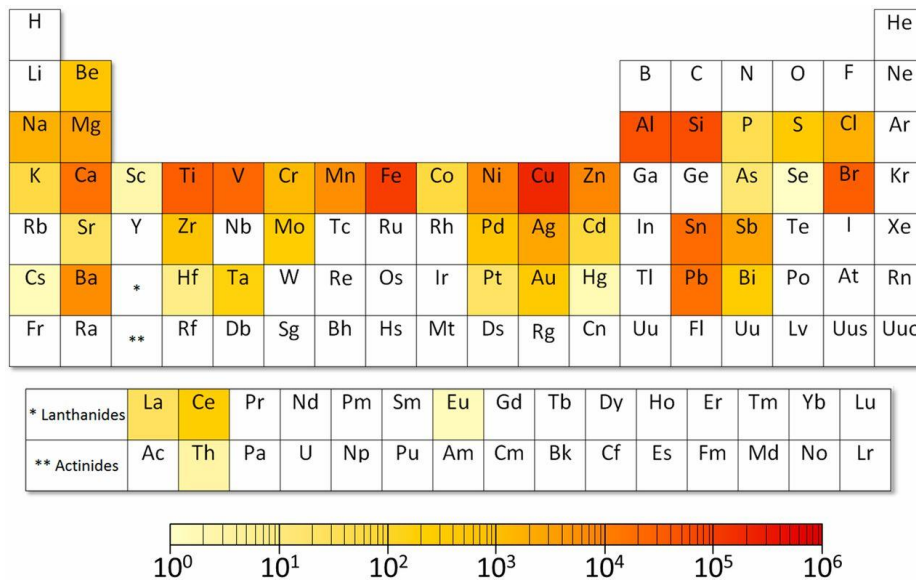


Fig 1.3. The concentration in parts per million of 44 elements typically found on printed circuit boards ranging from 10^0 to 10^6 parts per million (Reprinted from Graedel et al. (2015) with permission from Proceedings of the National Academy of Science of the United States of America. Please refer to Fig C.3 for permission details).

Obsolete PM containing objects such as spent catalysts, e-wastes and other sources have been referred to lately as “urban mines” and rightfully so due to their high metal concentrations [1]. While natural ores can contain anywhere from 1-30 ppm of PM, secondary sources may have concentrations up to 2000 ppm [1]. To further illustrate the high concentration of secondary sources, it has previously been reported that 1 ton of computer scraps can contain higher metal content than can be extracted from 17 tons of gold ore [1]. Not only would the standardized and environmentally regulated practice of recovering metals from e-wastes help to prevent toxic materials from entering the environment, it would also help generate financial gain. However,

conventional PM recycling including pyrometallurgical processing and hydrometallurgical methods such as solvent extraction, reduction of precipitates and adsorption with ion-exchange resins are expensive, time-consuming, laborious and creates secondary wastes [2].

The usage of biomass-based materials for metal adsorption from leach solutions, known as biosorption, can prove to be an environmentally friendly and economical alternative to conventional recovery methods. Properties found in biomass, whether microbial or plant-based have been shown to form ligand-substituted complexes with metallic ions. This concept is depicted in Fig 1.4 where a polyphenolic species commonly found in plant structures is shown forming a complex with Fe(III) ions [14]. In the present state of hydrometallurgical research, biosorption has gained notable traction. Fig 1.5 summarizes a PM recovery process using biosorption with crosslinked persimmon tannin (CPT) gel [5].

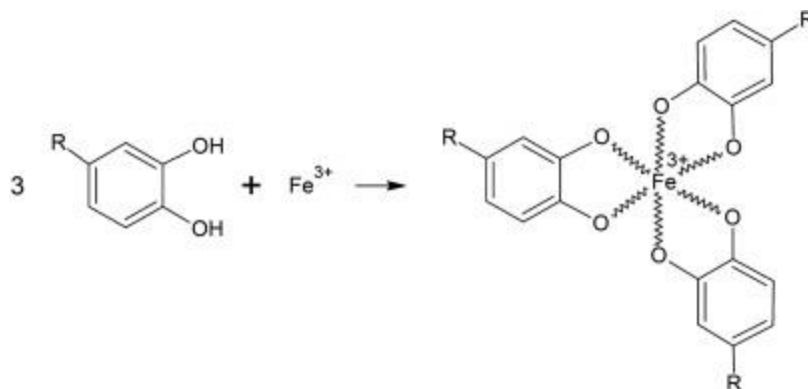


Fig 1.4. Proposed model for the complexation (indicated by serrated lines) between polyphenolic species and Fe(III) ions (adapted from Wang et al. (2015) with permission from Elsevier. Please refer to Fig C.4 for permission details).

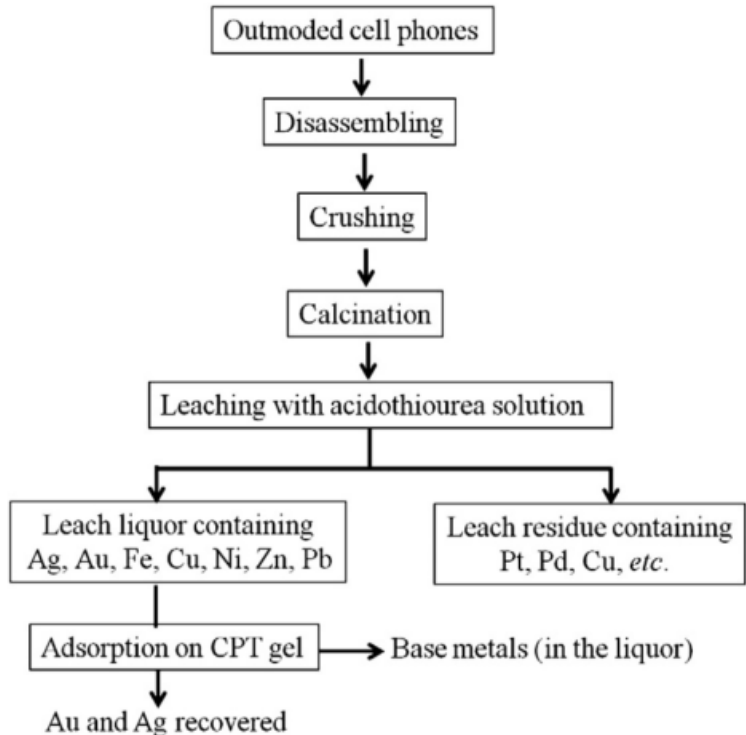


Fig 1.5. Flow chart for a typical method of recovering gold and silver via adsorption by crosslinked persimmon tannin gel (CPT) (Reproduced from Gurung et al. (2013) with permission from Elsevier. Please refer to Fig C.5 for permission details).

1.2 Knowledge gaps

From the study of present research done in the field of biosorption of PM, the following main knowledge gaps in the current status quo of hydrometallurgy research have been identified:

1. Most research is done using synthetic leach solutions derived from PM chloride salts and lab procured lixivants.
2. Although many research articles focus on the efficiency of biosorbents in recovering gold, few focus on PGMs such as platinum or palladium which are of higher value.
3. There are few research works done on the recovery of PM from industrial waste effluents which are primary sources of leached metal solutions.

1.3 Research objectives

The overall purpose of this thesis and its accompanying research work was to develop an effective biosorbent for recovering platinum and palladium from a secondary PM source. Specific objectives stemming from this are broken down as indicated below:

1. to select suitable biomass materials that can be found locally within Canada;
2. to prepare novel biosorbents from selected materials via immobilization methods previously reported;
3. to evaluate the efficacy of each biomass in recovering Pt and Pd from real leach solution and determine the optimal biosorbent;
4. to characterize the determined optimal biosorbents using FT-IR spectroscopy, CHNS content analysis, BET pore size analysis and particle size analysis;
5. to analyze the effect of various experimental parameters on the adsorption of Pt and Pd on the optimal biosorbent and conduct studies on its kinetic behavior, adsorption isotherm and thermodynamics.

1.4 Overall outline of the thesis

This thesis details the synthesis, characterization, experimental testing, results analysis and conclusion of the completed research as well as provide information for any context required for general understanding. Chapter 1 gives an introduction of the importance and demand for research work presented in the current thesis as well as outline knowledge gaps and objectives. Chapter 2 summarizes literature review in the field of biosorption, informing concepts that often arise with the research topic. Chapter 3 describes the experimental procedures, detailing the necessary materials, equipments and experimental methods used in the research work. Additionally, chapter 3 examines the characterization testing performed on the synthesized biosorbents and discusses their significance. Chapter 4 discusses the obtained experimental results and explains their significance in terms of biosorbent efficiency. Finally, chapter 5 concludes the thesis by summarizing the main findings of the research, pointing out any difficulties or limitations of the present research and provides suggestions for future research within the field.

CHAPTER 2: Literature Review

2.1 Mechanisms of metal biosorption

To properly understand the concept of biosorption, one must understand the components that are involved in its process. Dodson et al. [15] described the term “biosorption” as “the removal or binding of substances from solution by non-living bio-derived materials” which are referred to as biosorbents. However, in truth biosorption is difficult to define as various mechanisms are involved in the overall sorption process which includes, but are not limited to, adsorption, ion exchange, complexation, chelation and microprecipitation [16]. The general term of sorption itself is also defined as including the processes of absorption and adsorption which fundamentally differ. Adsorption is a phenomena in which interaction is defined as adhesion of gas, liquid or dissolved solid onto a surface whereas absorption is a process where a gaseous or liquid absorbate permeates or is dissolved by a liquid or solid absorbent [17]. For the scope of this thesis, the term “biosorption” will take upon the definition set by Dodson et al. and only refer to the adsorption of metallic ions onto the surface of biomass materials. In this thesis, the biochemical pathways between metal and adsorbent will not be considered.

As briefly mentioned in chapter 1, the key to biosorption from plant materials lies in the polyphenol content which is abundant in their structures. British chemist Edwin Haslam stated that in order to qualify as a polyphenol, a phenolic compound must [18]:

1. have water-soluble properties and must be found or derived from plants;
2. have molecular masses from 500 to 4000 Da;
3. possess anywhere from 12 to 16 phenolic hydroxyl groups;
4. include 5 to 7 aromatic rings per 1000 Da of molecular mass;

Polyphenols may exist in certain forms of organic polymers essential to the structural support of plants such as cellulose, lignin and tannin. Polyphenolic derivatives including flavonoids, carnosic acid and phenolic acid are also some examples of polyphenols commonly studied in biosorption research [14,19]. The chemical structure of lignin and tannic acid are displayed respectively in Fig 2.1 and Fig 2.2. Polyphenolic compounds are known to engage in redox reactions and can reduce Au(III) to elemental Au in their active sites [20]. For this reason,

polyphenols can demonstrate effective chelation with metal ions, typically with negatively charged hydroxyl groups [14].

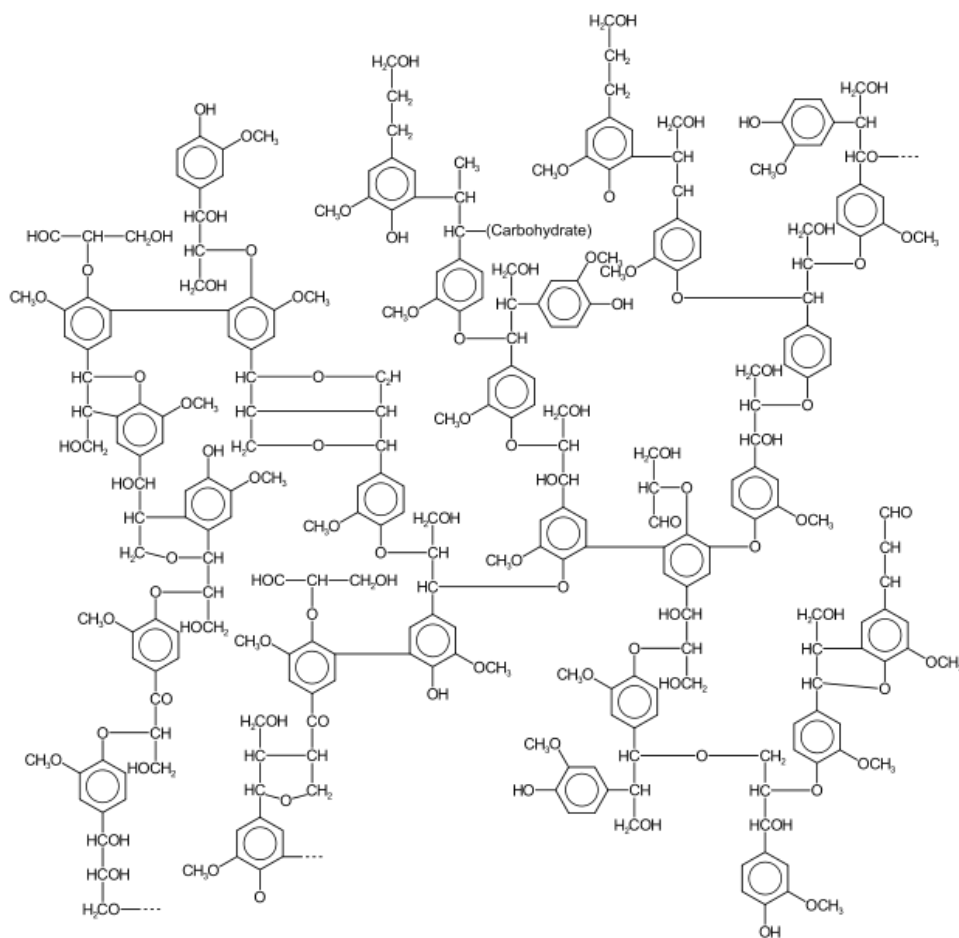


Fig 2.1. A proposed structure of lignin (by Karol Glqb (2007) under public domain. Please refer to Fig C.6 for permission details. Source: https://upload.wikimedia.org/wikipedia/commons/e/ee/Lignin_structure.svg).

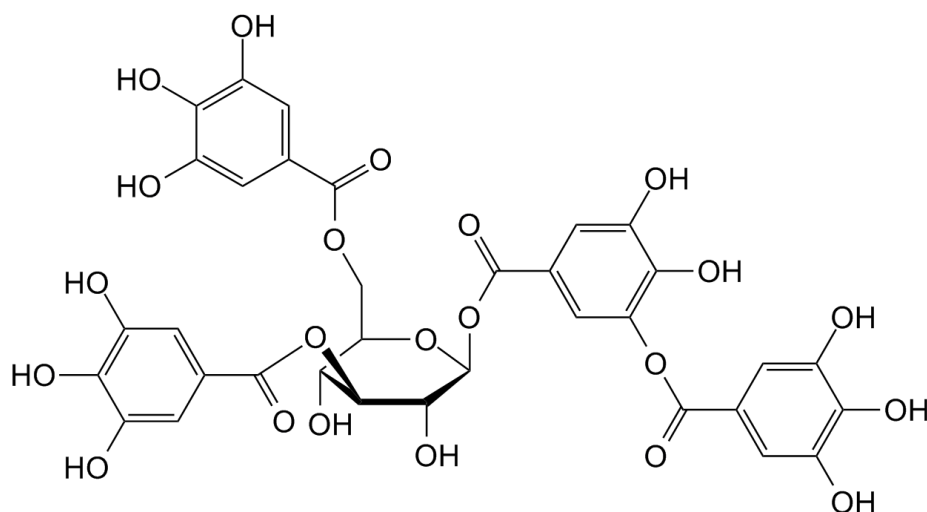
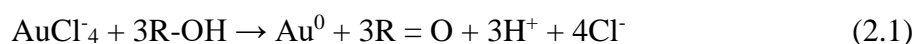


Fig 2.2. Structure of tannic acid, a form of tannin (by Michał Sobkowski (2008) under creative commons. Please refer to Fig C.7. Source: https://upload.wikimedia.org/wikipedia/commons/9/96/Tannic_acid.png).

In the same nature as hydroxyl groups, other functional groups such as carboxy, amino and thiol group can form complexes with metal ions. Plants are not the only type of biomass that can be used for biosorption as polysaccharides, proteins and lipids found on bacterial cell surfaces have also been found to be effective in recovering PM [21]. Effective biosorbents can be created by using fungi, yeast and cyanobacteria to form coordinate bonds with metal ions via intracellular uptake of metal through the cell surface and subsequent chemical transformation of the metal ion [21,22]. Whether the created biosorbent are microorganism-based or plant-based, the mechanism of biosorption may vary greatly.

In general, biosorption interactions can be explained as physical or chemical adsorption [2]. Physical sorption involves electrostatic interactions or ion-exchange between effective biosorbent functional groups and metal ions whereas chemical sorption includes chelation, microprecipitation and microreduction [23]. A common phenomenon occurring with the biosorption of Au(III) is the spontaneous reduction of the ion to elemental Au(0). In the case of tannin gel, this can occur from a redox reaction occurring between biosorbent and AuCl₄ species in which Au(III) is reduced and hydroxyl groups are oxidized to carbonyl groups [23]. The chemical reaction of this redox reaction is shown in Eq. 2.1 [23]:



Electrostatic interaction plays a key role in the case of PGM biosorption with Pt and Pd as focus. It was previously reported that in a study using glutaraldehyde cross-linked chitosan, the addition

of chloride and nitrate ions could decrease the uptake of Pt due to competition with negatively charged Pt ions for positive sites on the surface of the adsorbent, proving that the mechanism of electrostatic binding is present [2]. It should be noted that these two mechanisms are specific to their respective biosorbents, as the mechanisms responsible for PM sorption will depend largely on the type of sorbent used [23].

2.2 Lignin content of wheat straw, canola meal and wood bark

Lignin is a major structural component present in plant cell wall which supplements cellulose [24]. Lignin can comprise up to 10-30% of total content in wood and is unique in its complicated molecular structure, containing different monomers of varying functional groups including hydroxyl, ether and carbonyl groups [25]. Previous research works have shown that lignin-based biosorbents are effective in recovering PM [25–27]. Raw, un-immobilized lignin was able to exhibit a maximum Au(III) adsorption capacity of 6.0 mol/kg at 40°C, proving that even without any modifications, the polyphenol is able to adsorb a significant amount of PM [27]. For this research, three plant-based biomasses were utilized to create novel biosorbents, those being wheat straw (WS), canola meal (CM) and wood bark nuggets (WB). Wheat is a major agricultural product from Saskatchewan and for that, it was selected as a biomass for the current thesis. WS is a major byproduct in wheat grain production however, it can contain up to approximately 21% lignin content, making it a potentially effective biosorbent for PM recovery [28].

Rapeseed, also known as canola, is another major agricultural product from Saskatchewan and is widely extracted for its oil. After oil extraction, the residual canola meal is often used as animal feed due to its high protein content of at least 36% [29]. The typical composition of CM as used in animal feed is displayed in Table 2.1. CM is comprised of 8% lignin, which is regarded as a rather high amount when compared to other categories of residual products, such as soybean meal, which contains only 1% lignin [24]. Al-Asheh and Duvnjak [30] have previously reported findings that raw CM was effective in recovering copper, zinc and cadmium ions from leach solution with the content of protein and phytic acid hypothesized as playing a major role in adsorption. Along with the presence of lignin, it can be predicted that the protein content of CM can greatly aid in recovery of PM.

Table 2.1. Typical component values of canola meal in animal feed with North American and Export standards (Adapted from Newkirk (2009) with permission from the Canola Council of Canada. For written permission to use please refer to Fig C.8).

Characteristics (as fed)	Canada and US	Export
Protein, % minimum (set by Canadian Oilseed Processors Association or industry standard at time of production)	36	
Fat (oil), % typical minimum	2	
Protein + fat, % minimum		37
Moisture + fat, % maximum		15
Moisture, % maximum	12	12
Crude fiber, % maximum	12	12
Glucosinolates, $\mu\text{mol/g}$ maximum	30	30
Sand and/or silica, % maximum		1
Screen analysis (pellets), % retained on 2 mm screen		90

Bark, the outermost layer of woody plants, is a byproduct of the wood processing industry and typically comprises approximately 9-15% of a wood log by volume [31]. Fig 2.3 shows the cross-section diagram displaying the bark in respect to a typical tree trunk. WB is often used as a soil conditioner, for this purpose it is referred as mulch and can contain approximately 44% lignin or more depending on the type of wood [28,31]. At the time of writing of this thesis, there is no known research that has been conducted on the usage of WB and WB-derived biosorbents for PM recovery. However, due to its very high lignin content, it can be hypothesized that such biosorbents would be the most effective out of the three base biomasses studied herein.

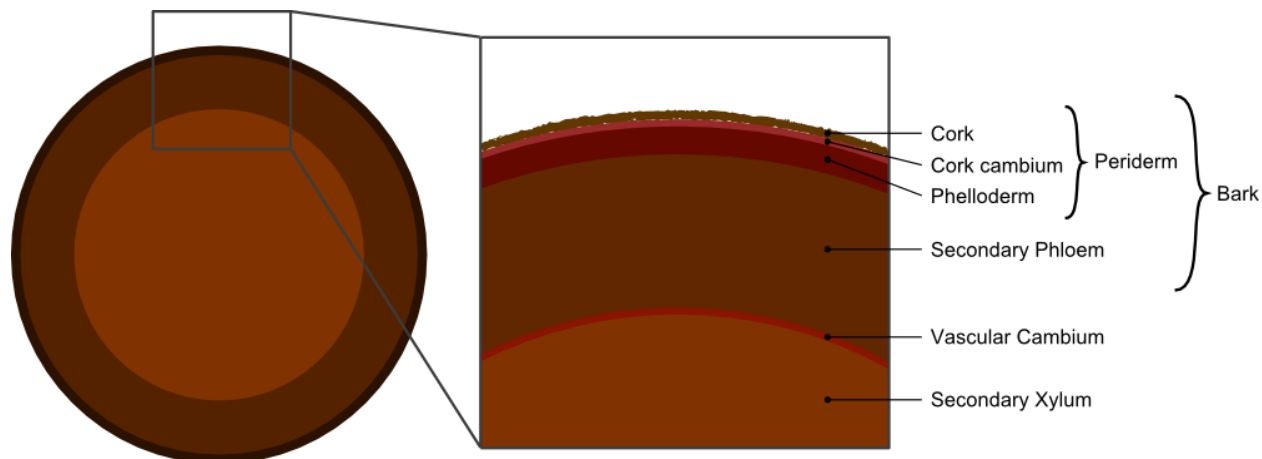


Fig 2.3. Cross-sectional diagram of a tree. The bark can be found in the outset layer of the tree (by Brer Lappin (2010) under the public domain. For permission details please refer to Fig C.9. Source: https://upload.wikimedia.org/wikipedia/commons/9/9b/Tree_secondary_components_diagram.png).

2.3 Conventional methods of recovery and advantages of biosorption

PM recovery can be conducted via two main paths: pyrometallurgy and hydrometallurgy. In pyrometallurgical methods, processes include the incineration, smelting, converting and refining of e-waste among other steps and is the standard method of recovering PM from secondary sources since the past few decades. During the process, wastes are first incinerated in a furnace or molten bath to remove any plastic components, then the remaining refractory oxides forms a slag phase and metal oxides [6]. The pyrometallurgical recycling of e-waste is commercially available and facilities exist all over the world to recover PM and other non-ferrous metals. The technology has been implemented in a refinery plant in Belgium which was reportedly able to treat up to 250,000 tons of wastes per annum [6]. However, pyrometallurgical methods are disadvantageous due to long settling times that are required to separate slag and metal collector [1]. The operating temperatures are also very high at the range of 1800-2000°C which requires excessive amounts of energy to maintain. Additionally, pyrometallurgical methods usually result in the undesired partial separations of PM. Due to these reasons, pyrometallurgy usually requires further hydrometallurgical or electrochemical processing to overcome any limitations of metal value upgrading [1].

Due to the issues related with pyrometallurgical processing, hydrometallurgical methods for the recovery of PM is now widely used by researchers and industry experts alike. Hydrometallurgy is advantageous due to its low capital requirement, ease and flexibility of operation and overall environmental sustainability when compared to pyrometallurgy [32]. In the

hydrometallurgical process, the recycling of PM begins with the leaching of solid e-wastes and other secondary sources by adding into a lixiviant. During leaching, PM containing sources are introduced into a tank containing the leaching agent where the metal is then dissolved from the ore or secondary source via complexation, forming a pregnant leach solution (PLS) from which PM can be extracted by further processing either through addition of precipitating agents or via electrowinning to reduce metallic ions into a usable form [33].

Traditionally, the usage of cyanide as a leaching agent for gold has gained widespread usage in not only the metal recovery industry, but in the mining industry in general [34]. Although highly effective and having been the industry standard since its first major industrial success in 1889, cyanide's toxic nature has caused industrial concerns to arise from numerous environmental disasters that have occurred over the years. Cases of industrial accidents involving cyanide contamination are usually a result from chemical leakage through tears, punctures or spillage from tailing storage areas and solution ponds that caused severe consequences [33]. Of all the environmental disasters associated with the mining industry, the collapse of the Guyanese Omai mine tailings dam in 1995 which released 2.9 million m³ of cyanide into the Omai river demonstrated just how devastating the usage of cyanide can be for surrounding communities [33]. To prevent such environmental catastrophes from happening in the future, other alternatives have been researched for their effectiveness as lixiviants in the leaching of PM.

Non-cyanide lixiviants such as aqua regia, thiourea, thiosulfate and acidic halide solutions have all gained attention within the industry for use in PM leaching, with usage of thiosulfate and thiourea being regarded as the most easily applicable alternatives [6]. As of recently, the usage of hydrochloric acid as a leach solution in the presence of chlorine gas has been regarded as a more advantageous and benign method of PM leaching [1]. A summary detailing the various possible alternatives to cyanide and their typical operation condition is showcased in Table 2.2 [33]. New research on the process of bioleaching has also introduced the usage of free cyanide (CN⁻) producing microorganisms as a viable low cost and environmentally friendly alternative to using liquid leaching agents. In their research, Is Bıldar et al. [35] were successful in developing a two-step bioleaching process of gold and copper from scrap PCB via the usage of microorganisms, achieving 44% and 98.4% leaching efficiency respectively.

Table 2.2. Various possible alternatives to cyanide as a leaching agent, their operating properties and extent of research and level of commercialization (Adapted from Hilson & Monhemius (2006) with permission from Elsevier. Please refer to Fig C.10 for permission details).

Reagent type	Concentration range	pH range	Basic chemistry	Research level	Extent of commercialisation
Ammonia	High	8–10	Simple	Low	Pilot tests, +100 °C
Ammonia/cyanide	Low	9–11	Simple	Extensive	Applied to Cu/Au ores
Ammonium thiosulphate	High	8.5–9.5	Complex	Extensive	Semi-commercial
Slurry CN-electrolysis	Low	9–11	Simple	Historical	Limited historical
Sodium sulphide	High	8–10	Simple	Low	Geological interest only
Alpha-hydroxynitriles	Moderate	7–8	Fairly simple	Fairly popular	None
Malononitrile	Moderate	8–9	Fairly complex	Low	None
Alkali cyanoform	Poorly defined	9?	Poorly defined	Low	None
Calcium cyanide	Poorly defined	9?	Poorly defined	Low	none
Alkaline polysulphides	High	8–9	Poorly defined	Low	None
Hypochlorite/chloride	High chloride	6–6.5	Well defined	Extensive	Historical and modern
Bromocyanide	High	6–7	Poorly defined	Historical	Historical
Iodine	High	3–10	Poorly defined	Low	None
Bisulphate/sulphur dioxide	High	4–5	Fairly simple	Low	None
Bacteria	High	7–10	Fairly complex	Low, growing	None
Natural organic acids	High	5–6	Fairly complex	Low	None
DMSO, DMF	Poorly defined	7	Poorly defined	Very low	None
Bromine/bromide	High	1–3	Well defined	Low	Historical
Thiourea	High	1–2	Well defined	Fairly popular	Some concentrates
Thiocyanate	Low	1–3	Well defined	Low	None
Aqua regia	High	Below 1	Well defined	Low	Analytical and refining
Acid ferric chloride	High	Below 1	Well defined	Low	Electrolytic Cu slimes
Ethylene thiourea	High	1–2	Poorly defined	Very low	None
Haber process	Poorly defined		Proprietary	One entity	None
“Bio-D leachant”	Poorly defined		Proprietary	One entity	None
High temperature chlorination	High	6–7	Simple	historical	Historical

After the leaching process, aqueous PM ions can be recovered from PLS using various hydrometallurgical methods such as solvent extraction, ion-exchange or via adsorption with activated carbon. Solvent extraction, also known as liquid-liquid extraction is utilized in the processing of a wide variety of metals and is characterized by the application of chemical extractants such as MIBK, Cyanex 471X, Cyanex 923 or Aliquat 336 amongst others [36]. These extractants can selectively isolate different PM depending on the metal content of PLS and the base lixiviant. Despite its popular and established usage, solvent extraction leaves behind secondary waste effluents that require further treatment prior to disposal making this method an unattractive one for the truly environmentally and financially conscious [37].

Ion-exchange resins and activated carbon are some existing agents that are commonly used as of present for the recovery of PM. Much like biosorbents, ion-exchange resins and activated carbon adsorbents recover metals via physical or chemical interactions depending on the type of adsorbent, properties of desired PM, content of PLS or operating condition [38]. These sorbents also extract metal ions through complexation and in a special case for activated carbon – high surface area and microporosity [15]. However, the usage of commercial ion-

exchange resins, besides their high costs, can potentially have negative impacts on the environment as they are petroleum-derived and thus not biodegradable [39]. A major disadvantage in the usage of activated carbon are their tendencies to suffer from diffusion limitations in scenarios with bulky adsorbates [15].

The development of biosorption methods are a potential in filling the gap required in the current PM recycling market as a more cost effective, environmentally friendly and in some cases, better performing method to extracting metal ions from PLS. As shown in Fig 2.4, in an experiment conducted by Inoue et al. [39], novel grape-seed based biosorbent Gravinol-GA₅₆₀ exhibited high selectivity towards Au when compared to conventional ion-exchange resin S1A0A and outperformed the resin in the total adsorption percentage of Au recovered by 4%.

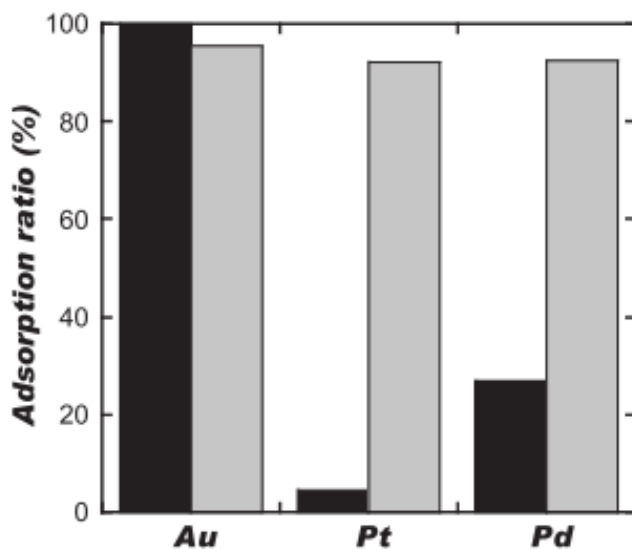


Fig 2.4. The adsorption ratios of gold, platinum and palladium at equilibrium using grape-seed based biosorbent Gravinol-GA₅₆₀ (black bar) versus conventional ion-exchange resin S1A0A (grey bar). It can be observed that Gravinol-GA₅₆₀ exhibited superior selectivity and recovery efficiency towards gold (Adapted from Inoue et al. (2015) with permission from Elsevier. Please refer to Fig C.11 for permission details).

The advantage of biosorbent use over conventional adsorbents is further exhibited by Khunathai et al. [40] where microalgal residue and modified microalgae biosorbents were observed to be effective in recovering Pd and Pt from PLS containing base metals as exhibited in Fig 2.5 [40]. However as demonstrated in Fig 2.6, by comparison, commercial ion-exchange

resin DIAION WA20 and activated carbon were unable to exhibit satisfactory selectivity towards the two PGM as significant amounts of Zn was also recovered [40].

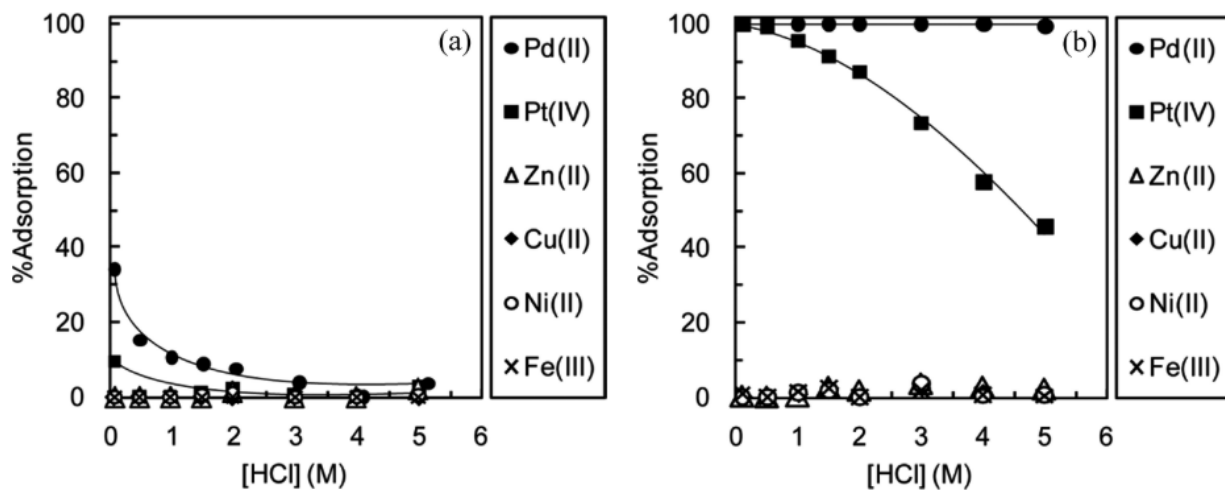


Fig 2.5. Adsorption percentage of various metals in pregnant leach solution on unmodified microalgal residue (a) and dithiooxamide-immobilized microalgae (b) in varying hydrochloric acid concentrations (Adapted from Khunathai et al. (2012) with permission from Taylor and Francis. Please refer to Fig C.12 for permission details).

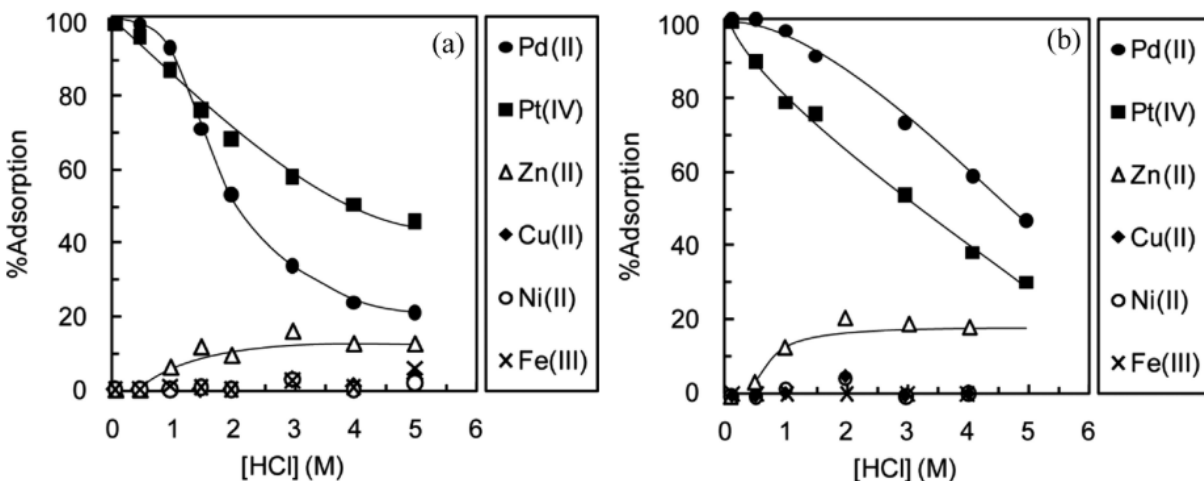


Fig 2.6. Adsorption percentage of various metals in pregnant leach solution on ion-exchange resin DIAION WA20 (a) and activated carbon (b) in varying hydrochloric acid concentrations (Adapted from Khunathai et al. (2012) with permission from Taylor and Francis. Please refer to Fig C.12 for permission details).

For an adsorbent to be truly efficient, its reusability must be accounted for. Desorption is a phenomenon defined by the release of one substance from another [17]. In the context of this research, desorption refers to the regeneration of biosorbents previously loaded with metal content however, desorption experiments have not been conducted for study in this thesis but should be considered for future projects [16]. For desorption to occur, the concentrated and

purified desired metal must be introduced to an eluent solution where metal will be released from the surface of the biosorbent into solution and can be reduced into usable form either via electrowinning or precipitation [1]. The selection of eluent solution for desorption experiment is important as they must be economically sound, environmentally friendly and non-destructive towards the biosorbent product to ensure its longevity for continued use. Previously, Park et al. [41] were successful in restoring Pd(III) and Au(III) loaded glutaraldehyde-crosslinked chitosan beads by performing desorption with 5 M HCl eluent solution. This desorption process was able to extract pure Pd ions into solution which can then be transformed into usable form by further addition of reduction agents to induce metal precipitation [41].

The above-mentioned experiments are just some examples of the clear advantages that biosorbent utilization has over conventional adsorbents particularly for their comparatively cheap operating costs in addition to a non-toxic and environmentally sustainable nature. Additionally, previous research conducted on biosorbents which were created from biomass sources largely available in Canada including paper [42], wood pulp [27] and wheat straw [26] demonstrates potential for biosorption to be adopted domestically by industries within the nation. However, as can be observed from Fig 2.5(a), often unmodified raw biosorbents show poor adsorption efficiency. Luckily, researchers have developed solutions to this problem and have been successful in bringing out the full potential of biomasses through a process called immobilization.

2.4 Significance of immobilization

The process of immobilization is defined in two parts: first by the incorporation of novel functional groups beneficial for metal adsorption onto the polyphenolic structure of biomass and the subsequent cross-linking of such structures or vice versa [2]. The reaction of biomass with substances such as dithiooxamide (DTO) [40], polyethyleneimine (PEI) [43,44] and dimethylamine [26] are just some examples of different methods researchers have used to incorporate functional groups with high metal ion affinity – particularly thiol and amino groups – to increase adsorption efficiency and even selectivity. Crosslinking of polyphenolic groups in immobilization can also improve the suitability of biomass in reaction mixtures by improving mechanical strength, rigidity and by making the biosorbent water insoluble [15,39].

The synthesis of novel biosorbents created for the thesis herein was modeled after three immobilization methods developed by Kunathai et al. and Parajuli et al. using DTO [40], ethylenediamine (EN) and primary amine (PA) [25]. As briefly mentioned in section 2.3, Khunathai et al. [40] were successful in creating a novel biosorbent by immobilizing microalgal residue with DTO which contains sulfur in place of oxygen in an oxamide group, as shown in Fig 2.7. By immobilizing microalgal residue with DTO, the biosorbent was able to achieve adsorption percentages of 85% and 96% for Pd(II) and Pt(IV) respectively [40].

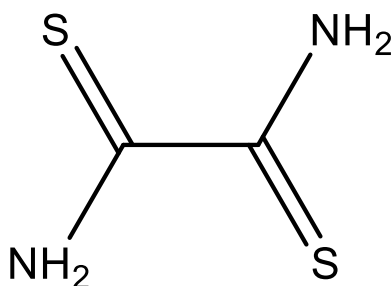


Fig 2.7. Structure of dithiooxamide (DTO).

In their research, Parajuli et al. [25] examined the effects of ethylenediamine and primary amine immobilization via ammonia to examine whether increased amine functional groups will improve efficiency of adsorption on PM. Each of the immobilization paths were separated into three parts. First, lignin-rich dried wood powder was subject to the addition of a phenolic group to create lignophenol. The lignophenol was then crosslinked using paraformaldehyde and sulfuric acid then finally, crosslinked lignophenol was reacted with either ethylenediamine or ammonia to create EN-lignin and PA-lignin respectively [25]. Experimental results revealed that despite having two amino groups instead of one as per the case of PA-lignin, EN-lignin did not exhibit a significantly higher adsorption capacity as the degree of amination in PA-lignin was higher than EN-lignin.

It can be theorized that the effectiveness of DTO, EN and PA as well as other thiol, hydroxyl or amino group containing immobilizations stems from the chemical concept of Hard-Soft Acid-Base (HSAB theory) proposed by American inorganic chemist Ralph Pearson [45]. Fig 2.8(a) and Fig 2.8(b) display a typical trend for hard and soft acids and bases. PM are considered soft electron accepting Lewis acids which contain positive charges whereas nitrogen and oxygen are hard electron donating bases and thus these two components are naturally drawn

towards each other. Although sulfur atoms are soft bases when compared to oxygen, their nucleophilic nature makes them effective in attracting PM.

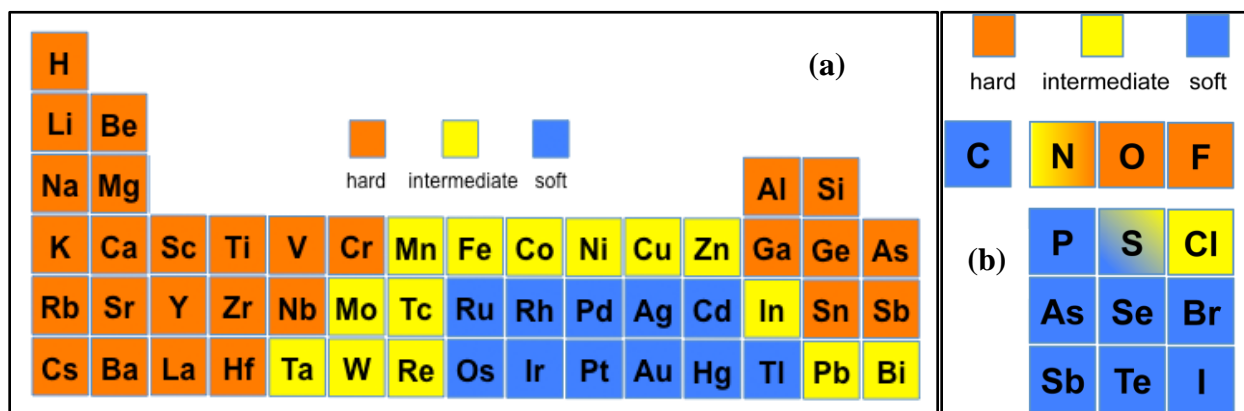


Fig 2.8. Trends of hard, soft and intermediate acids (a) and bases (b) (by Tem5psu under creative commons. Please see Fig C.13 and Fig C.14 for copyright details. Source: https://en.wikipedia.org/wiki/HSAB_theory#/media/File:Hardsoftacids.png and https://en.wikipedia.org/wiki/HSAB_theory#/media/File:Hardsoftbases.png).

2.5 Effect of experimental conditions

Biosorption research in the present is conducted mostly via batch method, allowing researchers to observe differences in adsorption efficiency depending on experimental conditions. Due to this nature of small-batch research, researchers can obtain the optimal experimental conditions required for maximum PM adsorption efficiency. Some commonly studied experimental condition variations include temperature, solution pH, sorbent dosage and initial concentration. It has been observed that since the adsorption of PM on many adsorbents are endothermic in nature, common trends point towards higher operating temperatures resulting in more efficient PM adsorption and recovery. Gurung et al. [5] observed that crosslinked persimmon tannin adsorbent exhibited higher Au recovery when temperature was increased from 30°C to 45°C. However, once temperature is increased to over 60°C recovery decreases. It was hypothesized that slight temperature increases are beneficial in activating reactant species and therefore propel extraction but large temperature increases can suppress this phenomena [5].

Factors important to the progression of redox reactions such as hydrolysis, precipitation and dissociation are all greatly dependent on the pH of leach solution during biosorption [46]. Because of this reason, proper solution pH plays an essential role in ensuring effective ion

sorption and therefore, PM recovery. Since pH is dependent upon the concentration of H^+ ions which in addition to being Arrhenius acids are also Lewis acids, their significant concentration and consequent low pH can cause competition between H^+ and PM ions, thus lowering adsorption efficiency [47]. In general, a solution pH range of 1 - 5 is particularly effective for the adsorption of gold because after leaching, gold ions are present in anionic forms such as $[AuCl_4]^-$ (in hydrochloric acid), $[Au(CN)_4]^-$ (in cyanide), $[Au(S_2O_3)_2]^{2-}$ (in thiosulfate) or others depending on lixiviant [2]. As demonstrated in Fig 2.9, Rubcumintara [37] observed that the solution for optimal Au recovery had a pH of 2 in an experiment using modified sugarcane bagasse biosorbent. At a higher pH of 4, the biosorbent required longer time to reach equilibrium and at pH 6, % Au recovery decreased by half. This phenomenon is hypothesized to be from the precipitation of $AuCl_4^-$ from solution at higher pH decreasing the total amount of aqueous Au available for recovery [37].

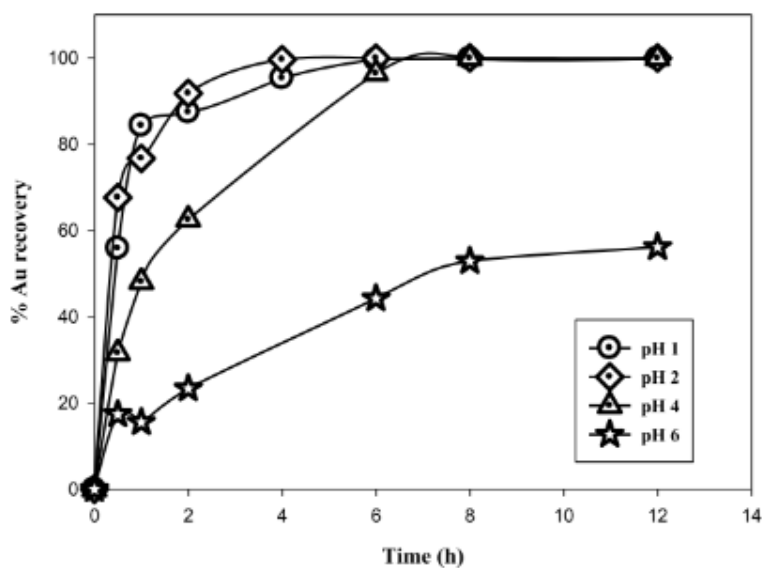


Fig 2.9. Effect of pH on recovery of Au at varying times for modified bagasse biosorbent (Adapted from Rubcumintara (2015) with permission from International Journal of Chemical Engineering and Applications. Please refer to Fig C.15 for written permission).

The amount of sorbent dosage used to reach optimal efficiency is an important criterion to understand for any biosorption experiment as this knowledge can save researchers and industry adopters the need for excessive adsorbent purchase or production for the desired amount of PM recovery. Additionally, sorbent dosage variations can strongly influence biosorption progression. Generally, increasing sorbent dosage usually increases the amount of adsorbed

solute due to the increase of surface area and thus binding sites available for PM ion adsorption [2]. In their experiment which studied the adsorption effects of kraft mill lignin, Adhikari et al. [27] observed that the Solid-Liquid (S/L) ratio (ratio of weight of biosorbent to the test solution volume) of 0.8 g/L caused the amount of Au remaining in solution to approach 0 ppm as displayed in Fig 2.10. This signifies that at 0.8 g/L S/L ratio, enough sorbent is used to achieve optimal Au recovery. However, when sorbent dosage is excessively high poor solute uptake may result from the lack of remaining available metal ions [2]. In addition to this, it was also theorized that interference between binding sites on biosorbent surface may occur, further contributing to low PM recovery [2].

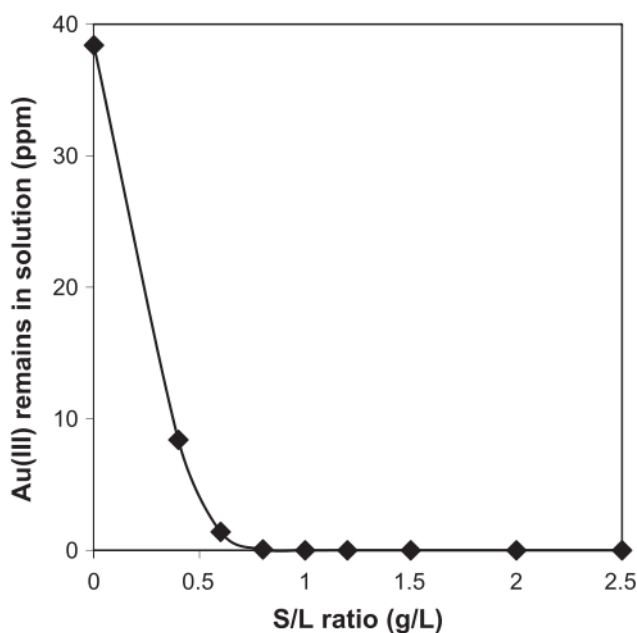


Fig 2.10. The effect of adsorbent dose on the amount of gold (III) remaining in solution using kraft mill lignin biosorbent. Solid-Liquid (S/L) ratio refers to the weight of biosorbent used per test solution volume (Reproduced from Adhikari et al. with permission from Elsevier. For additional permission details please refer to Fig C.16).

Initial PM concentration in leach solution is also a parameter that can affect solute uptake. Higher initial PM ion concentration generally results in higher adsorption percentage onto biosorbent due to the larger amounts of PM available for uptake while the opposite is true for solutions with low PM concentration. However, as initial PM concentration increases, the amount of available binding sites on biosorbent surface will also decrease accordingly as adsorption occurs [2]. Using modified chitosan resin biosorbent, Fujiwara et al. [19] demonstrated that increasing initial concentration in solution was able to increase Au(III)

adsorption up to a threshold of 2000 mg/L. However, concentration increase past this threshold resulted in a decrease in Au(III) recovery [19]. Modified sugarcane bagasse biosorbent displayed similar results as although recovery approaches 100% at an initial Au(III) concentration of 500 mg/L, further concentration increase to 800 mg/L decreased Au recovery to 93% [37].

2.6 Adsorption isotherm and thermodynamics

To understand the mechanism of adsorption, researchers utilize adsorption models to predict reaction outcomes from experimental data. Several types of adsorption models have been developed over scientific history with the most commonly used being the Langmuir, Freundlich, Temkin and Dubinin-Radushkevich isotherm models [48]. Biosorption models can be applied to experimental data by fitting data points generated at reaction equilibrium using information on the concentration of remaining metal ion in solution and the amount of desired metal ions that were adsorbed onto adsorbent surface [49]. For the scope of this research, only the Langmuir and Freundlich adsorption isotherms were analyzed.

The Langmuir adsorption isotherm was first presented by American scientist Irving Langmuir in 1918 and describes the adsorption of sorbate on adsorbent binding sites as monolayer and homogenous with uniform energy throughout [50]. The model simply assumes that despite the close proximity of adsorbed species on adsorbent surface, there is no interaction which occurs between them [2]. Eq. 2.2 details the Langmuir adsorption isotherm:

$$q_e = \frac{q_{max}K_L C_e}{1 + K_L C_e} \quad (2.2)$$

q_e describes the quantity of PM acquired per gram of biosorbent at equilibrium in mg/g, C_e is the equilibrium concentration of metal remaining in solution in mg/L, q_{max} represents the maximum adsorption capacity achieved by adsorbent in mg/g and K_L is the Langmuir equilibrium constant between adsorption and desorption in L/mg [2,47,48]. An example of a Langmuir plot from research by Sari et al. [47] is exhibited in Fig 2.11:

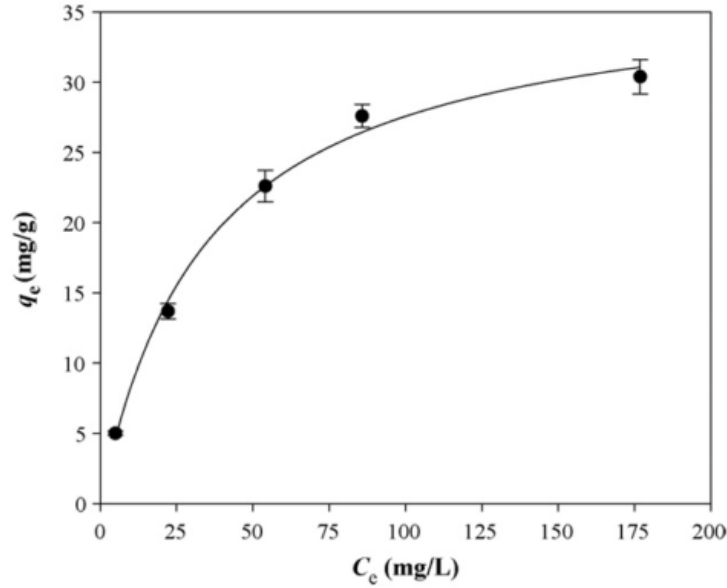


Fig 2.11. Langmuir isotherm plot of palladium (II) adsorption by moss biomass at equilibrium with $R^2 = 0.994$. C_e represents the concentration of metals remaining in solution at equilibrium and q_e is the quantity of PM acquired per gram of used biosorbent (Reproduced from Sari et al. (2009) with permission from Elsevier. For additional permission details, please refer to Fig C.17).

Unlike the Langmuir model which assumes a monolayer PM distribution with uniform energy, the Freundlich adsorption isotherm developed by German chemist Herbert Freundlich, describes the adsorption of PM on adsorbent surface as multilayer in fashion with a non-uniform and heterogenous energy distribution [51]. Also, unlike the Langmuir adsorption isotherm, the Freundlich model accounts for a scenario where adsorbed metal species interact with each other in adsorbent binding sites [19]. Eq. 2.3 expresses the Freundlich adsorption isotherm:

$$q_e = K_F C_e^{\frac{1}{n}} \quad (2.3)$$

Where K_F is a Freundlich constant which is related to the capacity of biosorption and n is a parameter which varies the heterogeneity of adsorbed material to the intensity of biosorption [47]. Again, using research by Sari et al. [47], an example of the Freundlich isotherm plot is displayed in Fig 2.12:

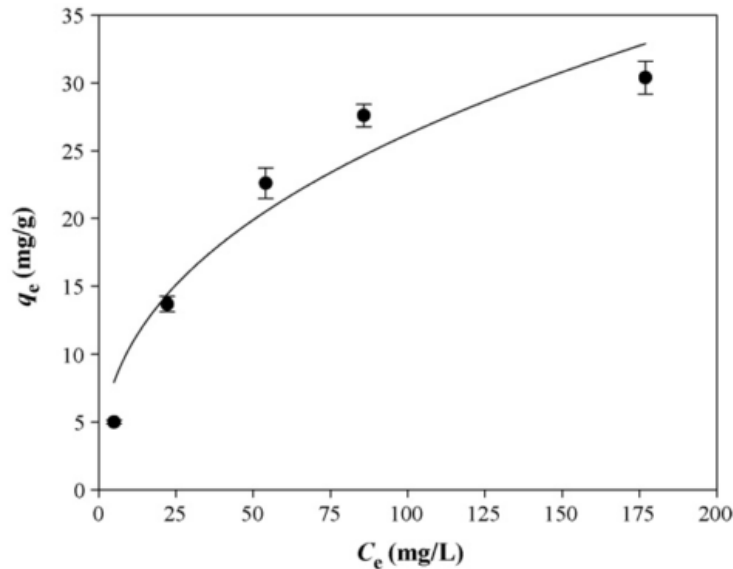
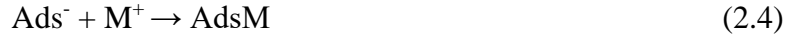


Fig 2.12. Freundlich isotherm plot for biosorption of palladium (II) on moss biomass at equilibrium with $R^2 = 0.935$. C_e represents the concentration of metals remaining in solution at equilibrium and q_e is the quantity of PM acquired per gram of used biosorbent (Reproduced from Sari et al. (2009) with permission from Elsevier. Please refer to Fig C.17 for permission details).

Examples from Fig 2.11 and Fig 2.12 reveals the R^2 fitting values of the Langmuir isotherm and Freundlich isotherm plot to be 0.994 and 0.935 respectively. This information signifies that the moss-based biosorbent studied by Sari et al. satisfies the Langmuir isotherm model over the Freundlich isotherm model due to the higher obtained R^2 value [47]. Although seemingly simple, the fitting of experimental data to both isotherm models can help other researchers hypothesize that the adsorption behavior of moss biomass is most likely monolayer and homogenous in nature with uniform energy distributions.

The study of activation energy from data obtained from biosorption experiments is also an important predictor for adsorption behavior as it can indicate whether adsorption processes occur via chemical reaction (chemisorption) or physical interactions (physisorption). Chemisorption has been defined as a form of adsorption “in which the forces involved are valence forces of the same kind as those operating in the formation of chemical compounds”, meaning that the adherence of metal to adsorbent surface is governed by chemical interactions which is typically irreversible [52]. On the other hand, physisorption is a process of adsorption in which intermolecular van der Waals forces are responsible for the interaction between metal and adsorbent which may be reversible [16]. A simple chemical reaction of chemisorption and

physisorption in the context of biosorption between biosorbent (Ads) and metallic ion (M⁺) to form metal loaded biosorbent (AdsM) are shown below in Eqs. 2.4 and 2.5 respectively:



Eq. 2.6 represents a linear form of the Arrhenius equation which is used to calculate activation energy (E_A):

$$\ln k_1 = \ln A - \frac{E_A}{R} \left(\frac{1}{T} \right) \quad (2.6)$$

Where R represents gas constant (usually 8.314 J/mol K), k₁ represents a rate constant and A signifies the Arrhenius constant. Typical values for physisorption can be up to 4.2 kJ/mol which is quite low as energies required for physical interactions are generally weak due to the nature of intermolecular forces [19]. Higher activation energies between 8.4 - 83.7 kJ/mol or above usually indicates that the forces required for chemical bonds to proceed are present for the interactions between adsorbent and metallic ions and thus adsorption proceeds via chemisorption [37].

Thermodynamic parameters in reference to the standard state, including entropy (ΔS°), enthalpy (ΔH°) and Gibb's free energy change (ΔG°) can also provide information on biosorption behavior to researchers and can be calculated via Eq. 2.7 and 2.8:

$$\Delta G^\circ = -RT \ln K_C \quad (2.7)$$

$$\ln K_C = \frac{\Delta S^\circ}{R} - \frac{\Delta H^\circ}{RT} \quad (2.8)$$

R again represents the universal gas constant (8.314 J/mol K), T is the temperature (in kelvins) and K_C signifies the equilibrium coefficient [47]. ΔS° measures the extent of order or lack thereof in a system and negative values suggest that a decrease in randomness, and therefore increased order is occurring [3]. ΔH° which describes the heat content of a system, indicate an exothermic (heat releasing) or endothermic (heat absorbing) adsorption process depending on negative or positive values calculated respectively [3,47]. ΔG° measures the favorability of an adsorption process given a constant temperature and pressure in the system (G = f(T,P)) and a negative calculated value indicates that biosorption is spontaneous in nature and therefore, thermodynamically feasible [3].

2.7 Summary of literature review

In chapter 2, the mechanisms and operational parameters of metal biosorption was explained along with a comparison of the usage of biosorption and its advantages versus conventional recovery methods. Plant materials contain structural and functional organic polymers that contain polyphenolic groups, of which have shown previously reported efficacy in adsorbing metal ions in solutions. Of the commonly researched polyphenol containing plant derivatives, lignin was determined to be widely abundant yet effective and as such was chosen to be the compound of choice in the selection of biomass material in the current research.

Present day methods of conventional PM recycling include pyrometallurgy and forms of hydrometallurgy which do not include biosorption. Although pyrometallurgical methods are commercially available, they are disadvantageous due to long processing time and large energy requirements to maintain operating temperatures. Additionally, pyrometallurgical methods are often not all inclusive – requiring further hydrometallurgical or electrochemical processing to improve metal value upgrading.

Although not as financially and environmentally demanding as pyrometallurgical processing, conventional hydrometallurgical methods of recovering PM has its own host of issues that makes the processing route disadvantageous. One major environmental obstacle is the traditional usage of cyanide based lixivants which have caused major ecological catastrophes in the past. Recent research and development work have shifted the usage of cyanide to alternatives such as thiourea, thiosulfate and other less toxic yet comparably effective means of leaching PM. Another environmental obstacle against conventional hydrometallurgical methods are the unsustainable nature of commercially available ion-exchange resins. Used during processing as adsorbents, ion-exchange resins are non-biodegradable as they are petroleum derived. Activated carbon, which is also often used as adsorbents are considered a commercial alternative of ion-exchange resins. However, they often suffer from diffusion limitations which can affect recovery efficiency.

Due to the disadvantages regarding conventional pyrometallurgical and hydrometallurgical PM recovery, the usage of biosorbents is presented as a low-cost, environmentally sustainable and potentially better performing alternative. Although raw, unmodified biomass already possess an inherent ability to adsorb metals to a certain extent, the

crosslinking of polyphenolic compounds and the addition of novel functional groups can greatly enhance adsorption efficiency. Known as immobilization, such modification methods can add value to raw biomass by increasing metal recovery as well as adsorption selectivity.

By understanding the disadvantages of conventional PM recovery methods and the advantages of biosorption in fulfilling the environmental and performance standards which pyrometallurgical and hydrometallurgical methods cannot, three biomass types were chosen to create biosorbents for PM adsorption in the current research. Wheat straw, canola meal and wood bark were selected as the base biomass materials which are to be further immobilized and experimented upon to determine each biosorbent's efficacy in recovering PM.

CHAPTER 3: Experimental Procedures

3.1 Materials and instrumentation

All chemicals used in the experiments of this research were purchased from Sigma Aldrich (St. Louis, MO) and Fischer Scientific (Hampton, NH) and were all of reagent grade. The acid chloride based PLS used in this research work was provided by Asahi Refining (Brampton, ON) and was used in varying levels of dilution with 0.4 M hydrochloric acid in the experiment. WS used in this study were procured from the Department of Biological Engineering at the University of Saskatchewan and Viterra. Inc (Regina, SK) generously provided the CM used for this research. In this experiment, WB or “wood bark” refers to a commercially available wood bark product used for heating which was purchased from Canadian Tire (Saskatoon, SK).

FT-IR analyses used throughout this experiment were conducted at the Saskatchewan Structural Sciences Center or within the Department of Chemical Engineering. Particle size analysis was conducted using Malvern Mastersizer 3000 (Malvern Panalytical, Malvern, United Kingdom) shown in Fig 3.1. BET pore size analysis and CHNS elemental analysis were performed by a technician from the Department of Chemical Engineering within the university. The Geoanalytical Laboratory in the Saskatchewan Research Council performed all the ICP testing required for this research.



Fig 3.1. The Malvern Mastersizer 3000 used for determination of biosorbent particle size.

3.2 Pre-treatment of biomass

Before any chemical treatment can be performed on the biomass, raw WS and WB had to be reduced in size using a wood grinder. After grinding, wheat straw was reduced to grinds shown in Fig 3.2 while WB was ground into a coarse powder. Fig 3.3(a) and (b) shows the original WB as received and in powdered form after grinding respectively. As raw biomass may contain waxes and other impurities, WS and WB had to undergo pre-treatment prior to further chemical processing. 1200 mL of benzene and 600 mL of ethanol were used to create a 2:1 ratio solution and 50 g of dry biomass were added to the mixture and stirred thoroughly for 48 hours at room temperature to remove extractants. The mixture was then vacuum filtered using a büchner funnel and left to air dry overnight. As mentioned previously in section 2.2, raw CM contains high protein content of approximately 36% or more [29]. To maintain comparable compositions for all biomass species in this research, protein content of CM had to be removed by mixing 200 g of CM into 1 L of 2% sodium hydroxide solution which was then stirred for 2 h at 80°C. Afterwards, the mixture was vacuum filtered and air dried and a black CM cake was obtained. Raw CM before any treatment and the subsequent black CM cake are exhibited in Fig 3.4(a) and (b) respectively. The CM cake was then ground into a smaller size using a conventional blender.



Fig 3.2. Raw wheat straw (WS) after grinding.

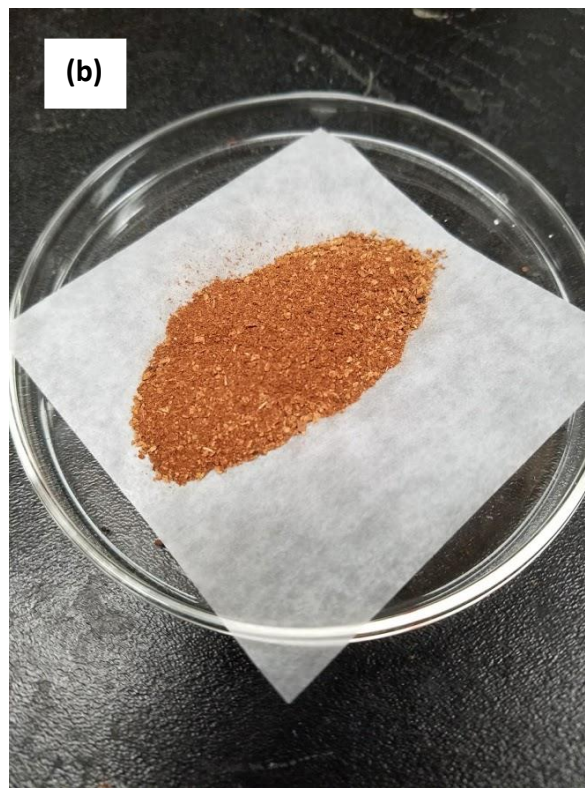


Fig 3.3. Wood bark (WB) as received (a) and after grinding (b).

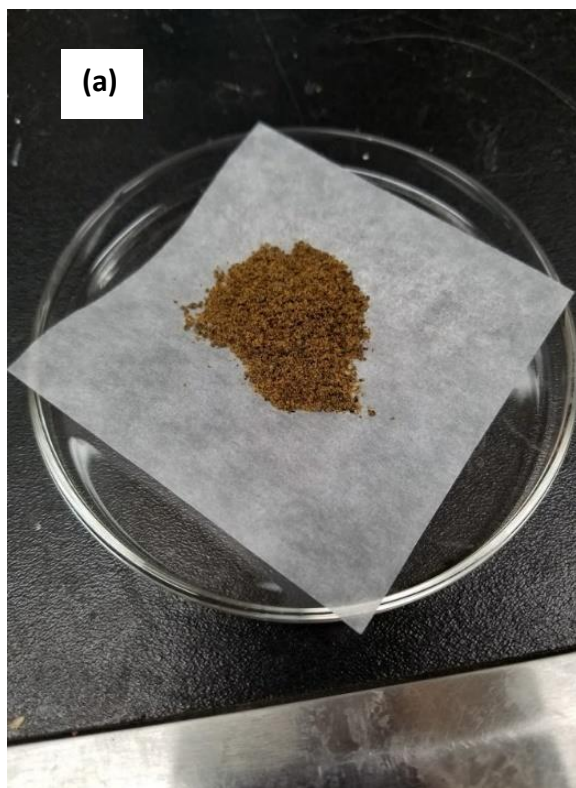


Fig 3.4. Raw canola meal (CM) as received (a) and after protein removal (b).

3.3 Dithiooxamide immobilization

The method of DTO incorporation on all biomass in this research was conducted after processes that Khunathai et al. [40] developed to immobilize microalgal residues. Fig 3.5 explains the route of synthesis as described in literature for which a similar process occurs in our lignin-based biomasses. The immobilization process is divided into two steps: 1) Initial chlorination of the biomass and 2) Following reaction with DTO. Chlorination is essential in the immobilization process as chlorine atoms which replace hydroxyl groups on lignin serve as leaving groups and are substituted with DTO in step 2. For chlorination, 50 g of dried biomass is mixed with 200 mL of pyridine in a three-necked flask which was submerged in an ice bath. Then a tube was fed into the flask to introduce inert N₂ atmosphere into the system. Using a separatory funnel, 150 mL of thionyl chloride was added dropwise into the flask which was then stirred at 75°C for 5 h before filtering. The filtered biomass was then washed thoroughly with distilled water then dried in a convection oven overnight at 60°C. The equipment arrangement for this process is displayed in Fig 3.6. For immobilization with dithiooxamide, 21 g of dried chlorinated biomass was put into a round bottom flask along with 1.4 g of DTO, 8.4 g of sodium carbonate and 100 mL of N,N-Dimethylformamide. The mixture was stirred thoroughly at 70°C for 48 h after which it was filtered, washed with 0.1 M hydrochloric acid and distilled water then air dried overnight at room temperature. The final product, dubbed DTO-biomass, was then obtained.

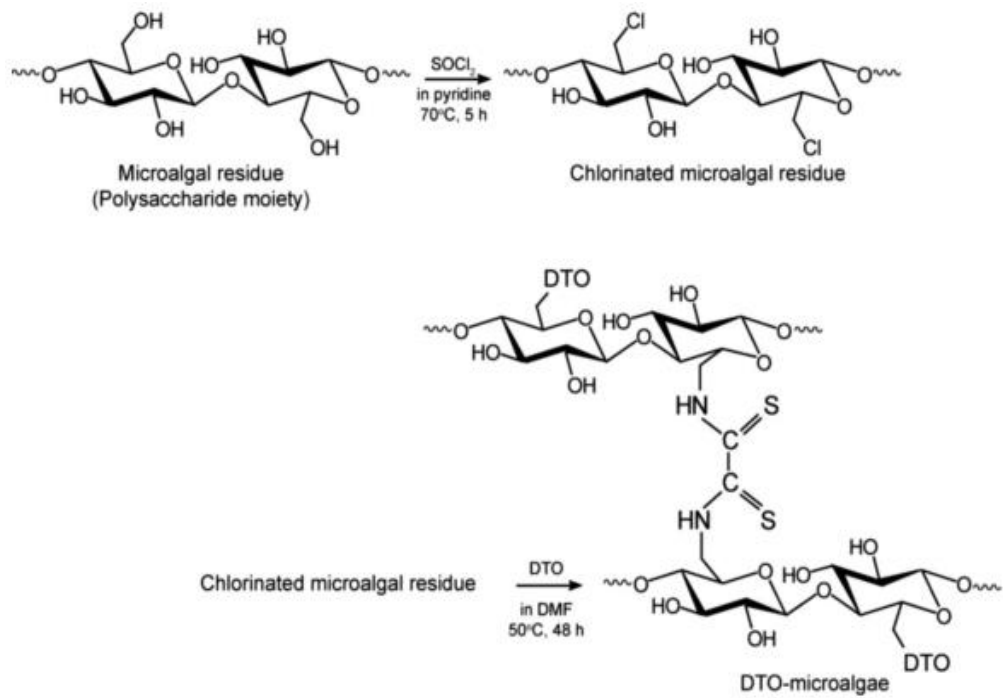


Fig 3.5. Schematic for the synthesis of dithiooxamide-immobilized microalgae (Reproduced from Khunathai et al. (2012) with permission from Taylor and Francis. Please refer to Fig C.12 for permission details).

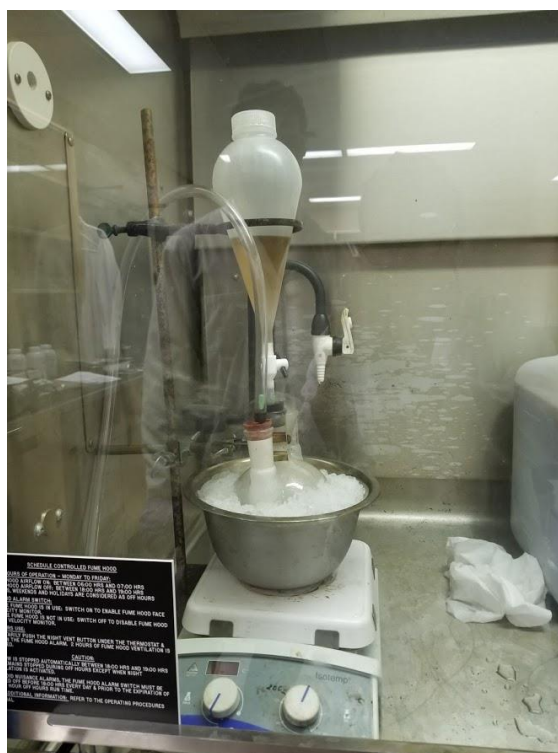


Fig 3.6. Laboratory set-up exhibiting the chlorination of biomass.

3.4 Synthesis of crosslinked-lignophenol

Parajuli et al. [25] previously developed a method of immobilizing raw wood powder with ethylenediamine and primary amine to create effective biosorbents for recovering Au(III), Pd(II) and Pt(IV). However, before the process of immobilization biomass must first be synthesized into crosslinked-lignophenol. The route of crosslinked-lignophenol synthesis from Parajuli et al. can be viewed in Fig 3.7. For this purpose, 40 g of purified (ethanol/benzene treated) biomass was submerged in a 1 M phenol solution in a round bottom flask then stirred vigorously for 10 minutes at 60°C then cooled to 30°C with continuous stirring. Subsequently, 800 mL of 72% sulfuric acid was then slowly added into the flask using a separatory funnel and the mixture was stirred for an additional 12 h. Fig 3.8 shows the addition of sulfuric acid. The contents of the flask were then centrifuged at a speed of 2000 rpm for 20 min after which a top organic layer and bottom ethanol layer were obtained. The top organic layer which contains the biomass was collected in a flask inside an ice bath. 1 L of diethyl ether was added to the organic mixture with 1 h of continuous stirring. After the stirred mixture was allowed to set, separation of the product occurs again with the lignophenol portion settling in the bottom. The top ether portion was discarded and the lignophenol mixture was dissolved in acetone, filtered, washed and air dried overnight at room temperature.

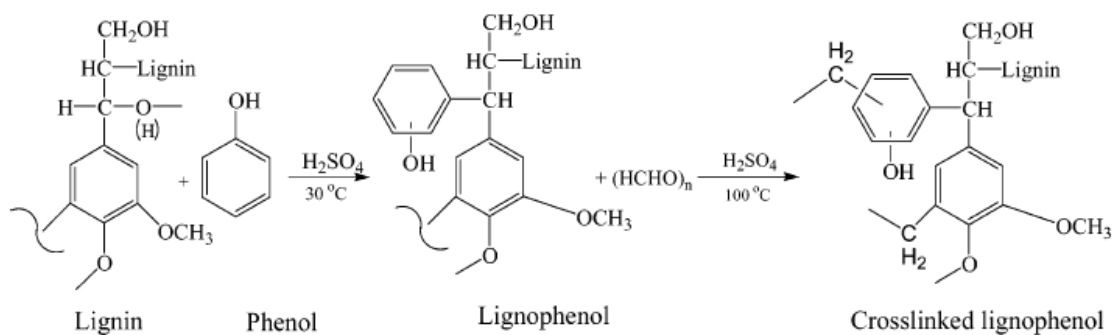


Fig 3.7. Creation of crosslinked-lignophenol biomass (Reprinted from Parajuli et al. (2006) with permission from American Chemical Society. Please refer to Fig C.18 for permission details).

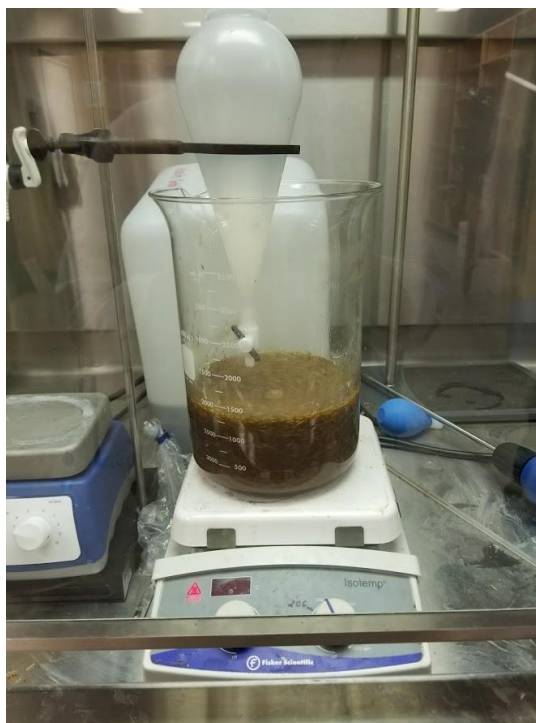


Fig 3.8. Schematic illustrating the addition of H_2SO_4 into phenolic mixture in the creation of lignophenol.

To crosslink the lignophenol biomass, paraformaldehyde was used to add characteristics including enhanced rigidity and water insolubility. These improvements are beneficial for the biosorbent to endure long contact with PLS solutions which are often highly corrosive. For this procedure, 50 g of lignophenol biomass was introduced to a flask containing 500 mL of 72% sulfuric acid and then stirred for 5 min. Afterwards, 65 g of paraformaldehyde was added and 24 h of stirring at 100°C follows. The mixture was then cooled to room temperature and 60 mL of 5% sodium hydrogen carbonate solution was added. After another 3 h of stirring, the mixture was filtered and washed with 0.1 M HCl solution to remove any impurities then followed with distilled water washing for pH neutralization. Finally, the crosslinked-lignophenol biomass was dried in a convection for 48 h at 70°C.

3.5 Ethylenediamine immobilization

To synthesize ethylenediamine onto the biomass, 5 g of crosslinked-lignophenol biomass was added to a round bottom flask containing 50 mL of dimethyl sulfoxide and stirred until all solids were dissolved. 8 g of sodium carbonate and 22 mL of ethylenediamine were then added to the mixture and the flask was stirred for 24 h at 80°C. Afterwards, the mixture was filtered and washed thoroughly with 0.1 M HCl and distilled water until neutral pH was reached. After

washing, the product was dried in a convection oven at 70°C for 24 h. Fig 3.9 shows the route of ethylenediamine immobilization from literature by Parajuli et al. [25].

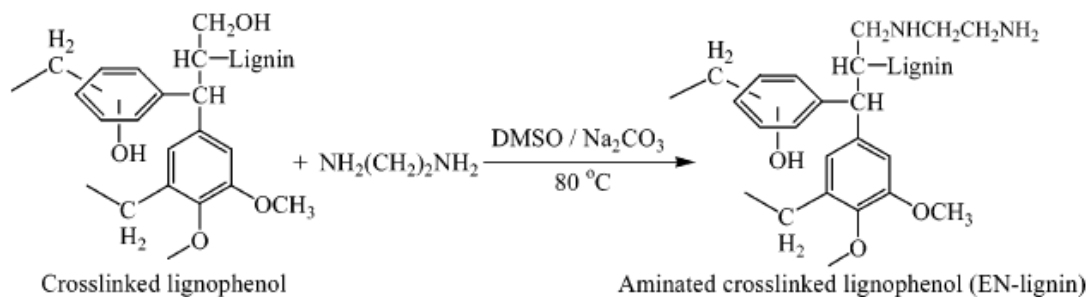


Fig 3.9. Reaction of crosslinked-lignophenol with ethylenediamine (Reprinted from Parajuli et al. (2006) with permission from American Chemical Society. Please refer to Fig C.18 for permission details).

3.6 Primary amine immobilization

The process of immobilizing crosslinked-lignophenol with a primary amine group, like with DTO immobilization involves chlorination of the compound before actual immobilization. During the chlorination process, 5 g of crosslinked-lignophenol was mixed with 200 mL of pyridine in a three-necked flask containing inert N_2 atmosphere and 30 mL of thionyl chloride was added dropwise into the mixture. After 5 h of constant stirring at 70°C, the chlorinated crosslinked-lignophenol was filtered, washed with distilled water and dried at 70°C in a convection oven overnight. Subsequently, 5 g of the dried product was then added to a flask and reacted with 40 mL of 1.18 M ammonia solution in ice bath and stirred for 10 min. 100 mL of dimethyl formamide was then introduced into the mixture which was then stirred at 75°C for another 48 h. The obtained product was filtered, washed with distilled water, dried in a convection oven at 70°C for 24 h and the final PA-biomass product was obtained. Synthesis route of PA-lignin as created by Parajuli et al. [25] is demonstrated in Fig 3.10.

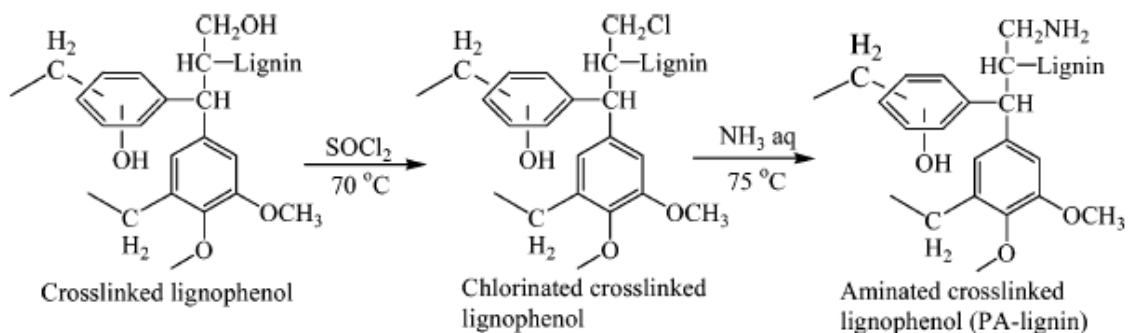


Fig 3.10. Reaction of crosslinked-lignophenol with primary amine (Reprinted from Parajuli et al. (2006) with permission from American Chemical Society. Please refer to Fig C.18 for permission details).

A flowchart summarizing the three immobilization routes and a table explaining the created products are shown in Fig 3.11 and Table 3.1.

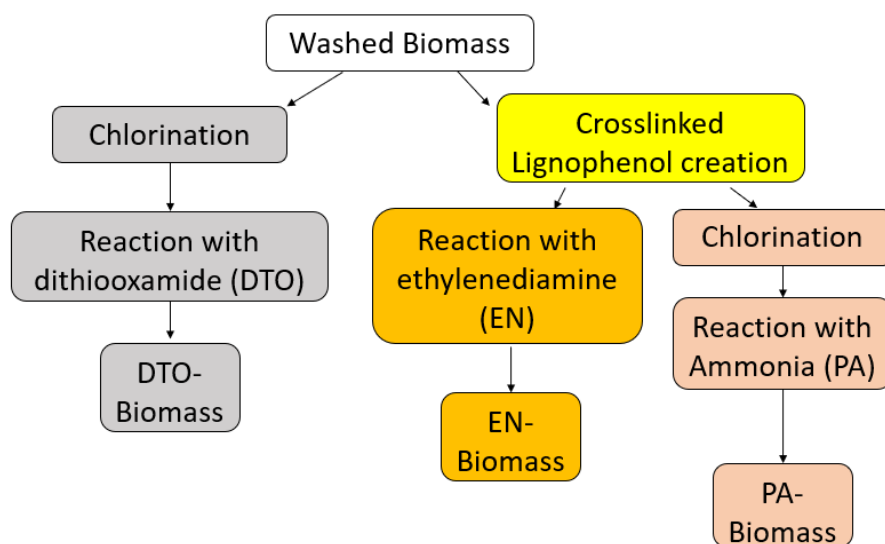


Fig 3.11. Summary of all immobilization routes for biosorbent production.

Table 3.1. All created adsorbents according to precursor biomasses and immobilization routes.

Immobilization Route	Precursor Biomass		
	Wheat Straw (WS)	Canola Meal (CM)	Wood Bark (WB)
Dithiooxamide (DTO)	DTO-WS	DTO-CM	DTO-WB
Ethylenediamine (EN)	EN-WS	EN-CM	EN-WB
Primary amine (PA)	PA-WS	PA-CM	PA-WB

3.7 Determination of the biosorbent of focus

Due to the limited time allotted for a master's thesis research, the characterization and subsequent analysis of each adsorbent species would have been a herculean task. Thus, one biosorbent which displays optimal recovery of Pd and Pt must be chosen out of the prepared 12 adsorbents. For this purpose, a preliminary experiment was conducted using a one-point adsorption test.

During the initial adsorption test, each of the 12 biosorbents were introduced into diluted PLS which was then recovered after a sufficient period of agitation and measured for remaining Pd and Pt content. To do this, first the received PLS was diluted to ensure that adsorbent binding sites would not be oversaturated with metal ions. See Table 3.2 for details of PLS concentration as received:

Table 3.2. Elemental assay of received pregnant leach solution without dilution.

Element	Concentration (ppm)	Element	Concentration (ppm)
Ag	25.7	Hg	0.7
Au	6.5	Ni	147
Pt	706.8	Pb	220
Pd	1816.5	Rh	4
Cd	21	Se	1976
Co	3	Sn	4
Cu	10405	Te	25
Fe	8221	Zn	573

By using the concentration of Pd as a reference, the leach solution was diluted by a factor of 9 with 0.4 M hydrochloric acid to obtain a new solution containing 204 ppm Pd and 76 ppm Pt from ICP assay. As explained above in section 2.5, changes in solution pH may cause metal to precipitate. As pH is not one of the parameters which was varied in this experiment due to the highly unpredictable nature of a real leach solution, the original pH of 0.39 must be maintained.

Once the diluted solution was obtained, 20 mL was decanted into vials in which 1 g of adsorbent was added to. The 12 vials were then shaken at 200 rpm in room temperature of around 25°C for 24 h. For observational purposes, the mixture was then left to settle undisturbed for 48 h and then filtered with Whatman no.40 filter paper. The filtrate was collected and analyzed with ICP-OES for Pd and Pt concentration. A photo of all biosorbent-solution mixtures after shaking along with diluted and raw PLS can be observed in Fig 3.12. From the image, it is evident that there have been various changes in solution color with CM standing out as having the starkest difference. From this qualitative observation, it can be hypothesized that CM, EN-CM, DTO-WS and EN-WS were able to adsorb a significant amount of PLS out of solution. Images showing all 12 leach solutions after adsorption and filtration can be viewed in Appendix A.



Fig 3.12. All biosorbent and pregnant leach solution mixtures with diluted and undiluted leach solutions. Operation conditions: 1 g biosorbent and 20 mL diluted PLS mixture after shaking for 24 h at room temperature and 48 h of settling.

Concentration measurements generated from ICP were evaluated for the amount of adsorption (q) and adsorption percentage that each biosorbent exhibited on Pt and Pd. Eqs. 3.1 and 3.2 were used respectively to determine these values:

$$q = \frac{(C_i - C_e)V}{W} \quad (3.1)$$

$$\% \text{ Adsorption} = \frac{(C_i - C_e)}{C_i} \times 100 \quad (3.2)$$

C_i and C_e represent the ppm concentration of metal ions in solution initially and after equilibrium has been reached respectively. V is the test solution volume in mL and W signifies the weight of

adsorbent used in mg. It must be clarified that in calculations of this experiment, ppm values of metal ions are defined as mg of metal present per L of leach solution. It should be noted that for the purpose of this experiment, equilibrium is the point in which concentration of metals in solution no longer shows significant changes.

Results of the one-point adsorption test is displayed in Fig 3.13. High recovery was observed for all PA type biomasses and DTO-WS. DTO-CM and EN-WS exhibited intense selectivity towards Pd and Pt respectively, showing no adsorption behavior for the other metal. Surprisingly, CM displayed significant adsorption for both metals despite the lack of immobilization, recovering 94.9% for Pt and 99.2% for Pd. Overall, DTO-WB was the optimal adsorbent as it was able to recover 97.4% of Pt and 99.8% of Pd and for this reason it was selected as the biosorbent of focus for the rest of this research work.

In comparison of results to previous findings, Khunathai et al. [40] reported that DTO-immobilized microalgal residue was effective in recovering 99% of Pt and Pd from solution under similar experimental conditions however, the unmodified microalgal residue exhibited poor adsorption of 40% for Pd and 10% for Pt. This contrast in adsorption efficiency between the modified and unmodified versions of biosorbents is reflected in the results between DTO-WB and WB as well as DTO-WS and WS where adsorption efficiency increased greatly with immobilization. However, surprisingly DTO-CM exhibited poorer Pd adsorption efficiency when compared to its precursor and did not show any signs of Pt recovery. In general, Khunathai et al. attributed this increase in adsorption efficiency from immobilization to the presence of sulfur and nitrogen in the modified biomass which acts as specific donor atoms for complexation.

Parajuli et al. [25] observed that EN-immobilized lignin exhibited adsorption percentages of up to 93% for Pt and 55% for Pd with PA-immobilized lignin achieving 80% and 42% recovery of Pd and Pt adsorption respectively. These results signify that EN-lignin exhibits higher selectivity towards Pt over Pd whereas the reverse is true for PA-lignin. In the obtained experimental results of the present research work, it can be observed that these selectivity patterns were not observed between EN-immobilized and PA-immobilized biosorbents as with the exception of EN-WS, all adsorbents exhibited selectivity towards recovering Pd.

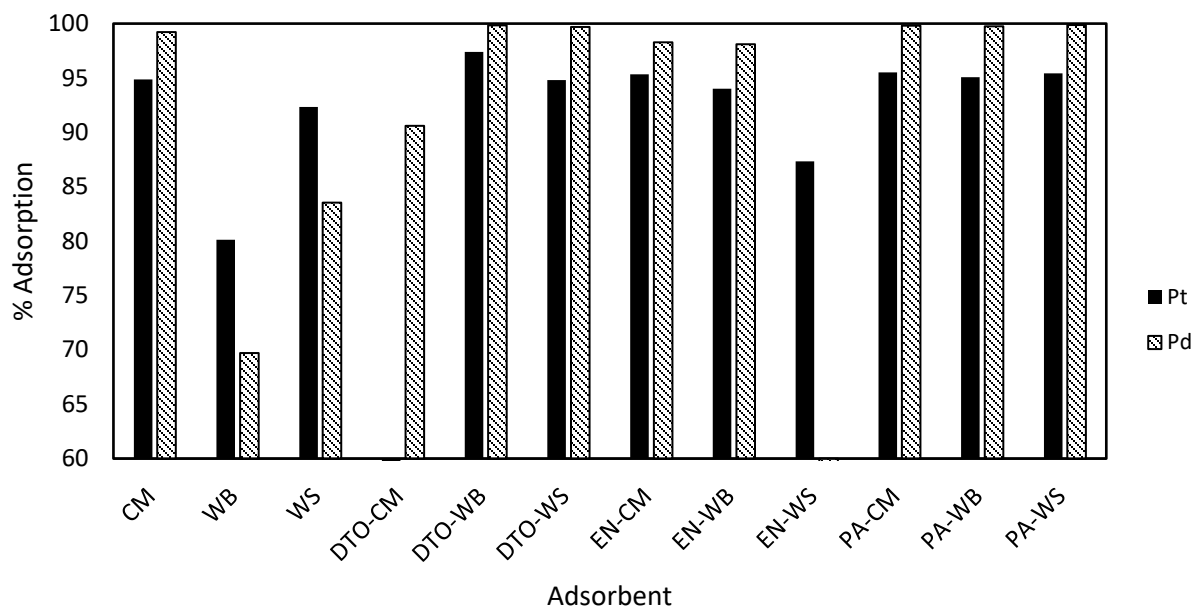


Fig 3.13. Comparison of all 12 biosorbents in their efficiency of adsorbing platinum (black bar) and palladium (grey bar) from solution. Operating conditions: Initial concentration of Pd and Pt = 204 ppm and 76 ppm respectively, sorbent dose = 1 g, solution volume = 20 mL, shaking speed = 200 rpm, shaking time = 24h, operating temperature = 25°C.

To confirm the adsorption results of DTO-WB, further adsorption of two additional trials were conducted using the same experimental conditions as the initial test, including 48 h of settling time after 24 h of shaking. The obtained results can be viewed in Fig 3.14. Adsorption of Pt appears to vary greatly as reflected in the generated error bars, ranging from 97.4% from the original trial to 98.8% in a repeated trial. By contrast, Pd adsorption is relatively consistent with all adsorption efficiencies reaching 99.8% after rounding to the tenth decimal place. Overall, one can conclude that the repeated trials confirms that DTO-WB is the most efficient biosorbent out of the initial 12 products.

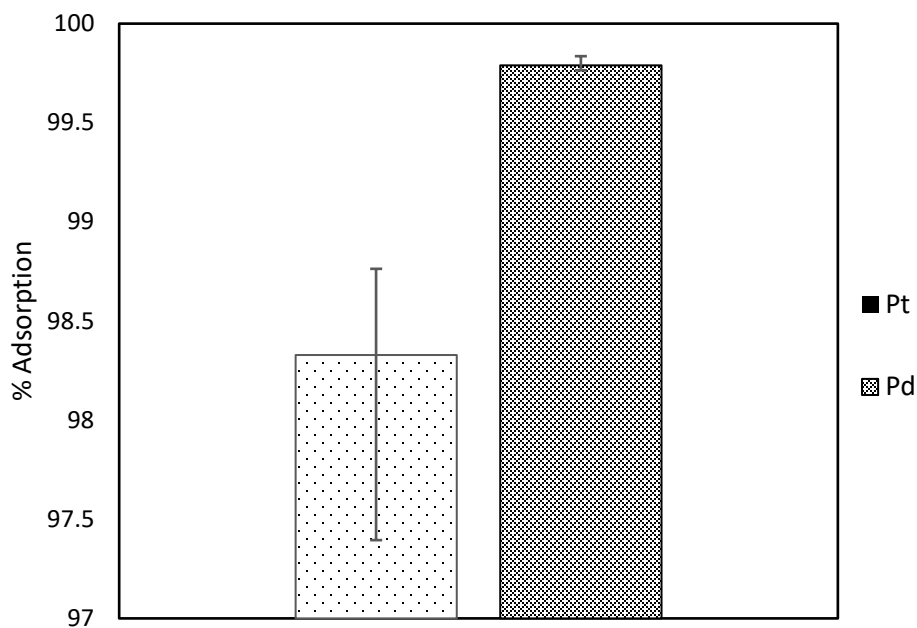


Fig 3.14. Average adsorption percentages achieved by dithiooxamide-immobilized wood bark on platinum and palladium recovery from three trials. Operating conditions: Initial concentration of Pd and Pt = 204 ppm and 76 ppm respectively, sorbent dose = 1 g, solution volume = 20 mL, shaking speed = 200 rpm, operating temperature = 25°C.

3.8 Adsorption experiments

Conventional batch methods were utilized in this research to evaluate adsorption behaviors of each biosorbent in recovering dissolved metal species of PLS. To determine the most effective sorbent dosage to adsorb Pt and Pd from solution, the optimal solid-liquid (S/L) ratio was necessary. For this purpose, 30 mg of DTO-WB was added to diluted leach solutions of varying volumes with initial concentration of 96 ppm Pd and 35 ppm Pt from assay. Solution volumes were varied using 60 mL, 30 mL, 20 mL, 15 mL, 12 mL and 10 mL aliquots, generating S/L ratios that varied from 0.5, 1, 1.5, 2, 2.5 and 3 correspondingly. The mixtures were then shaken at 200 rpm and 30°C conditions for 48 h after which they were filtered, and the filtrates were analyzed. The shaking time of 48 h was determined according to point of equilibrium for DTO-WB obtained from adsorption kinetics experiments where 24 h was indicated to be enough time for adsorption to reach completion at higher temperatures.

The adsorption isotherms for DTO-WB were determined via batch experiments using 20 mg of DTO-WB and 20 mL of diluted leach solutions. Six leach solutions of concentrations ranging from 25 ppm Pd to 800 ppm Pd were used and the samples were shaken at 25°C and

30°C for 48 h. Afterwards, the mixtures were filtered, and the remaining solution was measured for Pt and Pd concentration.

The kinetics of adsorption behavior were observed to determine the rate of metal uptake onto the DTO-WB biosorbent. During this experiment, 200 mg of DTO-WB was mixed into a 200 mL beaker of diluted leach solution with Pd concentration of 50 ppm. The beaker was stirred using a magnetic stirrer with speed of 200 rpm and 10 mL of solution sample was drawn out at various time intervals for up to 96 h. The experiment was repeated three times to vary temperature conditions starting with room temperature at 25°C. To maintain temperatures of 30°C and 40°C, a temperature-controlled chamber was used to conduct the experiment. At sample drawing intervals, extracted samples were filtered immediately and contained, after which Pt and Pd concentrations were analyzed. Using concentration data obtained from the ICP, the following Eq. 3.3 was used to determine amount of metal adsorbed at time t (q_t):

$$q_t = \frac{(C_i - C_t)V}{W} \quad (3.3)$$

Where C_i represents the concentration of metals at initial time in hours and C_t is the concentration of metals in parts per million at time t.

3.9 Characterization of biosorbent

3.9.1 FT-IR analysis of DTO-WB

The FT-IR spectra of DTO-WB was examined to gain perspective in the chemical makeup of the biosorbent and is presented in Fig 3.15. In addition to DTO-WB, the FT-IR spectra of all 12 adsorbents may be viewed in Appendix B. According to the FT-IR spectra, there is evidence of a secondary amine moiety at 1624 cm^{-1} and 1570 cm^{-1} while peaks at 1153 cm^{-1} , 1096 cm^{-1} and 1022 cm^{-1} represents the stretching of thiocarbonyl groups. From the presence of these two groups, it can be assumed that the immobilization of DTO on the structure of WB was successful.

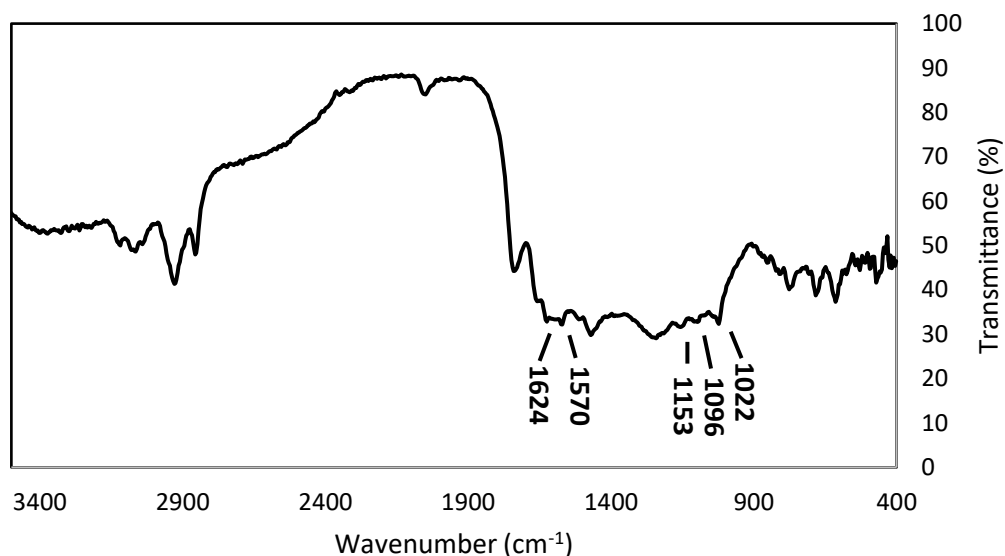


Fig 3.15. FT-IR spectra of dithiooxamide-immobilized wood bark. Peaks at 1624 cm^{-1} and 1570 cm^{-1} represents secondary amine groups whereas peaks at 1153 cm^{-1} , 1096 cm^{-1} and 1022 cm^{-1} represents presence of thiocarbonyl groups.

3.9.2 Characterization of DTO-WB

The C, H, N and S contents of DTO-WB and raw WB were evaluated for comparison in Table 3.3. Results suggests that DTO immobilization of raw WB was successful and significantly increased the content of nitrogen from 0.254% to 2.42%. Sulfur content increased dramatically to over 27%. In their research, Khunathai et al. [40] also observed a large increase in the content of nitrogen and sulfur on microalgal residue after DTO-immobilization with nitrogen increasing from 4.04% to 5.28% and sulfur increasing from 1.34% to 18.7%. When compared to the current results, DTO-immobilization generated a more significant increase in sulfur content on WB than on microalgal residue as was previously reported.

Table 3.3. Carbon, Hydrogen, Sulfur and Nitrogen percentages of dithiooxamide-immobilized wood bark and raw wood bark.

Biomass	Elemental content (%)			
	Carbon	Nitrogen	Sulfur	Hydrogen
Raw WB	48.8%	0.254%	0.383%	5.82%
DTO-WB	37.7%	2.42%	27.2%	4.07%

BET analysis which is used to analyze surface area and pore characteristics of biosorbents was also performed on DTO-WB. Testing revealed that the adsorbent had a surface

area of 2.21 m²/g, pore volume of 0.0072 cm³/g and average adsorption pore size of 46.20 nm. Particle size analysis showed that DTO-WB has a D₉₀ of 346 μm, D₅₀ of 147 μm and D₁₀ of 32.8 μm. The particle size distribution of the adsorbent is shown below in Fig 3.16. From the graph, it is evident that a high amount of DTO-WB exists within the 20-400 μm range, peaking at around 250 μm.

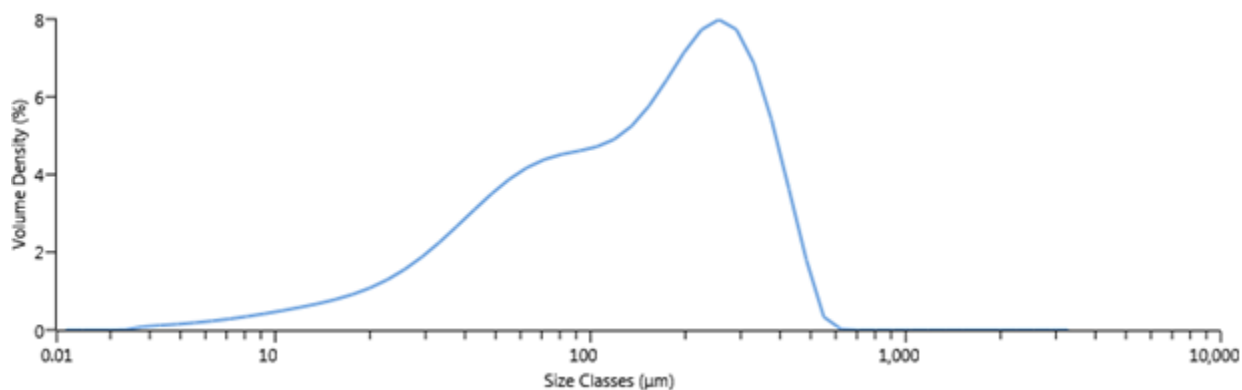


Fig 3.16. Particle size distribution of dithiooxamide-immobilized wood bark (X-axis not to scale).

3.10 Data analysis

To calculate the various parameters required for the analysis of data obtained from experiments, Microsoft Excel was used. By setting X and Y axes accordingly to calculated parameters required for equations, linear trendlines were able to be created giving values pertaining to desired information. For example, in the case of calculating activation energy E_A , the X and Y parameters required were determined from the linear Arrhenius equation (from Eq. 2.6) as $1/T$ and $\ln k_I$ respectively. By inputting the respective parameter values as calculated into excel and drawing a graph, a linear trendline with the format $y = mx + b$ could be created where b is equivalent to $\ln A$ and slope m is equivalent to $-E_A/R$. By utilizing some algebraic maneuvering, E_A could then be calculated by hand. It is by using this method that the data obtained from conducted kinetic, isotherm and thermodynamic experiments were analyzed.

4.1 Effect of adsorbent dose

The effect of solid to liquid (S/L) ratios in regards to the performance of adsorbent is displayed in Fig 4.1. As S/L ratio increased, there is a sharp decrease in the amount of Pd remaining in solution. The optimal S/L ratio for Pd adsorption was found to be at 2.5 where only 0.4 ppm remained in solution. However surprisingly, the highest S/L ratio of 3 was not as effective, leaving 0.9 ppm Pd unabsorbed in solution. In contrast to the adsorption behavior of Pd, the decrease of remaining Pt in solution was more gradual in fashion. The optimal S/L ratio in adsorbing Pt for DTO-WB was also shown to be at 2.5 in which only 0.9 ppm of the metal remained. In a similar case with Pd adsorption, S/L ratio of 3 was not as effective, leaving 1.5 ppm of metal to remain in solution. By interpreting these results, we can observe that in a case of constant solution volume although higher sorbent dosage may yield more effective recovery of both Pt and Pd, there is a threshold of effectiveness at 2.5 S/L ratio. In accordance to the previously discussed theory in chapter 2, if sorbent dosage is increased beyond the optimal threshold effectiveness may actually decrease as binding sites of the adsorbent saturated solution interact with each other, interfering with metal recovery.

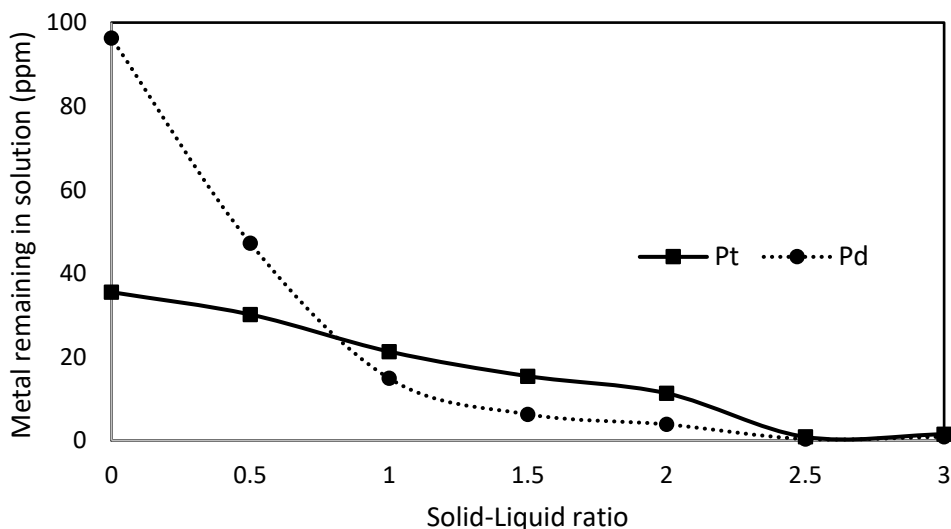


Fig 4.1. Effect of solid-liquid ratio on platinum and palladium recovery using dithiooxamide-immobilized wood bark. Operating conditions: Initial concentration of Pd = 96.3 ppm and Pt = 35.5 ppm, shaking speed = 200 rpm, operating temperature = 25°C, shaking time = 48 h.

4.2 Effect of initial solution metal concentration

For this analysis, six diluted PLS solutions with initial concentrations of 30, 50, 100, 150, 300 and 700 ppm Pd (10, 20, 35, 70, 150 and 300 ppm Pt) were created. Twenty milligrams of DTO-WB were added to 20 mL of the solution and the mixture was shaken for 48 h at 200 rpm with operating temperatures of 25°C and 30°C. Pt adsorption percentage is the highest at roughly 99.98% for both temperatures when initial concentrations are at its lowest, as can be observed in Fig 4.2(a). However, as initial concentration of Pt is raised to 35 ppm, adsorption percentage decreases sharply to 39.15% at 25°C. Fig 4.2(b) demonstrates that adsorption of Pd, like with the adsorption of Pt, reaches the highest percentages at low initial concentrations and was able to achieve up to 99.99% adsorption for both temperatures in 30 ppm Pd solution. Unlike with the case of Pt adsorption, the decrease in Pt adsorption percentage is more gradual as initial Pd concentration in solution was raised. For the case of both metals, adsorption efficiency is higher across almost all initial concentrations at the higher temperature of 30°C, signifying that adsorption efficiency can be improved by increasing the operating temperature. This phenomenon can be accounted for by DTO-WB's thermodynamic properties which will be discussed later in section 4.6.

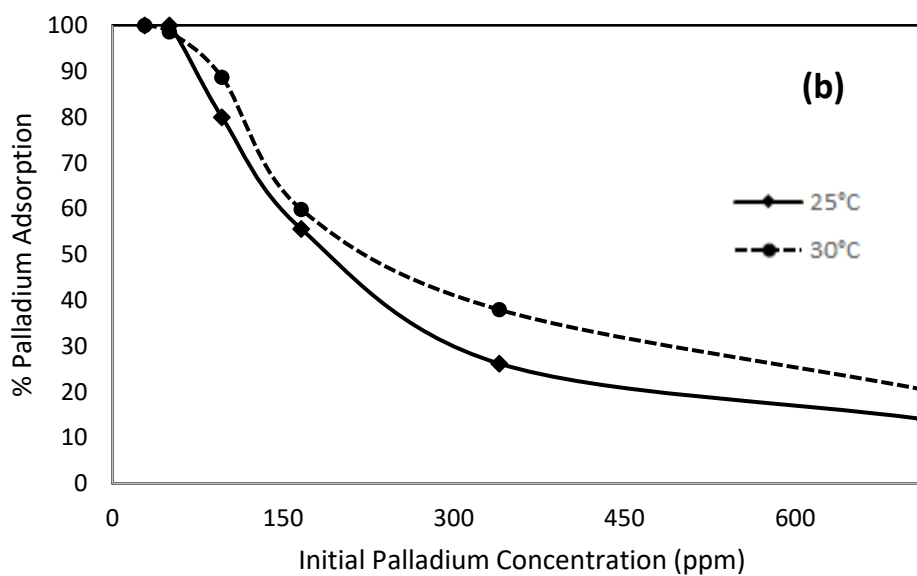
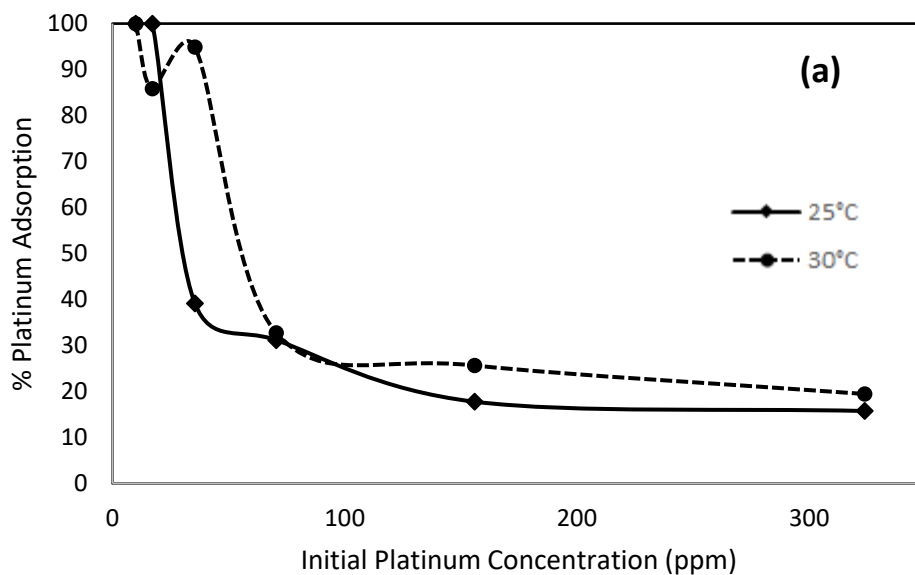


Fig 4.2. Effect of initial concentration on the adsorptions of platinum (a) and palladium (b) ions on dithiooxamide-immobilized wood bark. Operating conditions: Solution volume used = 20 mL, initial Pt and Pd concentrations = 10-300 ppm and 30-700 ppm respectively, shaking time = 48 h, shaking speed = 200 rpm. Note: lines present in this graph do not have any mathematical purpose and are drawn to guide reader's eyes only.

4.3 Biosorption kinetics

The obtained results from the kinetic studies conducted on DTO-WB for Pt and Pd adsorption are presented in Fig 4.3(a) and (b) respectively.

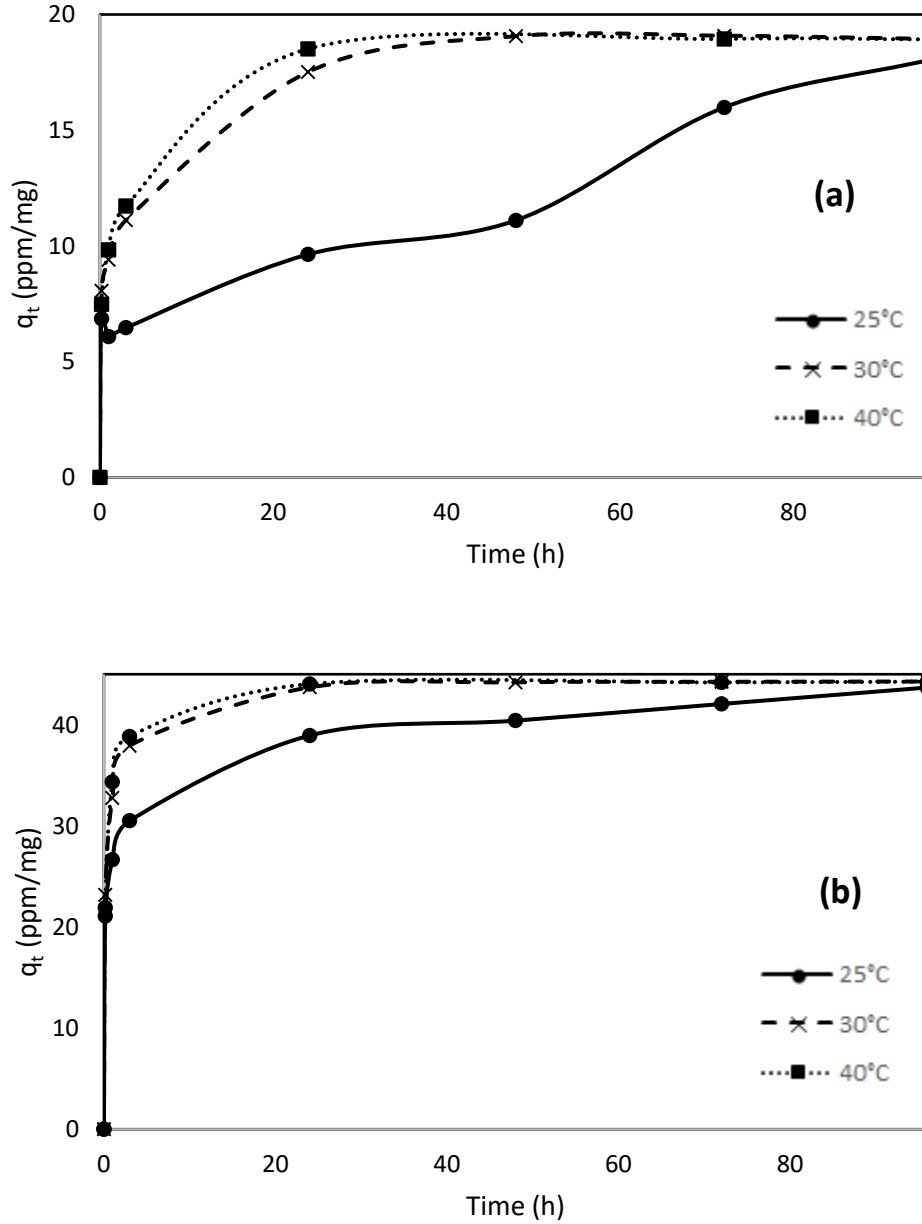


Fig 4.3. Effect of stirring time on the amount of platinum (a) and palladium (b) adsorbed by dithiooxamide-immobilized wood bark at 25°C, 30°C and 40°C. Operating conditions: Initial Pt and Pd concentrations = 20 ppm and 44 ppm respectively, solution volume = 200 mL, sorbent dosage = 200 mg, stirring speed = 200 rpm. Note: lines present in this graph do not have any mathematical purpose and are drawn to guide reader's eyes only.

It is indicated from the results that temperature increase clearly improves the adsorption capacity of DTO-WB and somewhat improves the rate of adsorption. Equilibrium of adsorption was reached quickly at approximately 24 h for Pt and Pd at 40°C but at 25°C, adsorption rate was sluggish and required 96 h to reach equilibrium. At these equilibrium times, the 40°C temperature proved to be superior in terms of adsorption capacity, reaching 19 ppm/mg adsorption for Pt at only a quarter of the time required to adsorb 18 ppm/mg at 25°C. In the case of Pd adsorption, the lower operating temperature of 25°C did not result in a significant difference in adsorption capacity when compared to higher temperatures as long as equilibrium times are reached. Surprisingly in the case of Pt adsorption, it seems that once 72 h of agitation times has been reached by both 30°C and 40°C temperatures, longer contact of DTO-WB in solution causes adsorption capacity to decrease.

Pseudo-first and pseudo-second order kinetic fitting were also performed on the results obtained for Pt and Pd adsorption on DTO-WB. To analyze the data according to the pseudo-first and pseudo-second order kinetic models, Eqs. 4.1 and 4.2 were used respectively. By setting boundary conditions of the equation from $t = 0$ to $t = t$ and $q_t = q_e$ and integrating, the linear forms of Eqs. 4.1 and 4.2 were obtained and expressed in Eqs. 4.3 and 4.4 respectively [53].

$$\frac{dq_t}{dt} = k_1(q_e - q_t) \quad (4.1)$$

$$\frac{dq_t}{dt} = k_2(q_e - q_t)^2 \quad (4.2)$$

$$\log(q_e - q_t) = \log q_e - \frac{k_1}{2.303} t \quad (4.3)$$

$$\frac{t}{q_t} = \frac{1}{k_2 q_e^2} + \frac{1}{q_e} t \quad (4.4)$$

In these equations, k_1 and k_2 correspondingly represent the rate constants of the pseudo-first order model in h^{-1} and pseudo-second order model in $\text{mg ppm}^{-1} \text{h}^{-1}$. After subjecting kinetic experimental data to Eqs. 4.3 and 4.4, the various parameters for both the pseudo-first and pseudo-second order kinetic models were obtained and are exhibited in Table 4.1. It has been previously explained that sorption processes which follow pseudo-second order fitting indicates that the rate controlling factor is the chemical reaction itself and thus can be identified as a chemisorption process [53]. Pseudo-first order reactions on the other hand indicates that a

sorption process operates via physisorption as the rate limiting step in the process is dependent on diffusion instead of the concentration of reactants as with chemical reactions [53].

According to obtained calculations for the pseudo-first order kinetic model, there is a 4-fold increase in the rate of adsorption of Pt as temperatures increased from 25°C to 30°C. An additional increase in 10°C from 30°C to 40°C further enhances the rate of adsorption of Pt another 2-fold. In the case of Pd, temperature increase from 25°C to 30°C was able to increase the rate of adsorption almost 3-fold. However, when temperatures are increased from 30°C to 40°C, it appears that the rate of Pd adsorption decreases. This result indicates that for DTO-WB, rate of Pd adsorption is optimal at 30°C whereas according to trend, higher temperatures generally increases rate of Pt adsorption.

Table 4.1. Summary of all obtained parameters from pseudo-first and pseudo-second order kinetic model fitting of the adsorption of platinum and palladium on dithiooxamide-immobilized wood bark. Note that (a) signifies values were obtained from experimental data and (b) signifies values were obtained from calculation.

Temperature (°C)	Pseudo-first order kinetic model			Pseudo-second order kinetic model		
	q_e^a (ppm/mg)*	k_1 (h ⁻¹)	R^2	k_2 (mg ppm ⁻¹ h ⁻¹) x 10 ⁴	R^2	q_e^b (ppm/mg)*
Pt						
25	18.07	0.02096	0.8751	0.06420	0.9214	17.54
30	18.95	0.08360	0.9978	0.5602	0.9995	19.27
40	18.93	0.1373	0.9991	0.7231	0.9998	19.16
Pd						
25	43.69	0.03409	0.9401	5.660	0.9985	43.48
30	44.28	0.09189	0.9586	25.65	1	44.44
40	44.27	0.07301	0.8074	31.35	1	44.44

* Unit of q_e is defined as amount of metals (mg) per liter of solution per mg of sorbent used.

Graphical data showing the pseudo-first order linear fittings of Pt and Pd adsorption by DTO-WB can be observed in Fig 4.4(a) and (b) respectively. R^2 correlation coefficient fitting of the plots obtained from trendline were examined to gain insight into whether kinetic behavior of DTO-WB followed the pseudo-first or pseudo-second order reaction. From Table 4.1, it can be observed that pseudo-first order fitting R^2 values for the adsorption of Pt was in the range of 0.8751 - 0.9991 for the various temperatures while Pd adsorption fitting values varied from 0.8074 - 0.9586. These R^2 values signify that in comparison to the behavior exhibited towards Pd, Pt adsorption on DTO-WB is a better fit with the pseudo-first order kinetic model.

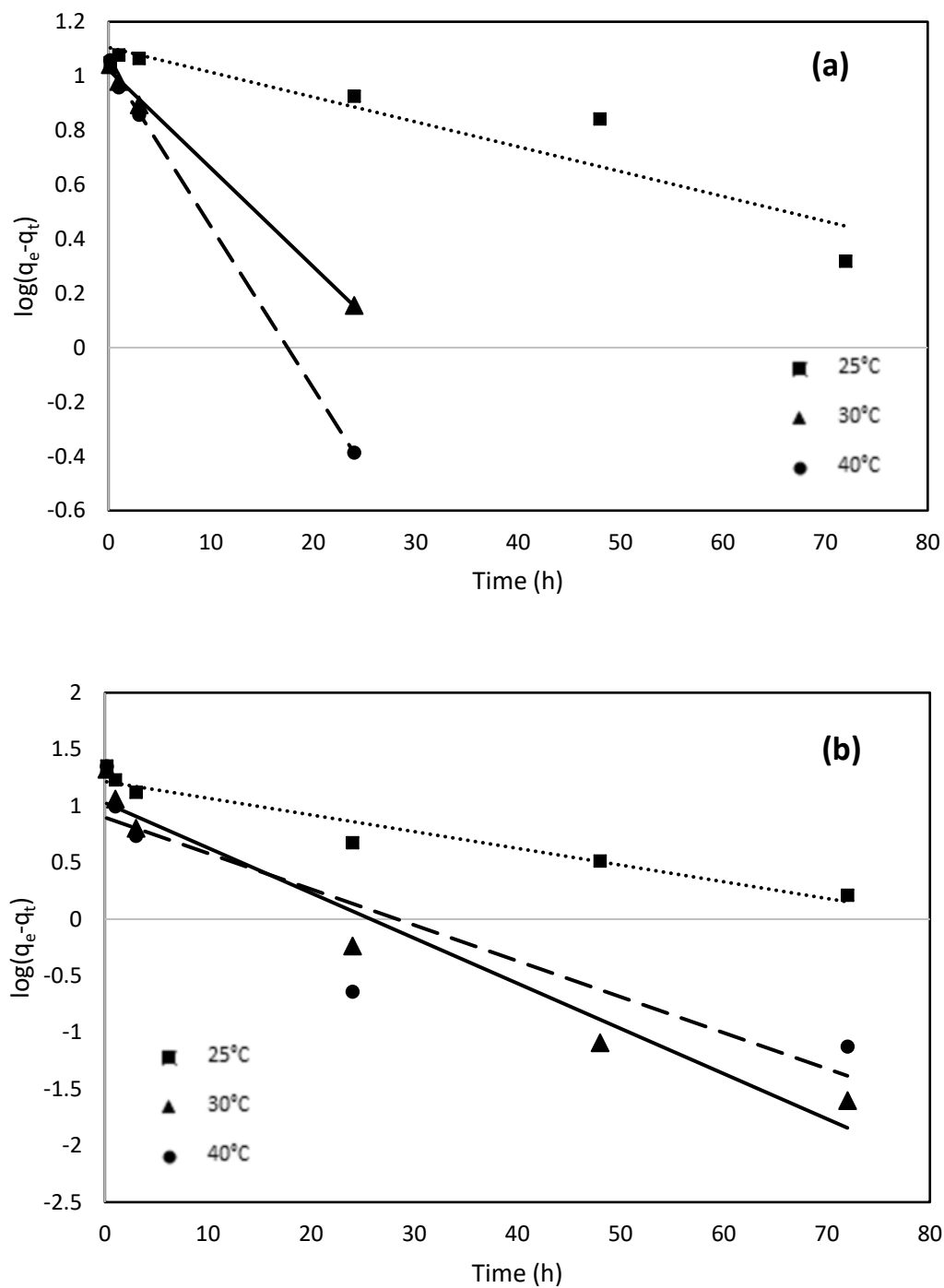


Fig 4.4. Pseudo-first order plot for the adsorption data of platinum (a) and palladium (b) on dithiooxamide-immobilized wood bark biosorbent at various temperatures. Operating conditions: Initial Pt and Pd concentrations = 20 ppm and 44 ppm respectively, sorbent dosage = 200 mg, solution volume = 200 mL, stirring speed = 200 rpm. Note: Lines represent trendline fitting of data.

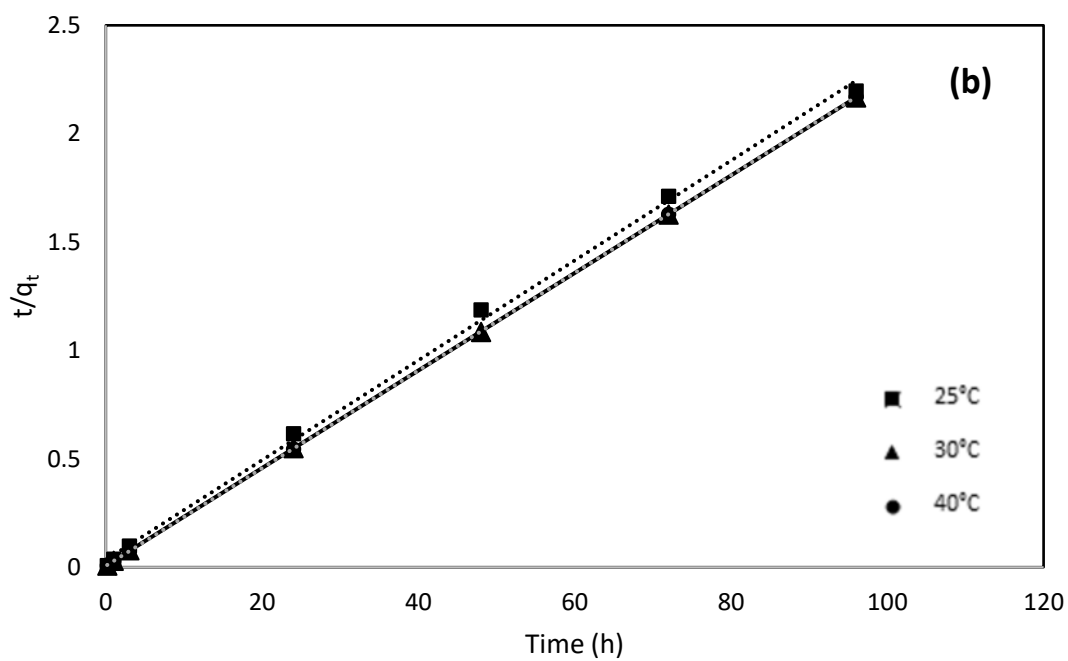
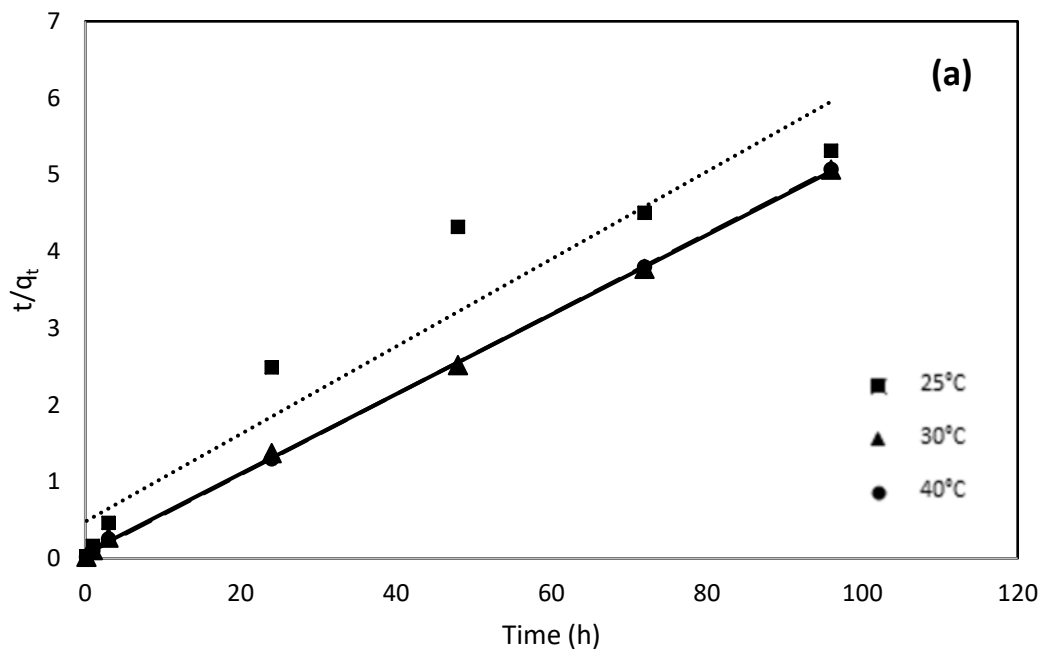


Fig 4.5 Pseudo-second order plot for the adsorption data of platinum (a) and palladium (b) on dithiooxamide-immobilized wood bark biosorbent at various temperatures. Operating conditions: Initial Pt and Pd concentrations = 20 ppm and 44 ppm respectively, sorbent dosage = 200 mg, solution volume = 200 mL, stirring speed = 200 rpm. Note: Lines represent trendline fitting of data.

In the same manner, results from the application of pseudo-second order linear fitting for the adsorption of both metals is shown in Fig 4.5. From the results, it can be observed just visually that linear fitting is more accurate for both Pt and Pd adsorption and this assumption is supported by R^2 values which range from 0.9214 - 0.9998 and 0.9985 - 1 respectively. From this information, we can predict that due to the higher R^2 values overall, the adsorption of both metals follows a pseudo-second order kinetic behavior. This information assumes that the rate-limiting step of adsorption is due to chemisorption from valency forces via electron exchange between DTO-WB and both metals which results in best data correlation [53]. As summarized in Table 4.1, the calculated and experimentally observed adsorption capacity at equilibrium were very similar. Therefore, it can be concluded that the methods used to fit obtained experimental data to the pseudo-second order model are reliable.

4.4 Activation Energies of Pt and Pd adsorption

Using rate constant k_1 calculated from the pseudo-first order kinetic model, the energy of activation (E_A) for the adsorption of both Pt and Pd by DTO-WB could be obtained using Eq. 2.6 from section 2.6. By evaluating the pseudo-first order rate constant k_1 against temperature in kelvins, an Arrhenius plot was created, as displayed in Fig 4.6.

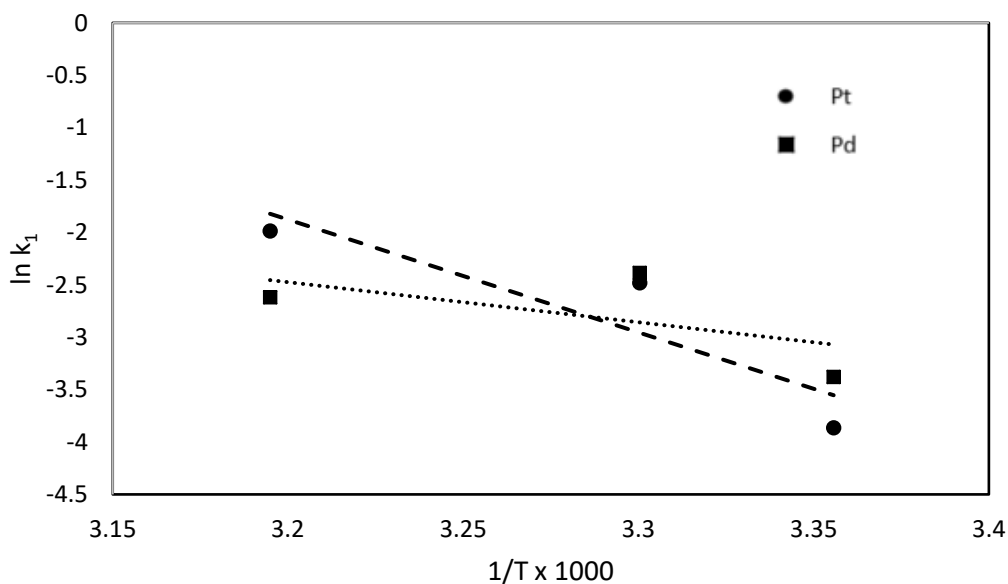


Fig 4.6. Arrhenius plot obtained from the pseudo-first order kinetic data of platinum and palladium adsorption by dithiooxamide-immobilized wood bark where T is temperature in kelvins and k_1 represents the rate constant calculated from the pseudo-first order kinetic model.

From calculations, it was determined that the corresponding E_A for Pt and Pd adsorption were 89.5 kJ/mol and 31.8 kJ/mol. Although the calculated E_A of Pt adsorption was higher than the previously established range of 8.4 - 83.7 kJ/mol required for physisorption, as E_A required to indicate physisorption is usually not over 4.2 kJ/mol, we can infer that the high activation energies expressed by DTO-WB for the adsorption of both metals is due to chemisorption and that adsorption is governed by chemical bonds and interactions beyond van der Waals forces.

4.5 Biosorption isotherm models

This section details the application of the Langmuir and Freundlich adsorption isotherms to the obtained experimental data of Pt and Pd adsorption on DTO-WB. The experimental adsorption data for the recovery of Pt and Pd are displayed accordingly in Fig 4.7. From the information in the experimental plot, we can apply the linear forms of the Langmuir and Freundlich isotherm models which were expressed in section 2.6 as Eqs. 2.2 and 2.3 respectively. In doing so we obtain the corresponding Eqs. 4.5 and 4.6 for the linear Langmuir and Freundlich isotherm equations:

$$\frac{C_e}{q_e} = \frac{1}{q_{max}K_L} + \frac{1}{q_{max}}C_e \quad (4.5)$$

$$\log q_e = \log K_F + \frac{1}{n}\log C_e \quad (4.6)$$

By applying results from Fig 4.7 to Eqs. 4.5 and 4.6, experimental results can be fitted to the Langmuir and Freundlich models to create Fig 4.8 and Fig 4.9. A summary of calculated Langmuir parameters is also shown in Table 4.2.

Table 4.2. Summary of various parameters obtained from the application of the linear Langmuir equation from experimental data for the adsorption of platinum and palladium by dithiooxamide-immobilized wood bark. Note: (a) indicates observed data and (b) indicates calculated data.

Temperature (°C)	Langmuir equation	q_{\max}^a (ppm/mg)*	q_{\max}^b (ppm/mg)*	K_L
Pt				
25	$y = 0.0197x + 0.7461$	51	50.76	0.026
30	$y = 0.0151x + 0.6005$	63	66.23	0.025
Pd				
25	$y = 0.0101x + 0.0636$	100	99.01	0.159
30	$y = 0.0068x + 0.0847$	146	147.06	0.080

* Unit of q_{\max} is defined as amount of metals (mg) per liter of solution per mg of sorbent used.

Table 4.2 confirmed that the experimental and calculated values of q_{\max} were sufficiently comparable. Therefore, one can assume that the method applied to experimental data with the linear Langmuir equation resulted in a reliable fitting. Although only 2 temperature conditions were tested, it was evident from both q_{\max}^a and q_{\max}^b that increasing the temperature by 5°C from 25°C to 30°C was able to improve the adsorption capacity of both Pt and Pd by DTO-WB.

Similarly, as in the case of the fitting of kinetic rate equations, the adsorption behavior of DTO-WB in terms of adsorption isotherm can be predicted with the obtained R^2 correlation coefficients. For the R^2 values obtained from trendlines of Langmuir and Freundlich isotherm plots, refer to Table 4.3.

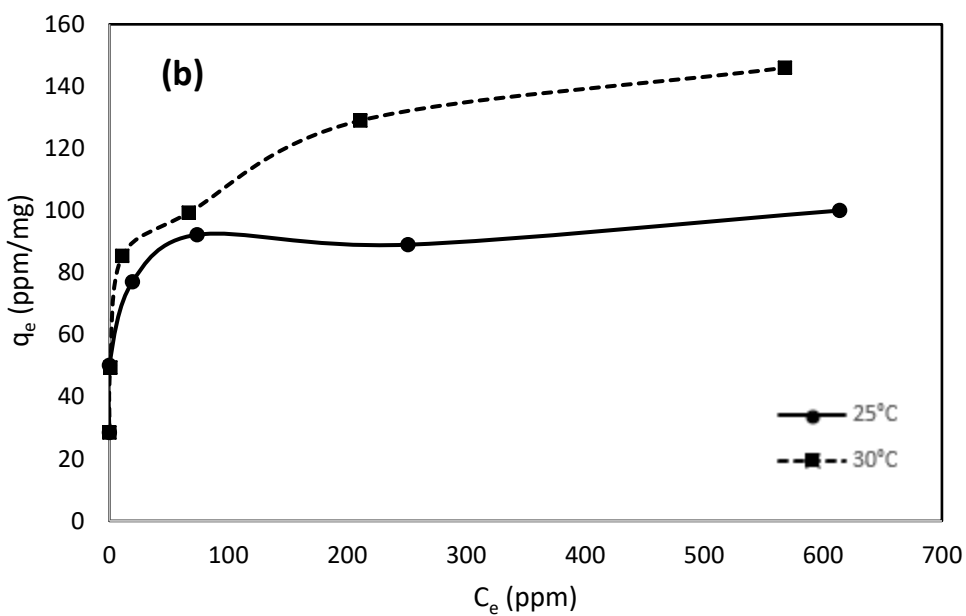
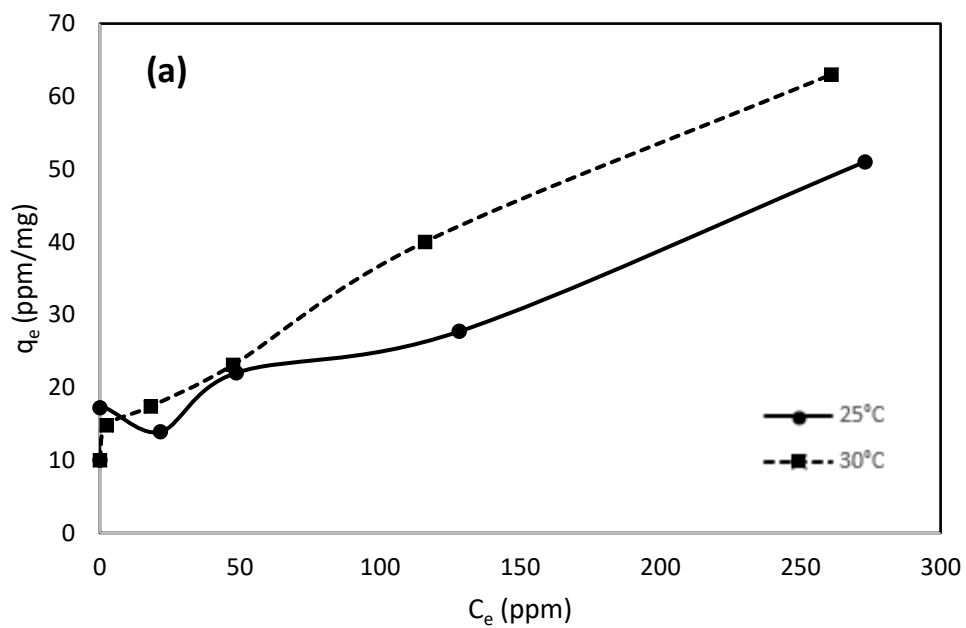


Fig 4.7. Experimental data plots for platinum (a) and palladium (b) adsorption by dithioamide-immobilized wood bark. Operating conditions: Solution volume = 20 mL, sorbent dosage = 20 mg, shaking time = 48 h, shaking speed = 200 rpm. Note: lines present in this graph do not have any mathematical purpose and are drawn to guide reader's eyes only.

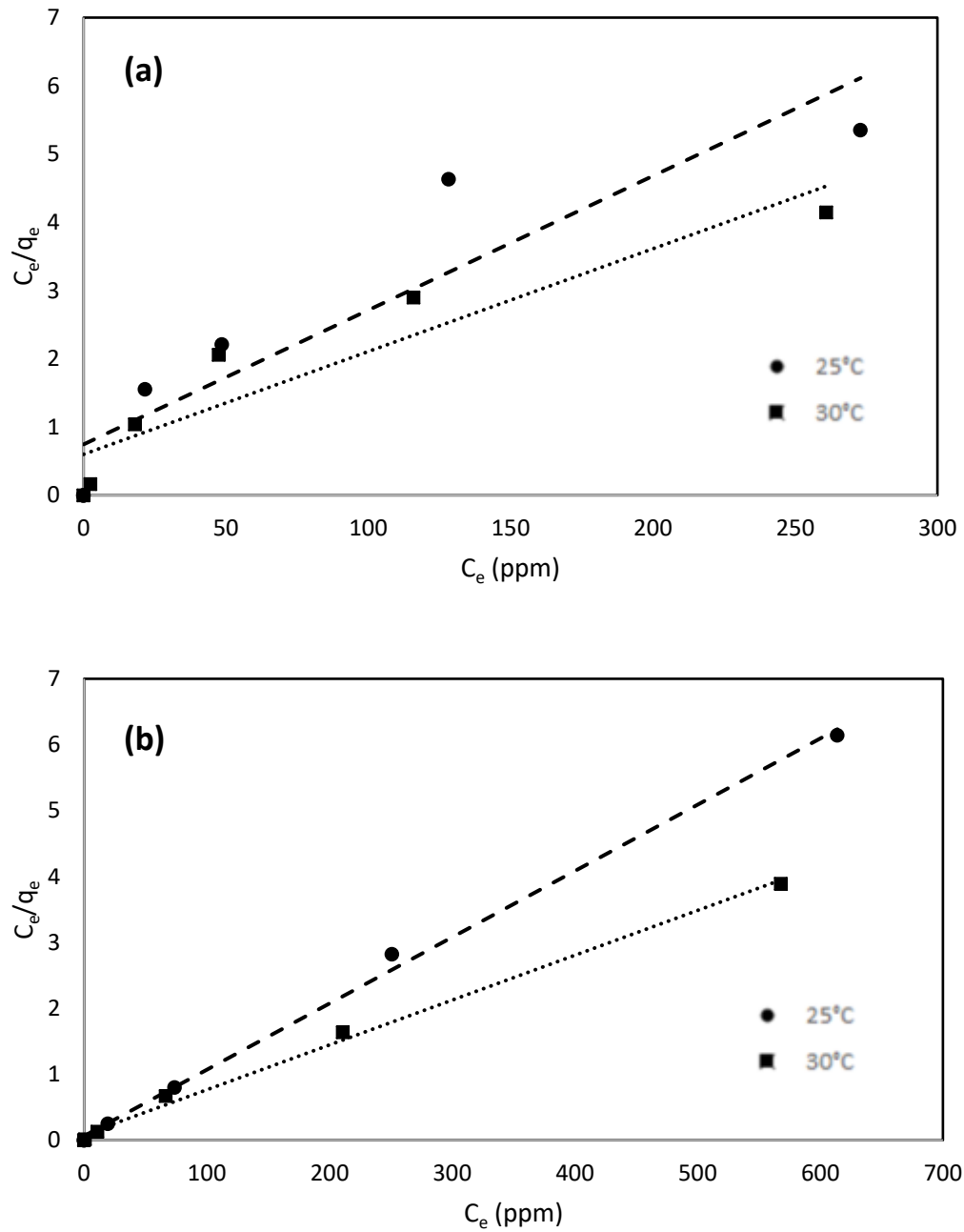


Fig 4.8. Langmuir isotherm plots of platinum (a) and palladium (b) adsorption by dithiooxamide-immobilized wood bark. Note: Lines represent trendline fitting of data.

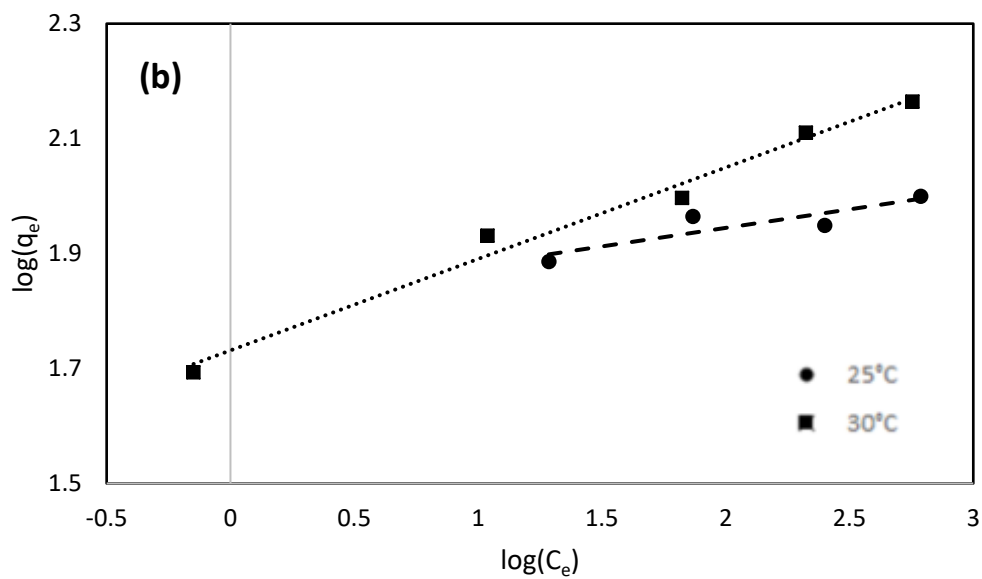
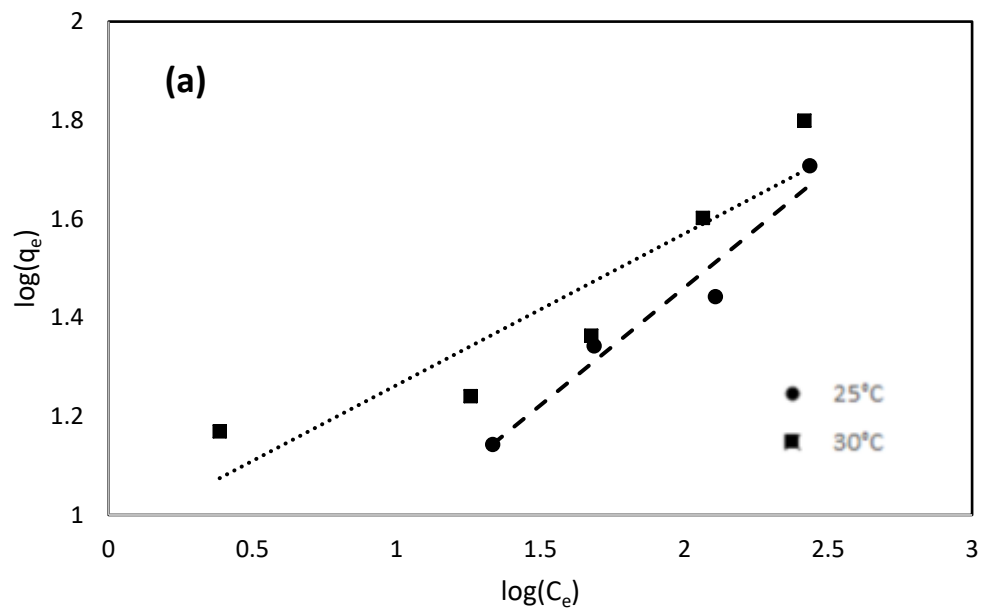


Fig 4.9. Freundlich isotherm plots of platinum (a) and palladium (b) adsorption by dithiooxamide-immobilized wood bark. Note: Lines represent trendline fitting of data.

Table 4.3. Summary of all obtained R^2 correlation coefficients for the Langmuir and Freundlich isotherm plots obtained from the adsorption of platinum and palladium by dithiooxamide-immobilized wood bark.

Temperature (°C)	R^2 coefficient values	
	Langmuir	Freundlich
Pt		
25	0.847	0.850
30	0.878	0.956
Pd		
25	0.998	0.789
30	0.996	0.984

According to the data obtained, R^2 coefficients of the Freundlich model were higher for Pt adsorption than for the Langmuir model. However, the reverse is true for Pd adsorption with both temperatures exhibiting higher R^2 values for fitting with the Langmuir model. This information suggests that Pt adsorbs onto the surface of DTO-WB in a heterogenous multilayer fashion whereas Pd adsorbs onto the biosorbent with homogenous monolayer arrangements of uniform energy. One hypothesis for this phenomenon of inconsistent isotherm model fittings for each metal may be due to the possibility of Pd adsorbing first onto the surface of DTO-WB in a monolayer fashion. It is possible that after a significant surface of DTO-WB had been saturated with Pd, Pt then adsorbs on top of the Pd layer, thus following the Freundlich model of multilayer adsorption.

Similar adsorption isotherm studies conducted by Khunathai et al. [40] on DTO-microalgae observed that experimental data plots (q_e vs C_e) of both Pt and Pd adsorption exhibited plateaus at high metal concentrations, adhering to the Langmuir adsorption model. When evaluated with the linear Langmuir model equation for the recovery of Pt and Pd, DTO-microalgae generated R^2 values of 0.9976 and 0.9895 at 25°C and 0.9976 and 0.9906 at 30°C respectively. By comparison to these previously reported results, the Langmuir fitting of the current research yielded discrepancies as Pd adsorption exhibited poorer fitting in the case of DTO-microalgae which was better suited for the model when analyzed against for DTO-WB.

However, as the Freundlich model was not studied for DTO-microalgae, an adequate comparison of the adsorption isotherm cannot be drawn between the two studies.

4.6 Thermodynamic analysis of adsorption

Throughout the research, there has been evidence that the increase of operating temperatures seemed to improve the efficiency of Pd and Pt adsorption by DTO-WB. This phenomenon was further analyzed by conducting a study on the thermodynamic behaviors of the biosorbent. In this section, the changes in Gibb's free energy (ΔG°), enthalpy (ΔH°) and entropy (ΔS°) were calculated using Eqs. 2.7 and 2.8 mentioned in section 2.6. In addition, the following Eq. 4.7 was also used [19]:

$$K_c = \frac{C_{Ae}}{C_e} \quad (4.7)$$

Where K_c represents the equilibrium constant. C_{Ae} is the concentration of metal ions on adsorbent at equilibrium and C_e is the concentration of metal remaining in solution at equilibrium. As both C_{Ae} and C_e are measured in ppm/mL, K_c is unitless. It should be noted that calculations made in for this thermodynamic analysis is based on assumptions that experimental conditions are in reference to the standard state. By plotting $\ln K_c$ against $1/T$ (where T represents temperature in kelvins) in what is known as a van't Hoff plot, it is possible to calculate ΔH° and ΔS° by using Eq. 2.8. The obtained van't Hoff linear plot and corresponding trendline equations are demonstrated in Fig 4.10.

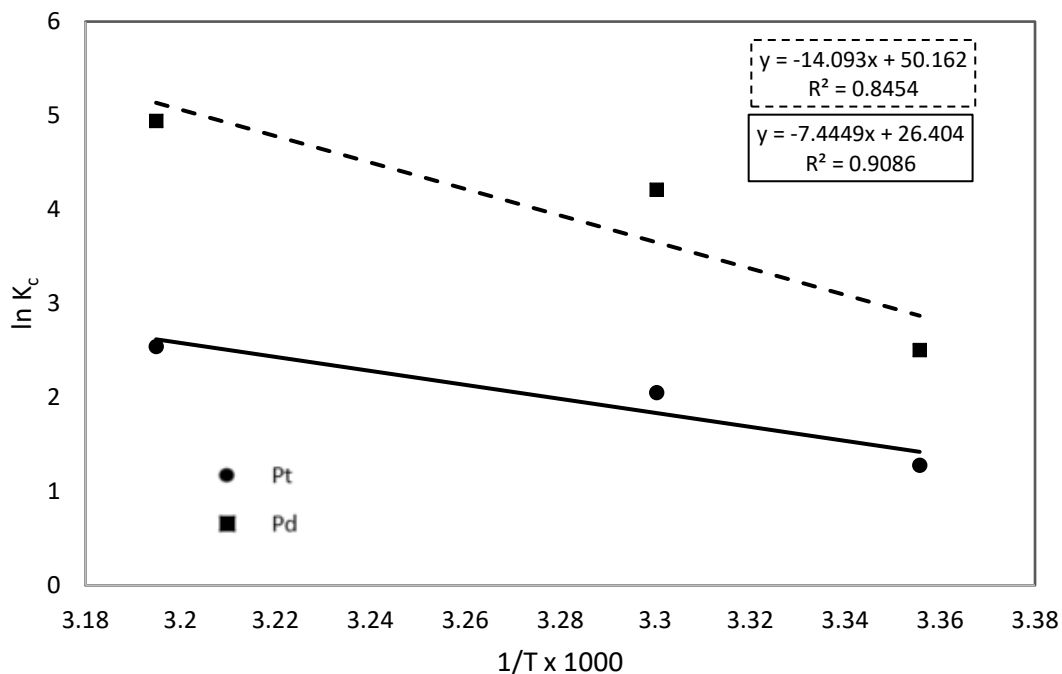


Fig 4.10. van't Hoff plot of the adsorption of platinum and palladium by dithiooxamide-immobilized wood bark. Trendline equations obtained are displayed for Pt (solid box) and Pd (dashed box) adsorption. Operating conditions: Initial platinum and palladium concentration = 20 and 44 ppm respectively, solution volume = 200 mL, sorbent dosage = 200 mg, stirring time = 24 h, stirring speed = 200 rpm.

Using the trendlines generated from the plot for Pd (displayed in dashed box) and Pt (displayed in solid box), thermodynamic parameters were calculated and are summarized in Table 4.4. The obtained ΔG° was revealed to be negative for both Pt and Pd adsorption, indicating that the adsorption process is spontaneous in nature and with increasing temperature, becomes more stable thermodynamically. Positive ΔS° signifies that randomness of the system during the adsorption process increases. This increase in entropy may be due to the increased amount of open space in solution as adsorption proceeds, thereby increasing the number of configurations that residual metal ions can exist in the space. Finally, the positive ΔH° confirms the trend previously observed that increasing temperatures also increases adsorption efficiency, explaining that the adsorption for Pt and Pd by DTO-WB is an endothermic process.

Similarly in previously conducted experiments, Khunathai et al. [26] observed that the adsorption efficiencies of DTO-microalgae on the recovery of Pt and Pd is enhanced with increasing temperature, indicating that adsorption progresses via an endothermic reaction. This hypothesis was confirmed by thermodynamic studies which determined that calculated ΔH°

values were positive at 25°C, 30°C and 40°C. Additionally, ΔS° values were also calculated for the case of DTO-microalgae and although numerically very dissimilar to the obtained results for DTO-WB, change of entropy values were also determined to be positive, indicating an increase in randomness. Khunathai et al. [40] also determined that ΔG° values of DTO-microalgae for adsorption were negative thus concluding that the adsorption process of Pt and Pd is spontaneous and favorable at increasing temperatures.

Table 4.4. Summary of all calculated thermodynamic parameters for the adsorption of platinum and palladium by dithiooxamide-immobilized wood bark.

Temperature (K)	K_c	ΔG° (kJ mol ⁻¹)	ΔS° (J mol ⁻¹ K ⁻¹)	ΔH° (J mol ⁻¹)	R^2
Pt					
298	3.59	-3.17			
303	7.79	-5.17	220	61.9	0.909
313	12.7	-6.62			
Pd					
298	12.2	-6.20			
303	67.4	-10.6	417	118	0.845
313	140	-12.9			

4.7 Trace metal co-adsorption

As exhibited by Table 3.2 in section 3.7, the PLS studied in the research herein contains other dissolved metal species of varying concentrations. As such a scenario will be a regular case due to the nature of real leach solution, the effectiveness of DTO-WB in co-adsorbing these metal ions was studied. Fig 4.11 demonstrates that DTO-WB was efficient in recovering silver (Ag) and rhodium (Rh), exhibiting high adsorption percentages of 73% at 25°C and 78% at 40°C respectively. This result indicates that DTO-WB is not only effective in the adsorption of Pt and Pd as was evident in the current research, it is also effective in recovering other noble metals. Selenium (Se), which according to the World Health Organization can be toxic to human health at consumption levels over 10 ppb in drinking water, was shown to be adsorbed in significant amounts with surprising selectivity at 25°C however, no sign of adsorption was shown at higher

temperatures [54]. This information suggests that not only is DTO-WB effective for use in the hydrometallurgical industry to recover PM, with further research the biosorbent may prove to have effective applications in the water treatment industry.

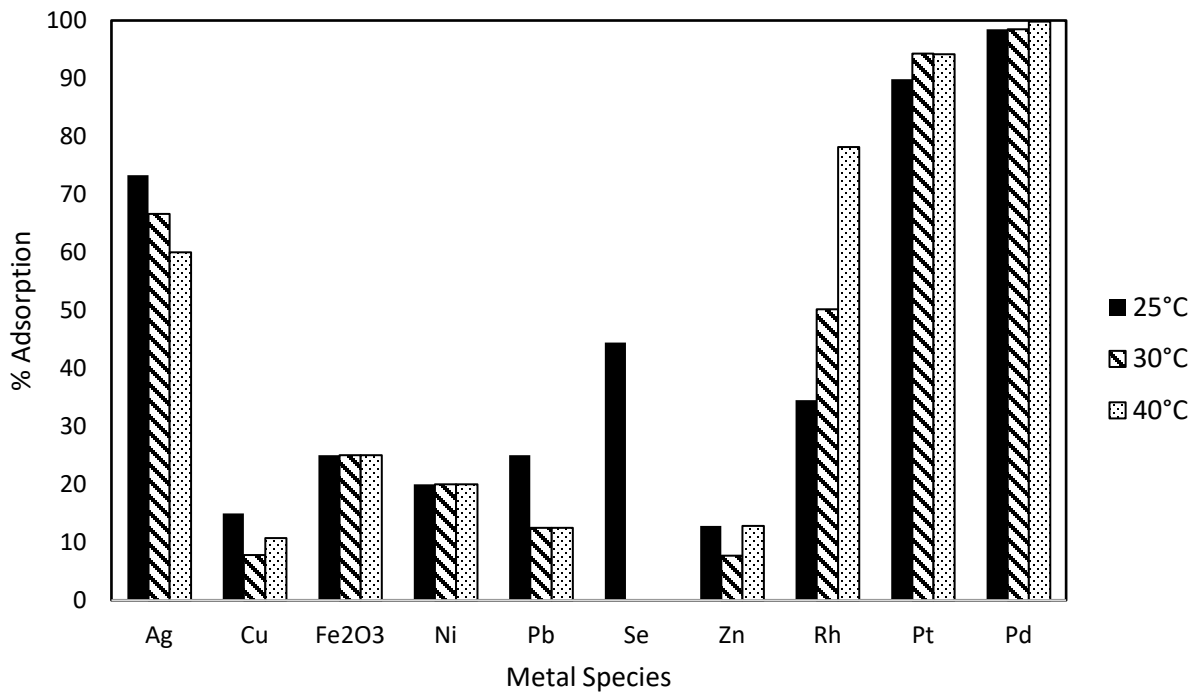


Fig 4.11. Comparison of effectiveness in co-adsorption of all detectable metal species in received pregnant leach solution by dithiooxamide-immobilized wood bark at various temperatures. Operating conditions: Initial platinum and palladium concentrations = 20 and 44 ppm, solution volume = 200 mL, sorbent dosage = 200 mg, stirring speed = 200 rpm.

CHAPTER 5: Conclusions and Recommendations

5.1 Summary of research and obtained results

The research work herein examined the development of 12 novel biosorbents created from wheat straw, canola meal and wood bark-based mulch which were immobilized with dithiooxamide, ethylenediamine and primary amine. These biosorbents were tested for their efficiency in recovering platinum (Pt) and palladium (Pd) from real pregnant leach solution obtained from a Canadian refinery plant.

From the initial one-point adsorption test, it was determined that out of all biosorbents that were created, Pt and Pd were most effectively recovered by dithiooxamide-immobilized wood bark (DTO-WB) which was able to recover 97.4% Pt and 99.8% Pd from leach solution. FT-IR spectra peaks of 1624 cm^{-1} and 1570 cm^{-1} which signify secondary amine moiety and peaks at 1153 cm^{-1} , 1096 cm^{-1} and 1022 cm^{-1} which indicate the existence of thiocarbonyl groups confirms that DTO immobilization on wood bark was successful. After synthesis with DTO, the sulfur and nitrogen content of wood bark were revealed to have increased by 26.8% and 2.2% respectively, further affirming that DTO immobilization was successful.

Solid-liquid ratio experiments concluded that the optimal dosage for DTO-WB was revealed to be at 2.5 S/L ratio. Adsorption kinetic studies explained that the rate of adsorption followed a pseudo-second order model in both the adsorption of Pt and Pd. Adsorption isotherm studies suggests that the adsorption of Pt by DTO-WB follows a multilayer Freundlich model whereas Pd adsorption is monolayer in nature, following the Langmuir model. The energy of activation for the adsorption process of Pt and Pd was calculated to be 89.5 kJ/mol and 31.8 kJ/mol respectively, signifying that the adsorption process progressed via chemisorption.

In terms of thermodynamics, positive enthalpy change that DTO-WB exhibits confirms that the adsorption process is endothermic in nature and an increase in temperature will produce a more favorable effect in adsorption. A negative change in Gibb's free energy suggests that the process of adsorption for both Pt and Pd is spontaneous in nature and becomes more stable with an increase in temperature. Due to the nature of real leach solution, an investigation in co-adsorption by DTO-WB on various existing trace metals was performed. It was discovered that DTO-WB was effective in recovering other noble metals, particularly silver and rhodium. The

significant adsorption of selenium by DTO-WB at room temperature also suggests that the biosorbent may have applications in water treatment.

In accordance to the objectives established at the beginning of this thesis in section 1.3, the present work achieved in the creation, experimentation and analysis of biosorbents and their effects in adsorbing Pt and Pd from real PLS by:

1. Selecting wheat straw (WS), canola meal (CM) and wood bark (WB) which were all obtained within Saskatchewan as the biomass of choice.
2. Preparing novel biosorbents from the three selected biosorbents via three methods of immobilization with dithiooxamide (DTO), ethylenediamine (EN) and primary amine (PA) to create 12 total biosorbents.
3. Determining the efficacy of all biosorbents via a one-point adsorption test to evaluate and compare the adsorption capabilities of all 12 biosorbents, after which DTO-WB was determined to be the optimal biosorbent.
4. Characterizing DTO-WB via FT-IR and CHNS analysis to exhibit the successful implementation of DTO functional groups on the compound structure. Further BET and particle size analyses gave insight into the surface area, pore volume, pore size and particle size distributions of the biosorbent.
5. Analysis of the effect of sorbent dosage and initial metal concentration along with the fitting of DTO-WB adsorption results to pseudo-first and pseudo-second order kinetic models, Langmuir and Freundlich adsorption isotherm models and the subsequent determination of E_A , ΔG° , ΔH° and ΔS° .

Overall, this research work successfully developed an alternative to conventional methods of PM recycling which is potentially more cost effective and environmentally friendly. The implications of the obtained results suggest that the value adding of WB which is often considered a waste product may generate financial gain recuperated in the extraction of PM. This indicates that DTO-WB has potential to fill the unexplored gap in the present state of the PM recycling industry by cost effectively and efficiently extracting Pt and Pd from real leach solutions using a seldom studied biomass. DTO-WB is superior in terms of environmental sustainability as it can be created and utilized without the excessive energy requirements and

generation of non-biodegradable secondary wastes associated with pyrometallurgical or other hydrometallurgical processing methods.

5.2 Challenges encountered in present research

Although useful results were obtained from the research and an effective adsorbent was successfully developed, the present research work was not without difficulties. In this section some challenges which were encountered during the experimental and analytical process will be discussed. Firstly, the lack of access to analytical instruments during the progress of this research meant that a large part of analysis work was outsourced to other laboratories. This was considered a disadvantage as opportunities in learning how to operate some analytical equipments were lost.

Due to the lack of sufficient research planning, some difficulties were encountered during the procurement process of chemicals. Thionyl chloride and ethanol are considered controlled chemicals in Canada and for such reason, it was not able to be delivered directly from the United States, causing a 6-week delay before DTO-type and PA-type biosorbents could be created. In the future, it should be ensured that proper planning must be implemented to ensure that all reactants and materials would have been procured ahead of time before any research work takes place to avoid delay.

The production process of PA-type adsorbent was extremely laborious due to the steps and reagents required for creating the adsorbent. With each consecutive step in synthesis, the yield decreases drastically until the original 50 g of raw biomasses that were used resulted in only generating 2 g or less of the final product. It must be acknowledged that again, higher efforts into preparing the experimental process before and during the synthesis of biosorbents would have ensured that proper amounts of raw materials and reagents are used to generate enough product.

In terms of the analytical process itself, it has been acknowledged that the obtained adsorption isotherm R^2 values for Pt and Pd adsorption were contradictory, with Pt adsorption following the Freundlich model and Pd adsorption following the Langmuir model. However, this may be due to the fact that such models were originally meant for solutions containing a low variety of solutes. Due to the nature of real PLS where many trace metals may co-exist and all

interact with each other within the solution, adsorption behavior is unpredictable with analytical methods of data generally used by conventional biosorption research which uses synthetic PLS.

Another factor which may have affected the accuracy of adsorption results in this thesis is the usage of Whatman no.40 filter paper throughout experiments. Paper contains a significant amount of cellulose which may have contributed to unnecessary additional adsorption of metals from solution samples. For this reason, it may very well be possible that obtained results regarding the recovery efficiency of biosorbent are not represented properly as calculated results may have been inaccurate.

Due to the novel nature of the current research work in which Pt and Pd were extracted from real PLS, there were very few studies which were similar enough to make comparison of results with. In addition to this point, DTO-immobilization is also a novel processing method which in the current study was applied to biomasses of which some had never been studied in its modified form before. Although DTO-microalgae which was previously synthesized by Khunathai et al. [40] was heavily referred to in this text for benchmarking results, the current work conducted some additional experimental analyses which could not be compared to for similarity.

5.3 The biosorption potential of canola meal

To confirm whether CM exhibits a high adsorption rate towards Pt and Pd, an additional one-point adsorption test was performed to compare the adsorption efficiencies of protein-free canola meal (CM), unwashed canola meal received as is (CM-NW) and protein-intact canola meal which has undergone benzene-ethanol washing (CM-P). For this experiment, 1 g of each adsorbent were introduced into vials containing 20 mL of diluted PLS with initial concentrations of 35 ppm and 135 ppm Pt and Pd respectively. The mixtures were then shaken at room temperature for 24 h at 200 rpm. Fig 5.1 and Fig 5.2 displays the three canola meal forms before and after the adsorption process. The adsorption percentage of each CM-based biosorbent is presented in Fig 5.3.

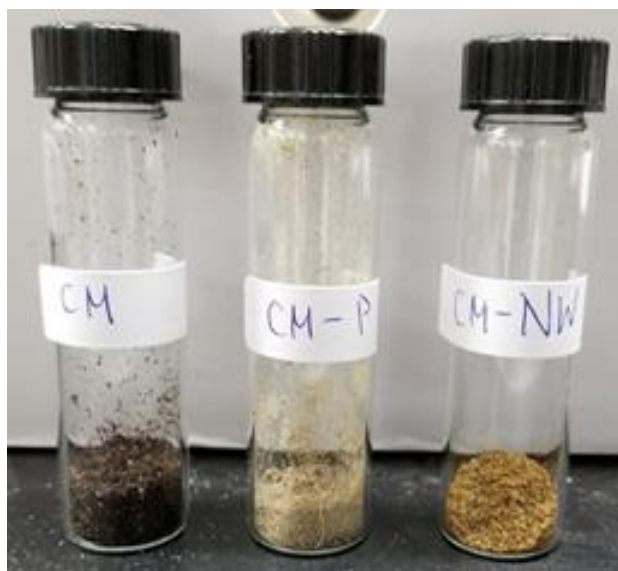


Fig 5.1. Protein-free canola meal (CM), protein-intact benzene-ethanol washed canola meal (CM-P) and protein-intact unwashed canola meal (CM-NW) before adsorption.

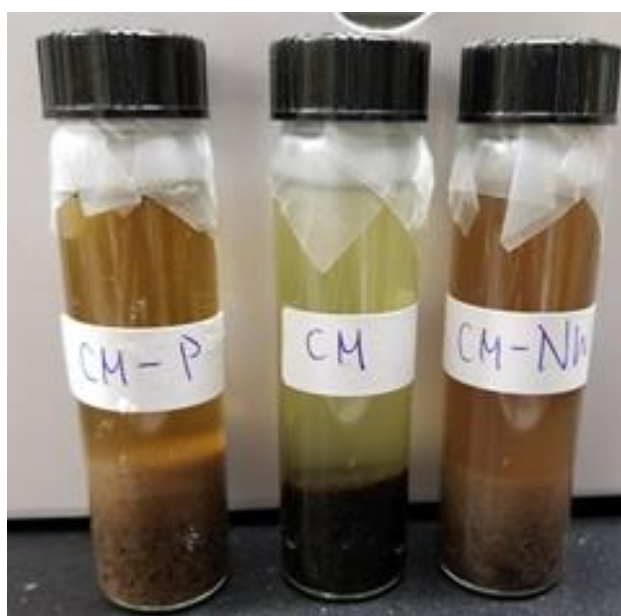


Fig 5.2. Protein-free canola meal (CM), protein-intact benzene-ethanol washed canola meal (CM-P) and protein-intact unwashed canola meal (CM-NW) in diluted pregnant leach solution after 24 hours of shaking.

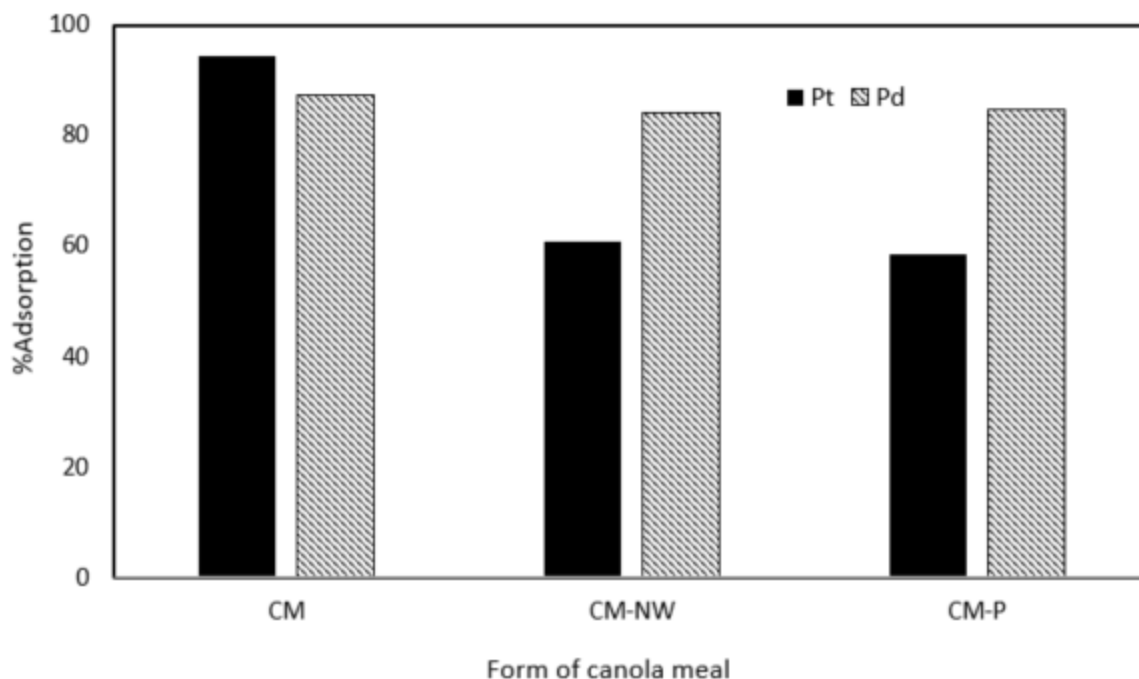


Fig 5.3. Adsorption efficiencies of protein-free canola meal (CM), protein-intact benzene-ethanol washed canola meal (CM-P) and protein-intact unwashed canola meal (CM-NW) in recovering platinum (black bar) and palladium (striped bar). Operating conditions: Initial palladium and platinum concentrations = 135 ppm and 35 ppm respectively, sorbent dosage = 1 g, solution volume = 20 mL, shaking speed = 200 rpm, shaking time = 24 h.

As can be observed in Fig 5.2, the filtrate solution for CM was more opaque and not as colorless as the filtrate solution from the one-point adsorption trial in Fig 3.12, suggesting that perhaps not as much of the metal ions in the solution were recovered. This qualitative hypothesis was confirmed as Fig 5.3 revealed that despite similar experimental conditions, CM was able to adsorb 94.4% and 87.1% Pt and Pd respectively compared to 94.9% Pt and 99.2% Pd adsorption in the first trial. However, this discrepancy in adsorption efficiency may be due to the lack of the 48-hour settling time which was implemented in the first trial. This suggests that Pt adsorption by CM was able to reach equilibrium faster than the adsorption of Pd as the adsorption efficiencies exhibited by Pt was minor.

CM-NW and CM-P exhibit very similar adsorption, both reaching approximately 60% adsorption for Pt and 84% adsorption for Pd respectively. The Pd adsorption efficiencies achieved by these two adsorbents were only 3% different from that of CM and are thus quite similar. This result suggests that the removal of protein from canola meal did not have a

significant impact on the recovery of Pd however, the presence of protein hinders the adsorption of Pt. The results of this one-point adsorption test reveals that CM may have an added value use in recovering precious metals and the selective recovery of Pd in the presence of Pt may be achieved by removing or retaining protein in the adsorbent. The overall results of CM-type adsorbents signify that an even more cost effective and environmentally friendly biosorbent may be used in the recovery of PM without sacrificing adsorption efficiency.

As previously mentioned in section 3.7, raw CM was observed to recover 94.9% of Pt and 99.2% of Pd despite its lack of any immobilization. This result suggests that there is potential for raw CM to be used as an adsorbent in the adsorption of PGM. If implemented on an industrial scale, raw CM may prove to be an even more economical and environmentally sustainable alternative to DTO-WB as it does not need expensive chemicals and laborious processing. However, CM as prepared for adsorption in this research work still required the removal of protein for the sake of comparability with wheat straw and wood bark.

5.4 Recommendations for future work

For future studies regarding DTO-WB, the exact lignin content in terms of percentages when compared to other polyphenols which may exist in wood bark should be observed. This testing is important for the understanding of the adsorbent as it may provide insight into whether lignin indeed plays a significant role in adsorption.

To determine whether the biosorbent may have real potential application on an industrial scale, research into the desorption and recycling of DTO-WB should be conducted. Experiments should be conducted to test different eluent solutions that can be used which will retain the highest adsorption potential for DTO-WB in additional PM recovery cycles. Furthermore, the study of metal yield obtained from start to finish of the adsorption process should be studied with consideration of metal reduction via electrowinning and precipitation.

As experiments conducted for the present research was entirely done via batch mode adsorption, future studies should examine how DTO-WB behaves in continuous adsorption mode experiments. In addition to the suggested work, it is advisable that feasibility studies and techno-economic analysis be conducted to gain insight into whether or not the biosorbent is an economically sound alternative to other more conventional methods of adsorption. To confirm

that DTO-WB is indeed an environmentally friendly product, thorough life-cycle analysis on the ecological impact of the biosorbent usage should be conducted.

Finally, although DTO-WB was the most effective and optimal adsorbent out of the 12 biosorbents which were tested in this research, the cost of reagents that were used to create it were very expensive. If recycling of the adsorbent was determined in the future to not be a viable option, this may negate any financial gain obtained from widescale applications in Pt and Pd recovering. Due to this, focus should be shifted towards use of CM as biosorbents.

REFERENCES

- [1] S.W. Won, P. Kotte, W. Wei, A. Lim, Y.-S. Yun, Biosorbents for recovery of precious metals, *Bioresour. Technol.* 160 (2014) 203–212. doi:10.1016/j.biortech.2014.01.121.
- [2] N. Das, Recovery of precious metals through biosorption - A review, *Hydrometallurgy.* 103 (2010) 180–189. doi:10.1016/j.hydromet.2010.03.016.
- [3] P. Ramakul, Y. Yanachawakul, N. Leepipatpiboon, N. Sunsandee, Biosorption of palladium(II) and platinum(IV) from aqueous solution using tannin from Indian almond (*Terminalia catappa* L.) leaf biomass: Kinetic and equilibrium studies, *Chem. Eng. J.* 193 (2012) 102–111. doi:10.1016/j.cej.2012.04.035.
- [4] R. Nuwer, What is the world's scarcest material?, *BBC.* (2014). doi:10.1111/j.1083-6101.2009.01474.x.
- [5] M. Gurung, B.B. Adhikari, H. Kawakita, K. Ohto, K. Inoue, S. Alam, Recovery of gold and silver from spent mobile phones by means of acidothiourea leaching followed by adsorption using biosorbent prepared from persimmon tannin, *Hydrometallurgy.* 133 (2013) 84–93. doi:10.1016/j.hydromet.2012.12.003.
- [6] J. Cui, L. Zhang, Metallurgical recovery of metals from electronic waste: A review, *J. Hazard. Mater.* 158 (2008) 228–256. doi:10.1016/j.jhazmat.2008.02.001.
- [7] B.H. Robinson, E-waste: An assessment of global production and environmental impacts, *Sci. Total Environ.* 408 (2009) 183–191. doi:10.1016/j.scitotenv.2009.09.044.
- [8] S. Sthiannopkao, M.H. Wong, Handling e-waste in developed and developing countries: Initiatives, practices, and consequences, *Sci. Total Environ.* 463–464 (2013) 1147–1153. doi:10.1016/J.SCITOTENV.2012.06.088.
- [9] S. Honda, D.S. Khatriwal, R. Kuehr, Regional E-Waste Monitor East and Southeast Asia, 2016. <http://ewastemonitor.info/pdf/Regional-E-Waste-Monitor.pdf> (accessed June 2, 2018).
- [10] L. Zhang, Z. Xu, A review of current progress of recycling technologies for metals from waste electrical and electronic equipment, *J. Clean. Prod.* 127 (2016) 19–36. doi:10.1016/j.jclepro.2016.04.004.

- [11] T.E. Graedel, E.M. Harper, N.T. Nassar, P. Nuss, B.K. Reck, Criticality of metals and metalloids., *Proc. Natl. Acad. Sci. U. S. A.* 112 (2015) 4257–62.
doi:10.1073/pnas.1500415112.
- [12] K. Crowley, Gold Miners Are Running Out of Metal: Five Charts Explaining Why, *Bloom. Mark.* (2016). <https://www.bloomberg.com/news/articles/2016-12-21/gold-miners-are-running-out-of-metal-five-charts-explaining-why> (accessed April 2, 2017).
- [13] B. Volesky, Biosorbents for metal recovery, *Trends Biotechnol.* 5 (2017) 96–101.
doi:10.1016/0167-7799(87)90027-8.
- [14] Z. Wang, C. Fang, M. Mallavarapu, Characterization of iron–polyphenol complex nanoparticles synthesized by Sage (*Salvia officinalis*) leaves, *Environ. Technol. Innov.* 4 (2015) 92–97. doi:10.1016/j.eti.2015.05.004.
- [15] J.R. Dodson, H.L. Parker, A. Muñoz García, A. Hicken, K. Asemave, T.J. Farmer, H. He, J.H. Clark, A.J. Hunt, Bio-derived materials as a green route for precious & critical metal recovery and re-use, *Green Chem.* 17 (2015) 1951–1965. doi:10.1039/c4gc02483d.
- [16] S. Alam, *Biosorption: Theory and Application for Sustainable Hydrometallurgical Processing*, (2015) 120.
- [17] Adsorption, Absorption and Desorption — What’s the Difference?, *Chromatogr. Today.* (2014). <https://www.chromatographytoday.com/news/hplc-uhplc/31/breaking-news/adsorption-absorption-and-desorption-mdash-whatsquos-the-difference/31397> (accessed August 30, 2018).
- [18] S. Quideau, D. Deffieux, C. Douat-Casassus, L. Pouységu, Plant Polyphenols: Chemical Properties, Biological Activities, and Synthesis, *Angew. Chemie Int. Ed.* 50 (2011) 586–621. doi:10.1002/anie.201000044.
- [19] K. Fujiwara, A. Ramesh, T. Maki, H. Hasegawa, K. Ueda, Adsorption of platinum (IV), palladium (II) and gold (III) from aqueous solutions onto l-lysine modified crosslinked chitosan resin, *J. Hazard. Mater.* 146 (2007) 39–50. doi:10.1016/j.jhazmat.2006.11.049.
- [20] M. Gurung, B.B. Adhikari, K. Khunathai, H. Kawakita, K. Ohto, H. Harada, K. Inoue, Quaternary Amine Modified Persimmon Tannin Gel: An Efficient Adsorbent for the

- Recovery of Precious Metals from Hydrochloric Acid Media, *Sep. Sci. Technol.* 46 (2011) 2250–2259. doi:10.1080/01496395.2011.594698.
- [21] G. Colica, S. Caparrotta, G. Bertini, R. De Philippis, Gold biosorption by exopolysaccharide producing cyanobacteria and purple nonsulphur bacteria, *J. Appl. Microbiol.* 113 (2012) 1380–1388. doi:10.1111/jam.12004.
- [22] K. Alluri-Hima, S. Reddy Ronda, V. Saradhi Settalluri, J. Singh Bondili, Biosorption: An eco-friendly alternative for heavy metal removal, *African J. Biotechnol.* 6 (2007) 2924–2931. doi:10.4314/ajb.v6i25.58244.
- [23] C. Mack, B. Wilhelmi, J.R. Duncan, J.E. Burgess, Biosorption of precious metals, *Biotechnol. Adv.* 25 (2007) 264–271. doi:10.1016/j.biotechadv.2007.01.003.
- [24] V. Binhu, R. Li, J. Huang, S. Kaminskyj, A. Sharpe, A. Hannoufa, Perturbation of lignin biosynthesis pathway in *Brassica napus* (canola) plants using RNAi, *Can. J. Plant Sci.* 89 (2009) 441–453. http://www.usask.ca/biology/kaminskyj/pub/Binhu_CanJPISci.pdf (accessed May 26, 2017).
- [25] D. Parajuli, H. Kawakita, K. Inoue, M. Funaoka, Recovery of Gold(III), Palladium(II), and Platinum(IV) by Aminated Lignin Derivatives, *Ind. Eng. Chem. Res.* 45 (2006) 6405–6412. doi:10.1021/ie0603518.
- [26] K. Khunathai, M. Matsueda, B.K. Biswas, H. Kawakita, K. Ohto, H. Harada, K. Inoue, M. Funaoka, S. Alam, Adsorption Behavior of Lignophenol Compounds and Their Dimethylamine Derivatives Prepared from Rice and Wheat Straws for Precious Metal Ion, *J. Chem. Eng. JAPAN.* 44 (2011) 781–787. doi:10.1252/jcej.10we246.
- [27] B.B. Adhikari, M. Gurung, S. Alam, B. Tolnai, K. Inoue, Kraft mill lignin - A potential source of bio-adsorbents for gold recovery from acidic chloride solution, *Chem. Eng. J.* 231 (2013) 190–197. doi:10.1016/j.cej.2013.07.016.
- [28] A. Demirbaş, Relationships between lignin contents and heating values of biomass, *Energy Convers. Manag.* 42 (2001) 183–188. doi:10.1016/S0196-8904(00)00050-9.
- [29] R. Newkirk, *Canola Meal Feed Industry Guide*, 2009. https://cigi.ca/wp-content/uploads/2011/12/2009-Canola_Guide.pdf (accessed July 6, 2017).

- [30] S. Al-Asheh, Z. Duvnjak, Adsorption of copper by canola meal, *J. Hazard. Mater.* 48 (1996) 83–93. doi:10.1016/0304-3894(95)00141-7.
- [31] J.M. Harkin, J.W. Rowe, Bark and its possible uses, (1971).
<https://www.fpl.fs.fed.us/documnts/fplrn/fplrn091.pdf> (accessed July 17, 2017).
- [32] Q. Yi, R. Fan, F. Xie, H. Min, Q. Zhang, Z. Luo, Selective recovery of Au(III) and Pd(II) from waste PCBs using ethylenediamine modified persimmon tannin adsorbent, *Procedia Environ. Sci.* 31 (2016) 185–194. doi:10.1016/j.proenv.2016.02.025.
- [33] G. Hilson, A.J. Monhemius, Alternatives to cyanide in the gold mining industry: what prospects for the future?, *J. Clean. Prod.* 14 (2006) 1158–1167.
doi:10.1016/J.JCLEPRO.2004.09.005.
- [34] M. Soleimani, T. Kaghazchi, Activated Hard Shell of Apricot Stones: A Promising Adsorbent in Gold Recovery, *Chinese J. Chem. Eng. Eng.* 16 (2008) 12–1. http://ac.els-cdn.com/S1004954108600488/1-s2.0-S1004954108600488-main.pdf?_tid=755055bc-6e35-11e7-8a04-00000aab0f01&acdnat=1500656334_0fa430ab60f1e380cb0f685c38920b02 (accessed July 21, 2017).
- [35] A. Is Bildar, J. Van De Vossenberg, E.R. Rene, E.D. Van Hullebusch, P.N.L. Lens, Two-step bioleaching of copper and gold from discarded printed circuit boards (PCB), *Waste Manag.* 57 (2016) 149–157. doi:10.1016/j.wasman.2015.11.033.
- [36] T.H. Nguyen, L. Wang, M.S. Lee, Separation and Recovery of Precious Metals from Leach Liquors of Spent Electronic Wastes by Solvent Extraction, *Korean J. Met. Mater.* 55 (2017) 247–255.
- [37] T. Rubcumintara, Adsorptive Recovery of Au(III) from Aqueous Solution Using Modified Bagasse Biosorbent, *Int. J. Chem. Eng. Appl.* 6 (2015) 95–100.
doi:10.7763/IJCEA.2015.V6.459.
- [38] O.N. Kononova, T.A. Leyman, A.M. Melnikov, D.M. Kashirin, M.M. Tselukovskaya, Ion exchange recovery of platinum from chloride solutions, *Hydrometallurgy.* 100 (2010) 161–167. doi:<https://doi.org/10.1016/j.hydromet.2009.11.011>.

- [39] M. Inoue, T. Nakano, A. Yamasaki, Fabrication of precious metals recovery materials using grape seed-waste, *Sustain. Mater. Technol.* 3 (2015) 14–16. doi:10.1016/j.susmat.2014.11.005.
- [40] K. Khunathai, K. Inoue, K. Ohto, H. Kawakita, M. Kurata, K. Atsumi, S. Alam, Dithiooxamide-Immobilized Microalgal Residue for the Selective Recovery of Pd(II) and Pt(IV), *Sep. Sci. Technol.* 47 (2012) 1185–1193. doi:10.1080/01496395.2011.645384.
- [41] S.-I. Park, I.S. Kwak, S.W. Won, Y.-S. Yun, Glutaraldehyde-crosslinked chitosan beads for sorptive separation of Au(III) and Pd(II): Opening a way to design reduction-coupled selectivity-tunable sorbents for separation of precious metals, *J. Hazard. Mater.* 248–249 (2013) 211–218. doi:10.1016/j.jhazmat.2013.01.013.
- [42] B. Pangeni, H. Paudyal, K. Inoue, H. Kawakita, K. Ohto, S. Alam, An Assessment of Gold Recovery Processes Using Cross-Linked Paper Gel, *J. Chem. Eng. Data.* 57 (2012) 796–804. doi:10.1021/je201018a.
- [43] S.W. Won, J. Mao, I.-S. Kwak, M. Sathishkumar, Y.-S. Yun, Platinum recovery from ICP wastewater by a combined method of biosorption and incineration, *Bioresour. Technol.* 101 (2010) 1135–1140. doi:10.1016/j.biortech.2009.09.056.
- [44] K. Khunathai, K. Inoue, K. Ohto, H. Kawakita, M. Kurata, K. Atsumi, H. Fukuda, S. Alam, Adsorptive Recovery of Palladium(II) and Platinum(IV) on the Chemically Modified-Microbial Residue, *Solvent Extr. Ion Exch.* 31 (2013) 320–334. doi:10.1080/07366299.2012.757092.
- [45] R.G. Pearson, Hard and Soft Acids and Bases, *J. Am. Chem. Soc.* 85 (1963) 3533–3539. doi:10.1021/ja00905a001.
- [46] H. Song, X. Li, J. Sun, X. Yin, Y. Wang, Z. Wu, Biosorption Equilibrium and Kinetics of Au(III) and Cu(II) on Magnetotactic Bacteria, *Chinese J. Chem. Eng.* 15 (2007) 847–854. doi:10.1016/S1004-9541(08)60013-0.
- [47] A. Sari, D. Mendil, M. Tuzen, M. Soylak, Biosorption of palladium(II) from aqueous solution by moss (*Racomitrium lanuginosum*) biomass: Equilibrium, kinetic and thermodynamic studies, *J. Hazard. Mater.* 162 (2009) 874–879.

doi:10.1016/j.jhazmat.2008.05.112.

- [48] A. Dada, A. Olalekan, A. Olatunya, O. Dada, Langmuir, Freundlich, Temkin and Dubinin–Radushkevich Isotherms Studies of Equilibrium Sorption of Zn²⁺ Unto Phosphoric Acid Modified Rice Husk, IOSR J. Appl. Chem. 3 (2012) 38–45. doi:10.9790/5736-0313845.
- [49] Adsorption Isotherm and its Types, (2009).
<http://www.chemistrylearning.com/adsorption-isotherm/> (accessed April 5, 2017).
- [50] I. Langmuir, The adsorption of gases on plane surfaces of glass, mica and platinum., J. Am. Chem. Soc. 40 (1918) 1361–1403. doi:10.1021/ja02242a004.
- [51] R.O. Herzog, Kapillarchemie, eine Darstellung der Chemie der Kolloide und verwandter Gebiete. Von Dr. Herbert Freundlich. Verlag der Akademischen Verlagsgesellschaft. Leipzig 1909. 591 Seiten. Preis 16,30 Mk., geb. 17,50 Mk, Zeitschrift Für Elektrochemie Und Angew. Phys. Chemie. 15 (n.d.) 948–948. doi:10.1002/BBPC.19090152312.
- [52] Chemisorption and physisorption, Int. Union Pure Appl. Chem. (2009).
http://old.iupac.org/reports/2001/colloid_2001/manual_of_s_and_t/node16.html (accessed August 31, 2018).
- [53] Y.. Ho, G. McKay, Pseudo-second order model for sorption processes, Process Biochem. 34 (1999) 451–465. doi:10.1016/S0032-9592(98)00112-5.
- [54] N. Bleiman, Y.G. Mishael, Selenium removal from drinking water by adsorption to chitosan–clay composites and oxides: Batch and columns tests, J. Hazard. Mater. 183 (2010) 590–595. doi:10.1016/J.JHAZMAT.2010.07.065.

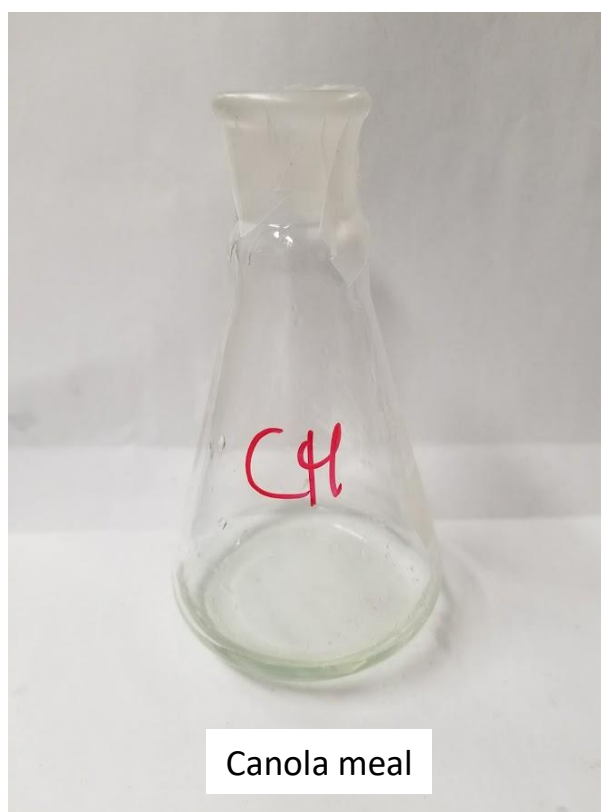
APPENDIX A: Filtrate solutions from one-point adsorption

Raw Biomasses:



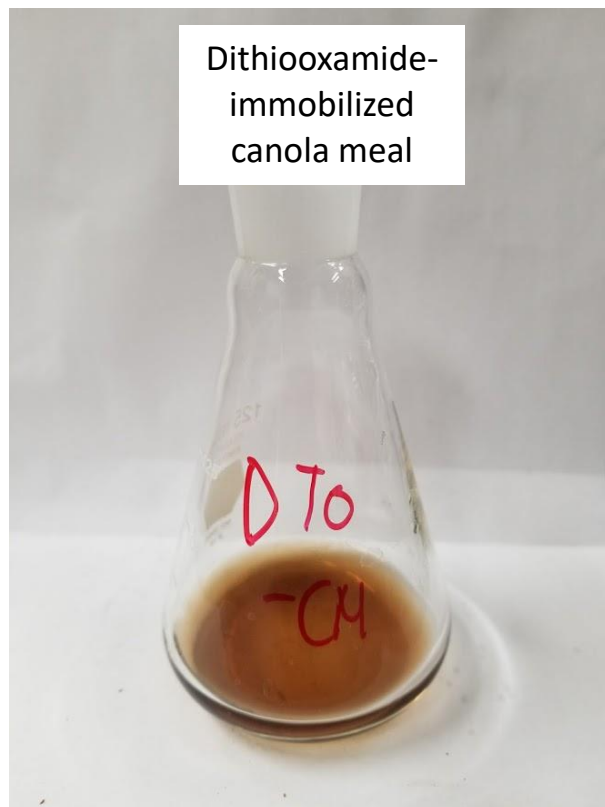
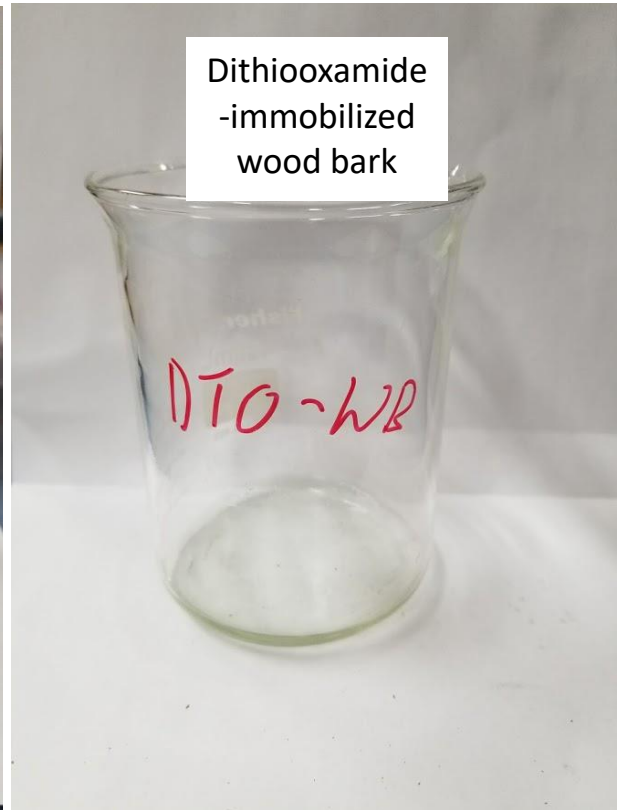
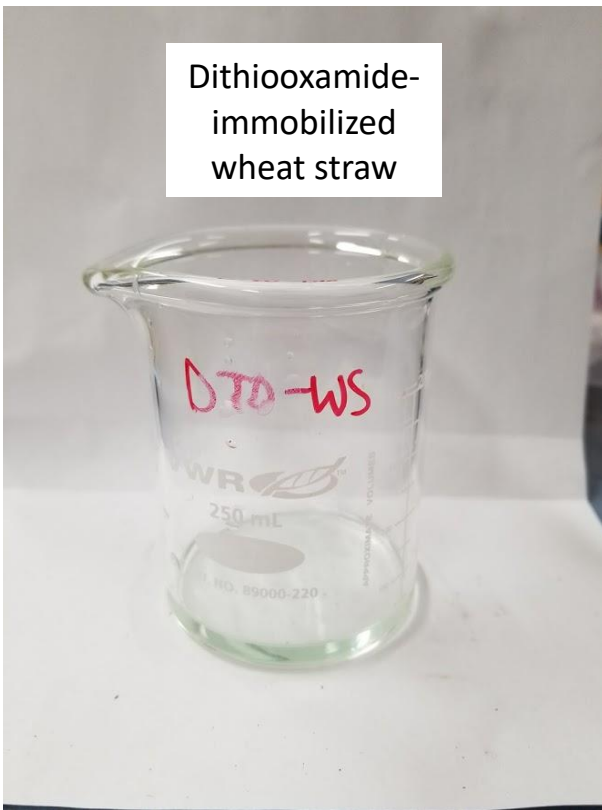
Wheat straw

Wood bark

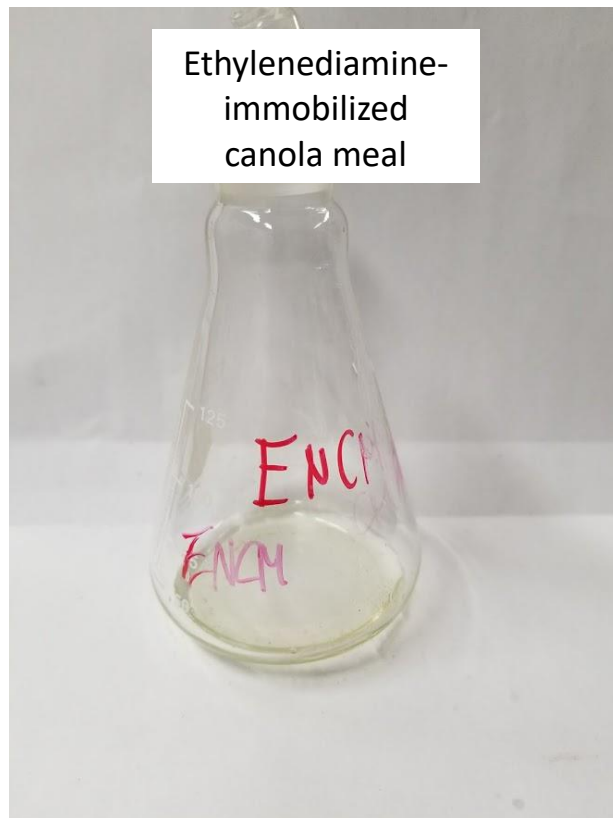
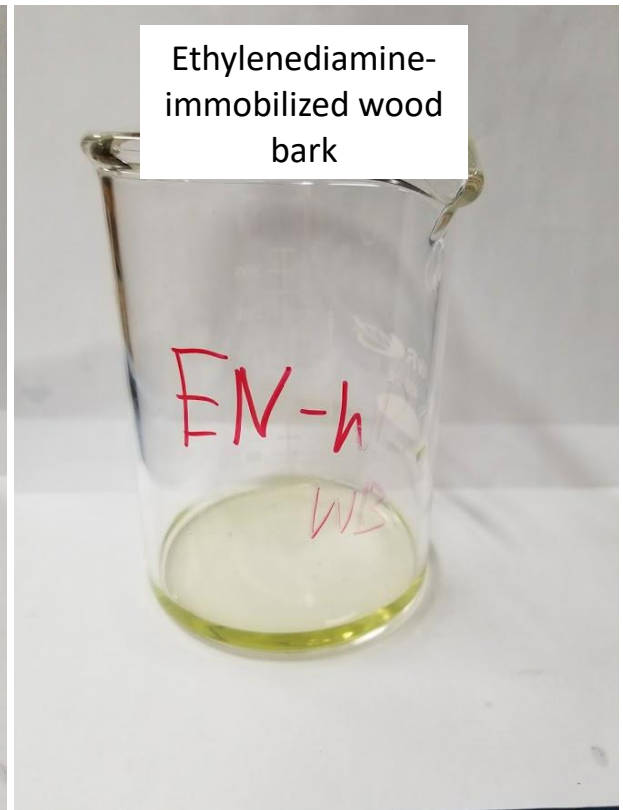
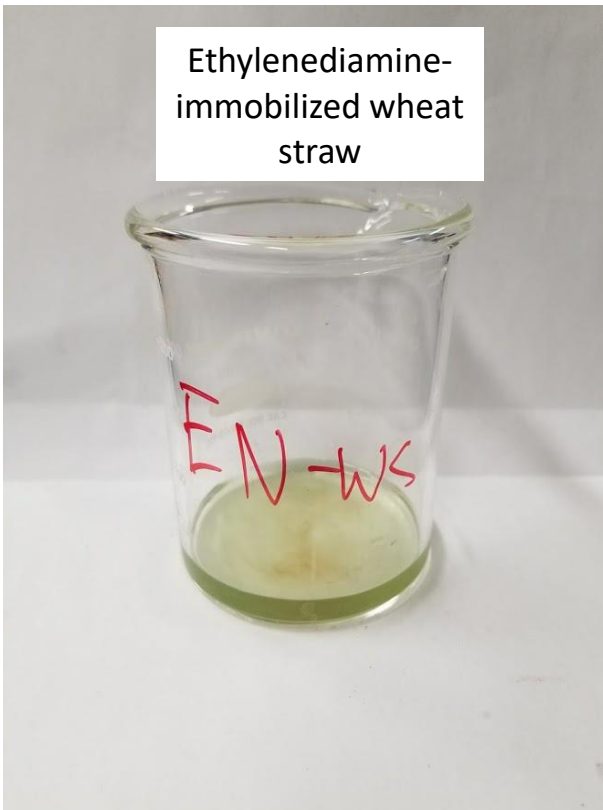


Canola meal

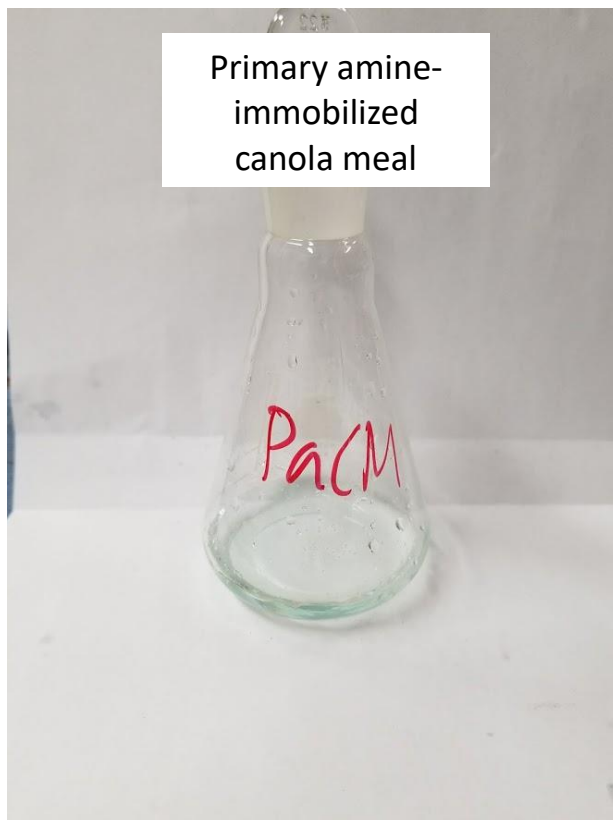
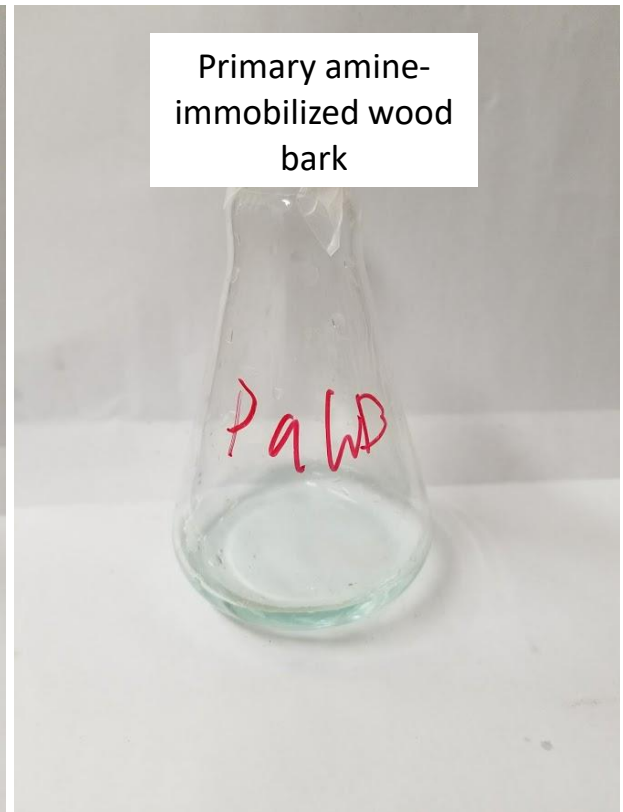
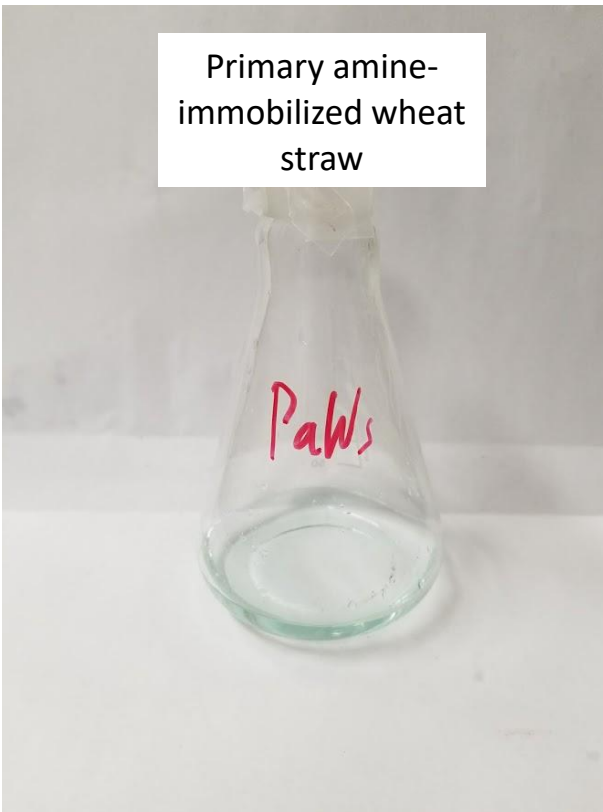
Dithiooxamide-immobilized biomass:



Ethylenediamine-immobilized biomass:



Primary amine-immobilized biomass:



APPENDIX B: FT-IR spectra of all biosorbents

Raw biomasses:

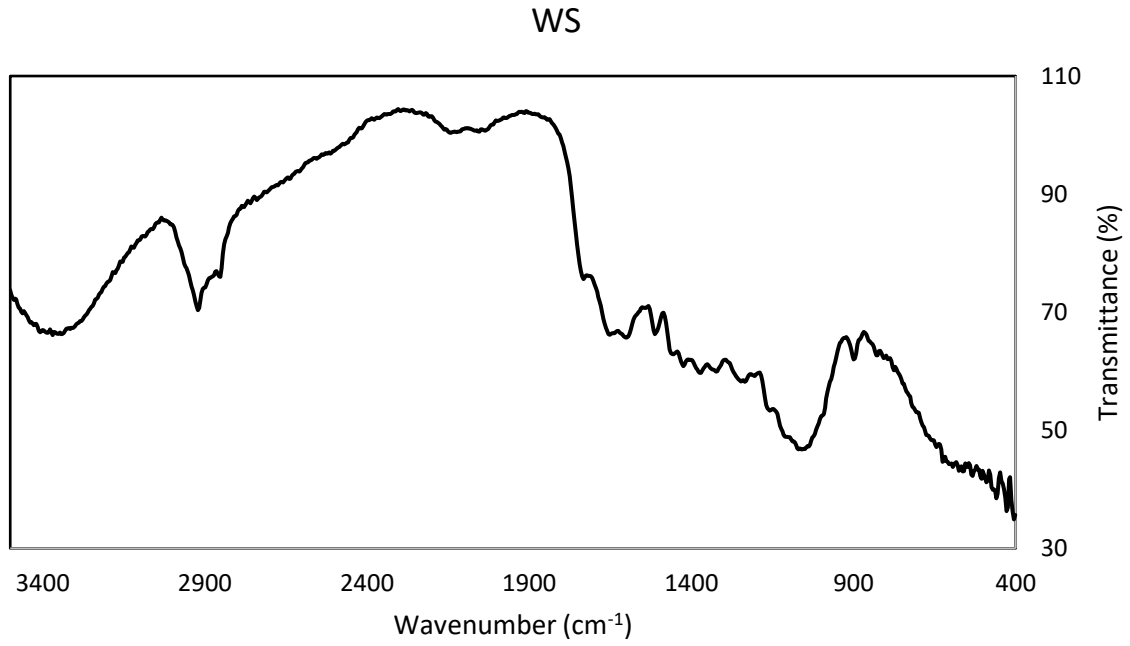


Fig B.1. FT-IR spectra of raw wheat straw.

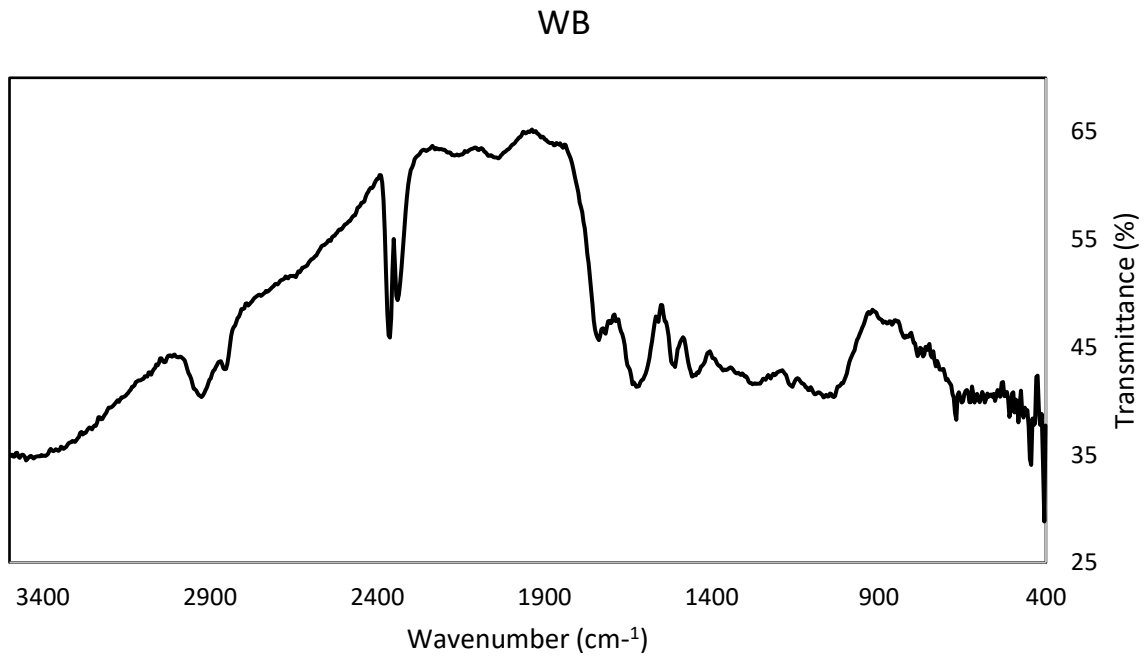


Fig B.2. FT-IR spectra of raw wood bark.

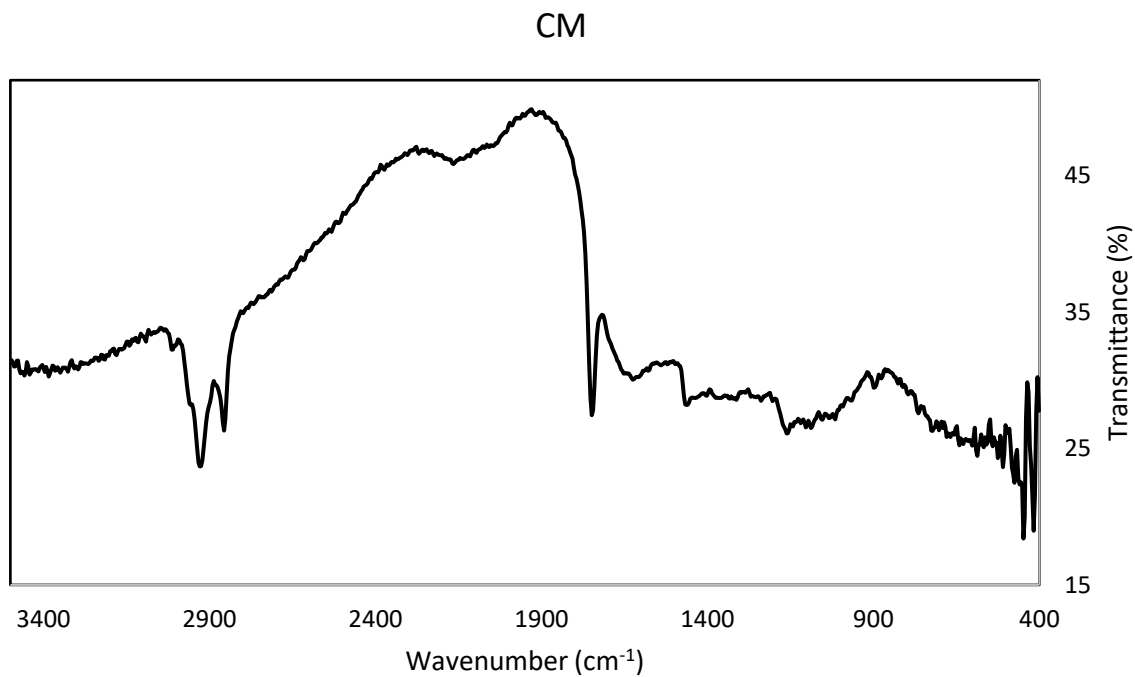


Fig B.3. FT-IR spectra of raw canola meal.

Dithiooxamide-immobilized biomass:

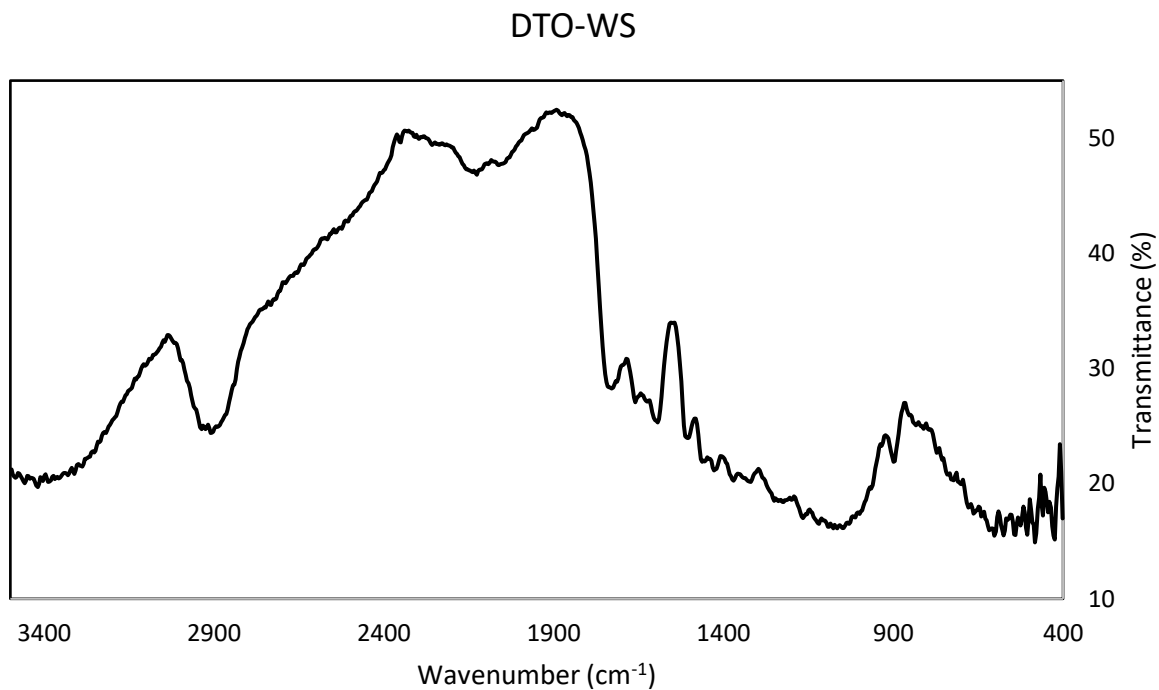


Fig B.4. FT-IR spectra of dithiooxamide-immobilized wheat straw.

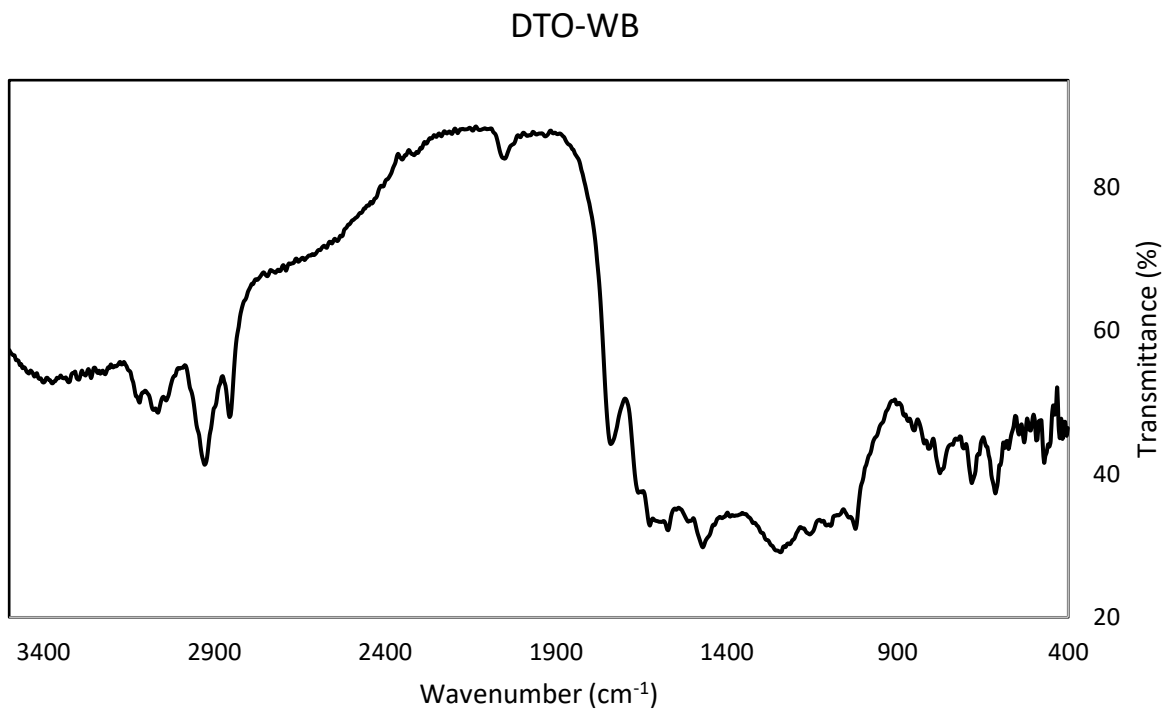


Fig B.5. FT-IR spectra of dithiooxamide-immobilized wood bark.

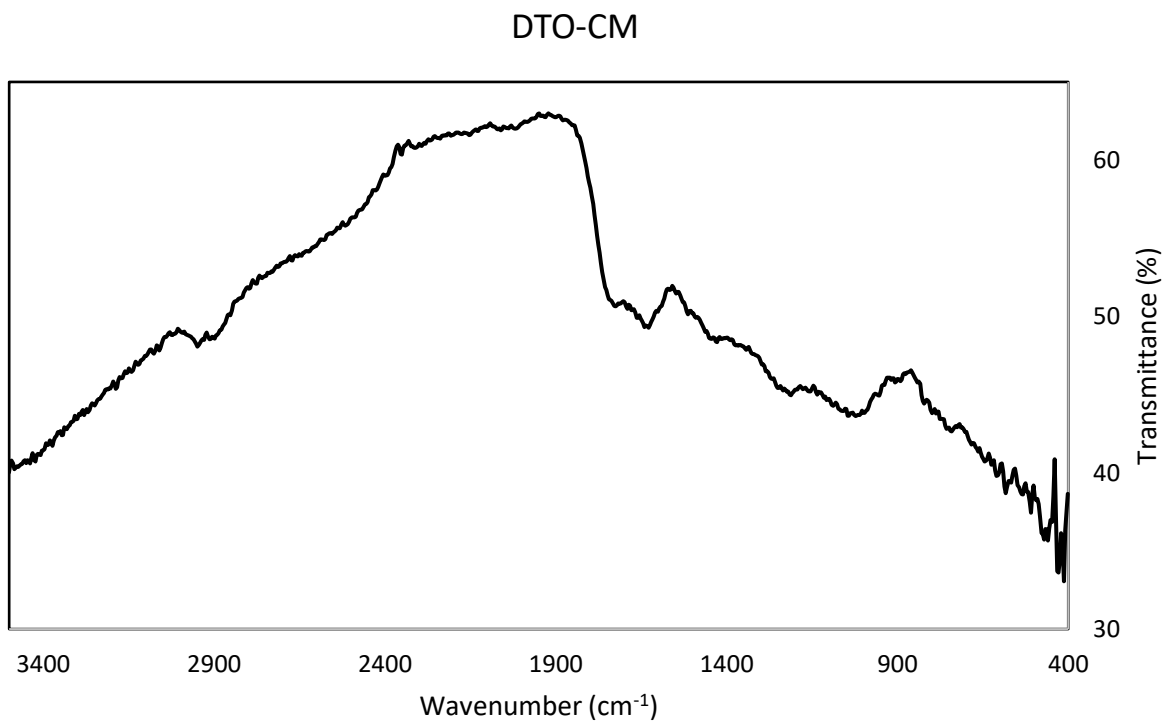


Fig B.6. FT-IR spectra of dithiooxamide-immobilized canola meal.

Ethylenediamine-immobilized biomass:

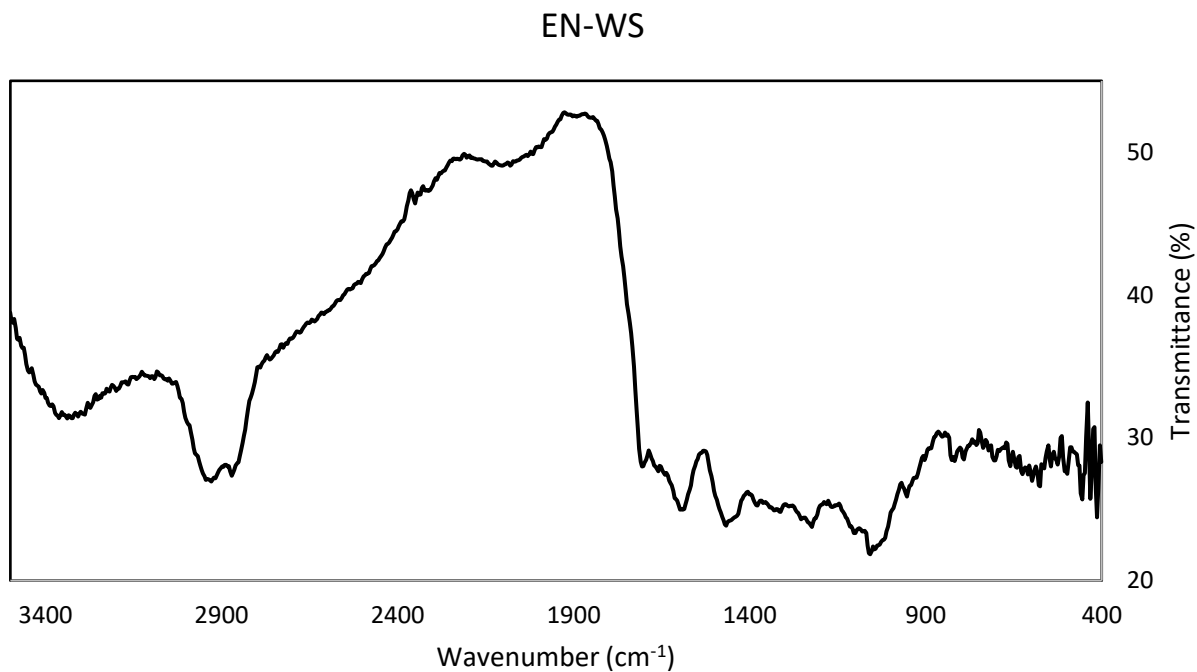


Fig B.7. FT-IR spectra of ethylenediamine-immobilized wheat straw.

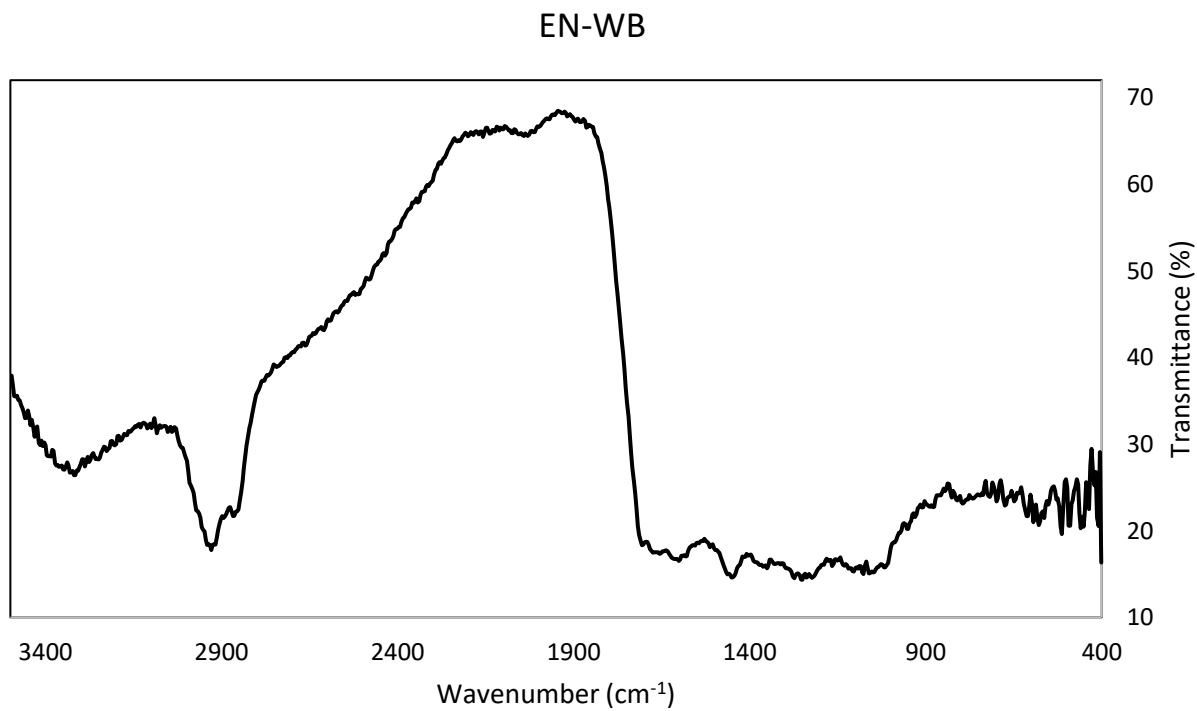


Fig B.8. FT-IR spectra of ethylenediamine-immobilized wood bark.

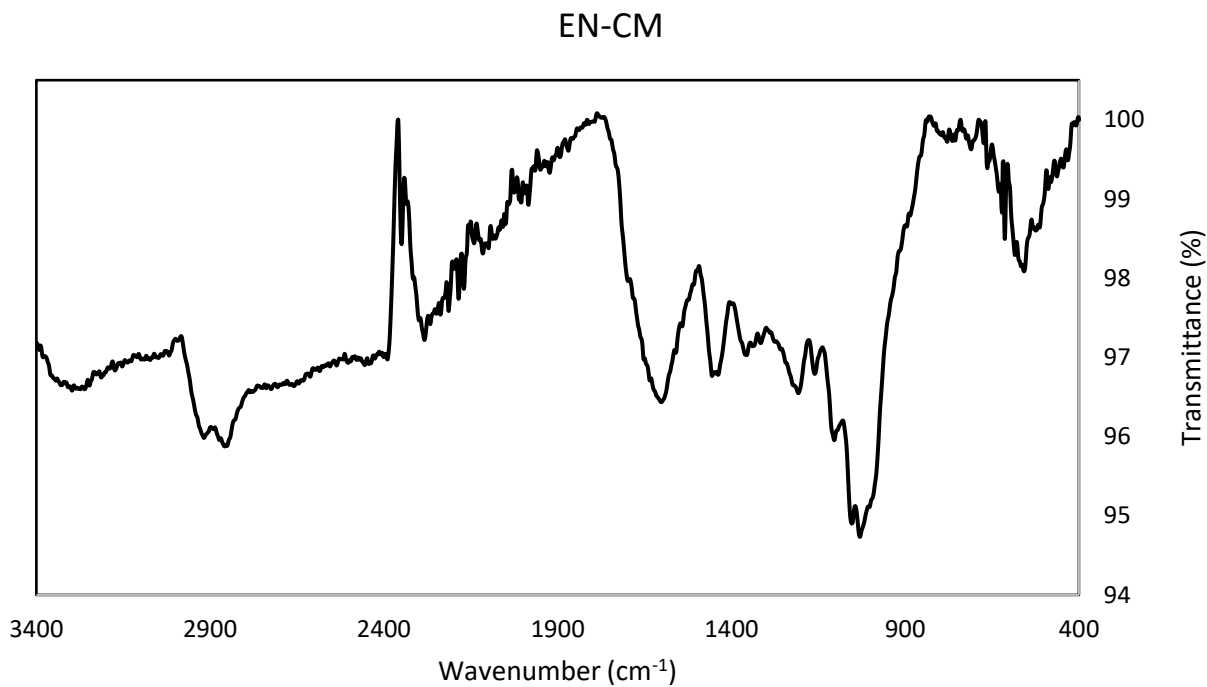


Fig B.9. FT-IR spectra of ethylenediamine-immobilized canola meal.

Primary amine-immobilized biomass:

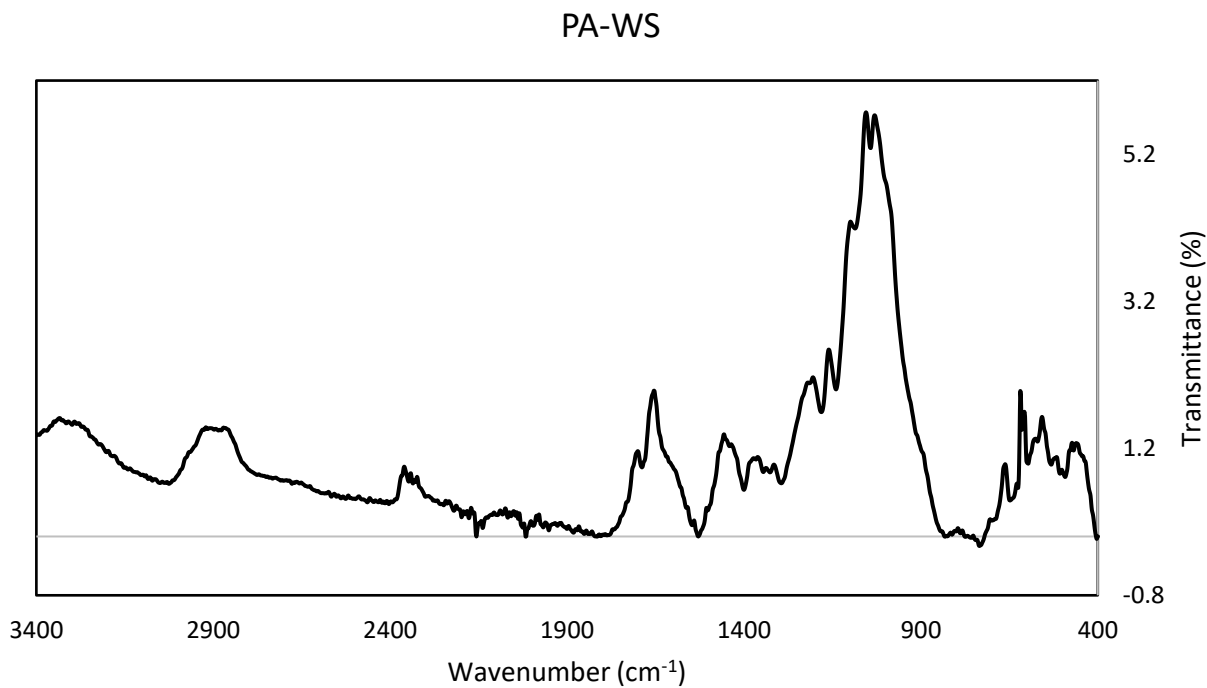


Fig B.10. FT-IR spectra of primary amine-immobilized wheat straw.

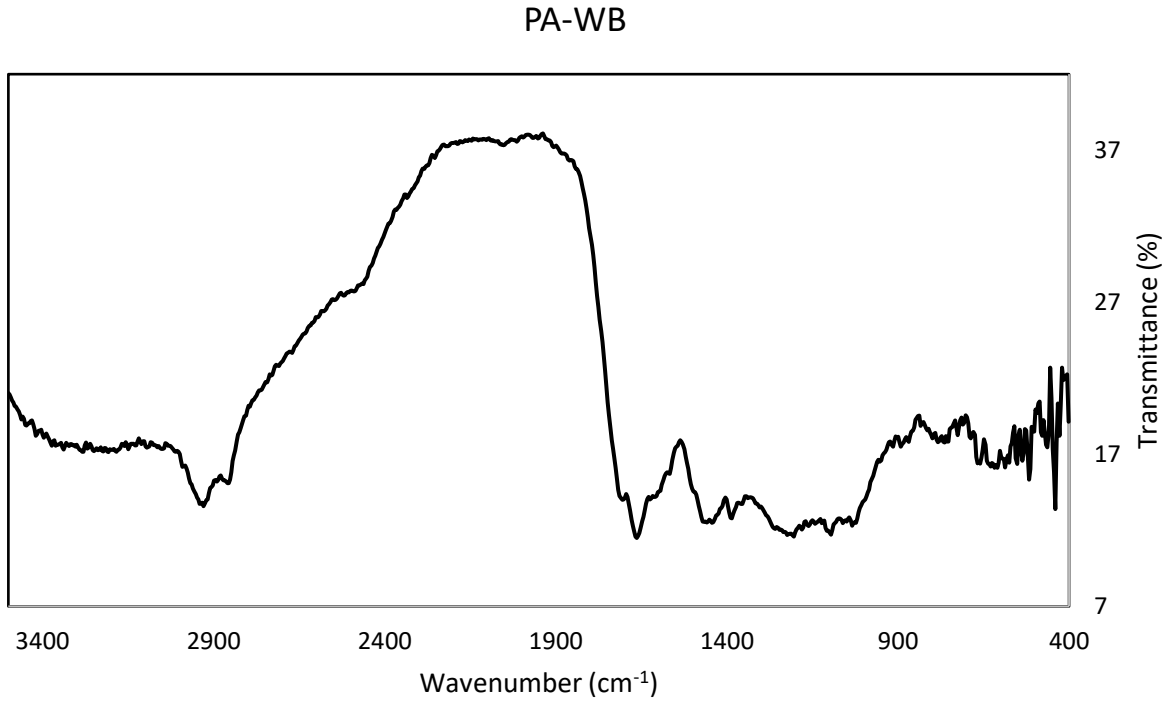


Fig B.11. FT-IR spectra of primary amine-immobilized wood bark.

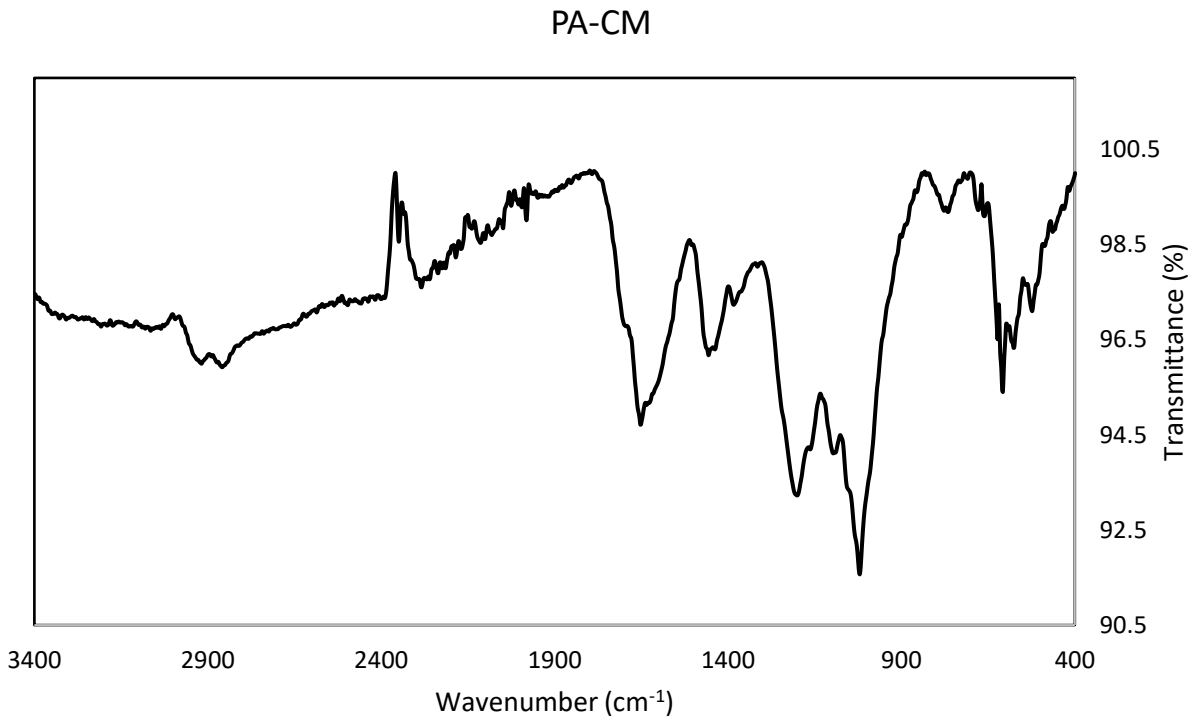


Fig B.12. FT-IR spectra of primary amine-immobilized canola meal.

APPENDIX C: Permission to reuse figures and tables from existing literature

The following copyright permission forms are arranged in order of table or figure appearance in the text.

This Agreement between Ms. Yen Ning Lee ("You") and Elsevier ("Elsevier") consists of your license details and the terms and conditions provided by Elsevier and Copyright Clearance Center.

License Number	4361060148375
License date	Jun 02, 2018
Licensed Content Publisher	Elsevier
Licensed Content Publication	Science of The Total Environment
Licensed Content Title	E-waste: An assessment of global production and environmental impacts
Licensed Content Author	Brett H. Robinson
Licensed Content Date	Dec 20, 2009
Licensed Content Volume	408
Licensed Content Issue	2
Licensed Content Pages	9
Start Page	183
End Page	191
Type of Use	reuse in a thesis/dissertation
Portion	figures/tables/illustrations
Number of figures/tables/illustrations	1
Format	both print and electronic
Are you the author of this Elsevier article?	No
Will you be translating?	No
Original figure numbers	Table 1
Title of your thesis/dissertation	The Biosorption of Platinum and Palladium in Chloride Based Real Leach Solution by Modified Biomass
Expected completion date	Jun 2018
Estimated size (number of pages)	90

Fig C.1

Regional E-waste Monitor: East and Southeast Asia

Honda, Shunichi, Khatriwal, Deepali S. and Kuehr, Ruediger, *Regional E-waste Monitor: East and Southeast Asia*, (Bonn: United Nations University and Japanese Ministry of the Environment, 2016).



Document type: Book
Collection: SCYCLE Books

METADATA	DOCUMENTS	VERSIONS	STATISTICS
Author	Honda, Shunichi Khatriwal, Deepali S. Kuehr, Ruediger		
Title	Regional E-waste Monitor: East and Southeast Asia		
Publication Date	2016		
Place of Publication	Bonn		
Publisher	United Nations University and Japanese Ministry of the Environment		
Pages	107		
Language	eng		
Copyright Holder	United Nations University		
Copyright Year	2016		
Copyright type	Creative commons		

Fig C.2

Requesting Permission

Anyone may, without requesting permission, use original figures or tables published in PNAS for noncommercial and educational use (i.e., in a review article, in a book that is not for sale), provided that the full journal reference is cited and, for articles published in volumes 90–105 (1993–2008), "Copyright (copyright year) National Academy of Sciences." Commercial reuse of figures and tables (i.e., in promotional materials, in a textbook for sale) requires permission from PNAS.

Text and data mining are permitted for noncommercial institutions with an active institutional site license to PNAS for internal noncommercial research purposes. Other requests should be sent to PNASpermissions@nas.edu.

Fig C.3

This Agreement between Ms. Yen Ning Lee ("You") and Elsevier ("Elsevier") consists of your license details and the terms and conditions provided by Elsevier and Copyright Clearance Center.

License Number	4362280423916
License date	Jun 04, 2018
Licensed Content Publisher	Elsevier
Licensed Content Publication	Environmental Technology & Innovation
Licensed Content Title	Characterization of iron-polyphenol complex nanoparticles synthesized by Sage (<i>Salvia officinalis</i>) leaves
Licensed Content Author	Zhiqiang Wang, Cheng Fang, Megharaj Mallavarapu
Licensed Content Date	Oct 1, 2015
Licensed Content Volume	4
Licensed Content Issue	n/a
Licensed Content Pages	6
Start Page	92
End Page	97
Type of Use	reuse in a thesis/dissertation
Portion	figures/tables/illustrations
Number of figures/tables/illustrations	1
Format	both print and electronic
Are you the author of this Elsevier article?	No
Will you be translating?	No
Original figure numbers	Fig 1
Title of your thesis/dissertation	The Biosorption of Platinum and Palladium in Chloride Based Real Leach Solution by Modified Biomass
Expected completion date	Jun 2018
Estimated size (number of pages)	90

Fig C.4



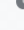
This Agreement between Ms. Yen Ning Lee ("You") and Elsevier ("Elsevier") consists of your license details and the terms and conditions provided by Elsevier and Copyright Clearance Center.

License Number	4360591239325
License date	Jun 02, 2018
Licensed Content Publisher	Elsevier
Licensed Content Publication	Hydrometallurgy
Licensed Content Title	Recovery of gold and silver from spent mobile phones by means of acidothiourea leaching followed by adsorption using biosorbent prepared from persimmon tannin
Licensed Content Author	Manju Gurung,Birendra Babu Adhikari,Hidetaka Kawakita,Keisuke Ohto,Katsutoshi Inoue,Shafiq Alam
Licensed Content Date	Feb 1, 2013
Licensed Content Volume	133
Licensed Content Issue	n/a
Licensed Content Pages	10
Start Page	84
End Page	93
Type of Use	reuse in a thesis/dissertation
Portion	figures/tables/illustrations
Number of figures/tables/illustrations	9
Format	both print and electronic
Are you the author of this Elsevier article?	No
Will you be translating?	No
Original figure numbers	Figure 9
Title of your thesis/dissertation	The Biosorption of Platinum and Palladium in Chloride Based Real Leach Solution by Modified Biomass
Expected completion date	Jun 2018

Fig C.5

Lignin

 real name: Karol Głęb pl.wiki: [Karol007](#) commons: [Karol007](#) e-mail: kamikaze007 (at) tlen.pl - own work from: Glazer, A. W., and Nikaido, H. (1995). Microbial Biotechnology: fundamentals of applied microbiology. San Francisco: W. H. Freeman, p. 340. ISBN 0-71672608-4 This vector image was created with [Inkscape](#).

 [CC BY-SA 3.0](#) [view terms](#)
 File: Lignin structure.svg
 Created: 24 April 2007

Permission details

GFDL ver. 1.2 or CC-by-sa ver. 2.5, 2.0, and 1.0 lub Public Domain (PD)

Fig C.6

Fig C.7

RE: Request for content usage



Crystal Klippenstein <klippensteinc@canolacouncil.org>

6/8/2018 7:39 AM

To: Lee, Yen Ning

Hello Yen Ning,

You have our permission to use table 2 from the Canola Meal Feed Industry Guide in your thesis.
Thanks,

Crystal Klippenstein

Communications Project Manager

400 – 167 Lombard Ave | Winnipeg MB | R3B 0T6

Office: 204.982.7762 | Cell: 204.298.5537 | klippensteinc@canolacouncil.org

www.canolacouncil.org

If you no longer want to receive emails, please let me know and I will remove you from my contacts list.

Fig C.8

Fig C.9

This Agreement between Ms. Yen Ning Lee ("You") and Elsevier ("Elsevier") consists of your license details and the terms and conditions provided by Elsevier and Copyright Clearance Center.

License Number	4363870444503
License date	Jun 07, 2018
Licensed Content Publisher	Elsevier
Licensed Content Publication	Journal of Cleaner Production
Licensed Content Title	Alternatives to cyanide in the gold mining industry: what prospects for the future?
Licensed Content Author	Gavin Hilson,A.J. Monhemius
Licensed Content Date	Jan 1, 2006
Licensed Content Volume	14
Licensed Content Issue	12-13
Licensed Content Pages	10
Start Page	1158
End Page	1167
Type of Use	reuse in a thesis/dissertation
Portion	figures/tables/illustrations
Number of figures/tables/illustrations	1
Format	both print and electronic
Are you the author of this Elsevier article?	No
Will you be translating?	No
Original figure numbers	Table 3
Title of your thesis/dissertation	The Biosorption of Platinum and Palladium in Chloride Based Real Leach Solution by Modified Biomass
Expected completion date	Jun 2018
Estimated size (number of pages)	90

Fig C.10

This Agreement between Ms. Yen Ning Lee ("You") and Elsevier ("Elsevier") consists of your license details and the terms and conditions provided by Elsevier and Copyright Clearance Center.

License Number	4363980064389
License date	Jun 07, 2018
Licensed Content Publisher	Elsevier
Licensed Content Publication	Sustainable Materials and Technologies
Licensed Content Title	Fabrication of precious metals recovery materials using grape seed-waste
Licensed Content Author	Motoki Inoue,Takeo Nakano,Akihiro Yamasaki
Licensed Content Date	Apr 1, 2015
Licensed Content Volume	3
Licensed Content Issue	n/a
Licensed Content Pages	3
Start Page	14
End Page	16
Type of Use	reuse in a thesis/dissertation
Portion	figures/tables/illustrations
Number of figures/tables/illustrations	1
Format	both print and electronic
Are you the author of this Elsevier article?	No
Will you be translating?	No
Original figure numbers	Figure 2
Title of your thesis/dissertation	The Biosorption of Platinum and Palladium in Chloride Based Real Leach Solution by Modified Biomass
Expected completion date	Jun 2018
Estimated size (number of pages)	90

Fig C.11



Title: Dithioamide-Immobilized Microalgal Residue for the Selective Recovery of Pd(II) and Pt(IV)
Author: Kanjana Khunathai, Katsutoshi Inoue, Keisuke Ohto, et al
Publication: Separation Science and Technology
Publisher: Taylor & Francis
Date: May 1, 2012
Rights managed by Taylor & Francis

Logged in as:
Yen Ning Lee
Account #:
3001293667

LOGOUT

Thesis/Dissertation Reuse Request

Taylor & Francis is pleased to offer reuses of its content for a thesis or dissertation free of charge contingent on resubmission of permission request if work is published.

Fig C.12

Acids

Tem5psu - Own work

Periodic table showing hard and soft acids

CC BY-SA 3.0

File: Hardsoftacids.png

Created: 7 July 2014

Fig C.13

Bases

Tem5psu - Own work

Periodic table showing hard and soft bases

CC BY-SA 3.0

File: Hardsoftbases.png

Created: 7 July 2014

Fig C.14

Re:Permission for content use



ijcea <ijcea@ejournal.net>

6/11/2018 12:34 AM

To: Lee, Yen Ning

Dear Yen Ning Lee,

Thanks for your email, you could cite it as a reference, and you have to note that the Figure is from IJCEA. I mean the reference source.

--

Best Regards,

Jennifer Zeng

IJCEA Associate Executive Editor

Email: ijcea@ejournal.net | **Website:** <http://www.ijcea.org>

Fig C.15

This Agreement between Ms. Yen Ning Lee ("You") and Elsevier ("Elsevier") consists of your license details and the terms and conditions provided by Elsevier and Copyright Clearance Center.

License Number	4364581477881
License date	Jun 09, 2018
Licensed Content Publisher	Elsevier
Licensed Content Publication	Chemical Engineering Journal
Licensed Content Title	Kraft mill lignin – A potential source of bio-adsorbents for gold recovery from acidic chloride solution
Licensed Content Author	Birendra Babu Adhikari,Manju Gurung,Shafiq Alam,Balázs Tolnai,Katsutoshi Inoue
Licensed Content Date	Sep 1, 2013
Licensed Content Volume	231
Licensed Content Issue	n/a
Licensed Content Pages	8
Start Page	190
End Page	197
Type of Use	reuse in a thesis/dissertation
Portion	figures/tables/illustrations
Number of figures/tables/illustrations	1
Format	both print and electronic
Are you the author of this Elsevier article?	No
Will you be translating?	No
Original figure numbers	Figure 2
Title of your thesis/dissertation	The Biosorption of Platinum and Palladium in Chloride Based Real Leach Solution by Modified Biomass
Expected completion date	Jun 2018
Estimated size (number of pages)	90

Fig C.16

This Agreement between Ms. Yen Ning Lee ("You") and Elsevier ("Elsevier") consists of your license details and the terms and conditions provided by Elsevier and Copyright Clearance Center.

License Number	4364610745039
License date	Jun 09, 2018
Licensed Content Publisher	Elsevier
Licensed Content Publication	Journal of Hazardous Materials
Licensed Content Title	Biosorption of palladium(II) from aqueous solution by moss (Racomitrium lanuginosum) biomass: Equilibrium, kinetic and thermodynamic studies
Licensed Content Author	Ahmet Sari,Durali Mendil,Mustafa Tuzen,Mustafa Soylak
Licensed Content Date	Mar 15, 2009
Licensed Content Volume	162
Licensed Content Issue	2-3
Licensed Content Pages	6
Start Page	874
End Page	879
Type of Use	reuse in a thesis/dissertation
Intended publisher of new work	other
Portion	figures/tables/illustrations
Number of figures/tables/illustrations	2
Format	both print and electronic
Are you the author of this Elsevier article?	No
Will you be translating?	No
Original figure numbers	Figure 3 Figure 4
Title of your thesis/dissertation	The Biosorption of Platinum and Palladium in Chloride Based Real Leach Solution by Modified Biomass
Expected completion date	Jun 2018
Estimated size (number of pages)	90

Fig C.17



ACS Publications
Most Trusted. Most Cited. Most Read.

Title: Recovery of Gold(III),
Palladium(II), and Platinum(IV)
by Aminated Lignin Derivatives

Author: Durga Parajuli, Hidetaka
Kawakita, Katsutoshi Inoue, et
al

Publication: Industrial & Engineering
Chemistry Research

Publisher: American Chemical Society

Date: Sep 1, 2006

Copyright © 2006, American Chemical Society

Logged in as:

Yen Ning Lee

Account #:
3001293667

LOGOUT

PERMISSION/LICENSE IS GRANTED FOR YOUR ORDER AT NO CHARGE

This type of permission/license, instead of the standard Terms & Conditions, is sent to you because no fee is being charged for your order. Please note the following:

- Permission is granted for your request in both print and electronic formats, and translations.
- If figures and/or tables were requested, they may be adapted or used in part.
- Please print this page for your records and send a copy of it to your publisher/graduate school.
- Appropriate credit for the requested material should be given as follows: "Reprinted (adapted) with permission from (COMPLETE REFERENCE CITATION). Copyright (YEAR) American Chemical Society." Insert appropriate information in place of the capitalized words.
- One-time permission is granted only for the use specified in your request. No additional uses are granted (such as derivative works or other editions). For any other uses, please submit a new request.

If credit is given to another source for the material you requested, permission must be obtained from that source.

Fig C.18